

# Discovery of Phenylpyrazole Derivatives as a New Class of Selective Inhibitors of MCL-1 with Antitumor Activity

Qineng Gong,<sup>§</sup> Chunpu Li,<sup>§</sup> Haojie Wang,<sup>§</sup> Jinrui Cao, Zuo Li, Mi Zhou, Yan Li, Yong Chu,\*  
Hong Liu,\* and Renxiao Wang\*



Cite This: *ACS Omega* 2024, 9, 27369–27396



Read Online

ACCESS |



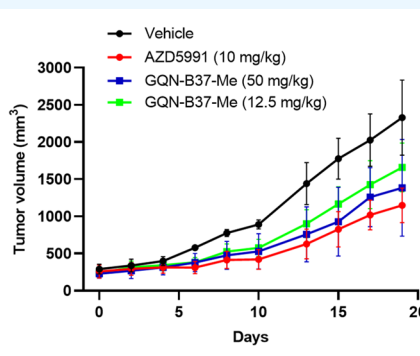
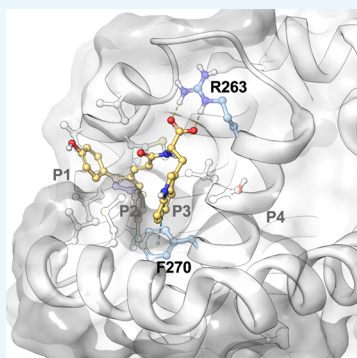
Metrics & More



Article Recommendations



Supporting Information



**ABSTRACT:** MCL-1, an antiapoptotic member of the BCL-2 family, is dysregulated and overexpressed in various tumors. In tumors with MCL-1 overexpression, selective inhibitors of MCL-1 are expected to overcome the drug resistance caused by BCL-2 inhibitors currently used in clinical treatment. Here, we employed docking-based virtual screening to identify an active hit, LC126, with binding affinity around 10  $\mu\text{M}$  for MCL-1 and BCL-2. Under the guidance of structure-based design, we obtained a few selective inhibitors of MCL-1 after three rounds of structural optimization. The representative compound GQN-B37-E exhibited binding affinity for MCL-1 at the submicromolar range ( $K_i = 0.6 \mu\text{M}$ ) without apparent binding to BCL-2 or BCL-X<sub>L</sub>. <sup>15</sup>N-heteronuclear single-quantum coherence NMR spectra suggested that this compound binds to the BH3-domain-binding pocket in the MCL-1 surface. Cellular assays revealed that GQN-B37-Me, the precursor of GQN-B37-E, is effective particularly on leukemia cells (such as H929 and MV-4–11) to induce caspase-dependent apoptosis. Its interaction with MCL-1 in cells was confirmed by coimmunoprecipitation. Administration of GQN-B37-Me to MV-4–11 xenograft mice at 50 mg/kg every 2 days for 20 days led to 43% tumor growth inhibition. GQN-B37-Me also exhibited reasonable in vitro stability in GSH and liver microsomes from several species. This new class of MCL-1 inhibitor may have potential to be further developed into a preclinical candidate for treating leukemia.

## 1. INTRODUCTION

In the past three decades or so, numerous studies have revealed the critical relationship between apoptosis and tumor progression, metastasis, and others.<sup>1–3</sup> In particular, mitochondrial apoptosis is normally triggered by the physiological stresses caused by anticancer therapies, and thus, evasion of apoptosis is a major mechanism for cancer cell resistance to such treatment.<sup>4–7</sup> BCL-2 family proteins are a group of key regulators of the mitochondrial apoptotic pathway, which include antiapoptotic proteins (e.g., BCL-2, BCL-x<sub>L</sub>, MCL-1, BCL-w, and BFL-1), proapoptotic proteins (e.g., BAX, BAK, and BOK), and BH3-only proteins (e.g., BIM, tBID, PUMA, BAD, NOXA, BIK, BMF, and HRK).<sup>8–11</sup> It is believed that BH3-only proteins can indirectly release proapoptotic BAX and BAK proteins from their binding to the antiapoptotic BCL-2 proteins. Then, BAX or BAK protein forms oligomers on the

outer mitochondrial membrane, which causes leak of the contents of mitochondria and eventually leads to apoptosis.<sup>12</sup>

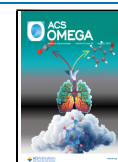
Overexpression of the antiapoptotic BCL-2 proteins are observed in various cancer cells.<sup>4–7</sup> Thus, small-molecule compounds targeting the antiapoptotic BCL-2 proteins may restore normal apoptosis and achieve benefits in clinical treatment.<sup>13,14</sup> In fact, discovery of small-molecule inhibitors of the antiapoptotic BCL-2 proteins has been actively pursued since the beginning of this century. So far, the most remarkable

Received: March 4, 2024

Revised: April 23, 2024

Accepted: May 30, 2024

Published: June 13, 2024



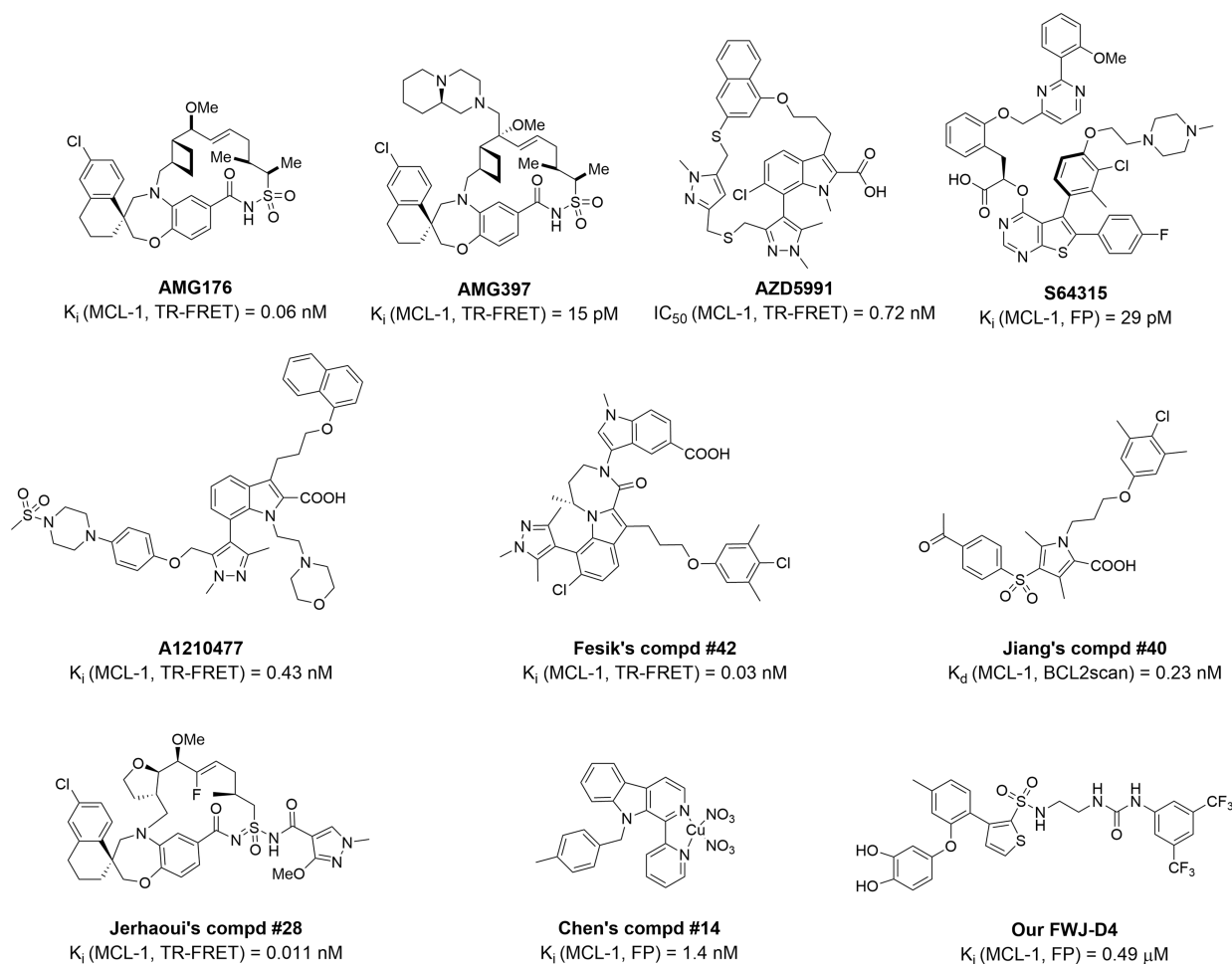


**Figure 1.** Some MCL-1 inhibitors reported in the literature which exhibit antitumor activity in vivo.

example of such efforts is the development of the ABT-series of compounds by Abbott, such as ABT-737,<sup>15</sup> ABT-263,<sup>16</sup> and ABT-199.<sup>17</sup> In 2016, Venetoclax (ABT-199) was approved by FDA for the treatment of chronic lymphocytic leukemia (CLL) with 17p gene deletion, which has validated the strategy of developing small-molecule compounds as BH3-domain mimetics to directly activate apoptosis in cancers.<sup>18</sup>

MCL-1, as a major antiapoptotic protein of the BCL-2 family, is overexpressed in various cancer cells, including leukemia,<sup>19</sup> lymphoma,<sup>20</sup> lung cancer,<sup>21</sup> breast cancer,<sup>22</sup> multiple myeloma,<sup>23</sup> colon cancer,<sup>24</sup> melanoma,<sup>25</sup> and others.<sup>26</sup> Overexpression of MCL-1 as a compensation of disabled BCL-2 can produce innate and acquired resistance to selective BCL-2 inhibitors such as ABT-199.<sup>27,28</sup> Although antiapoptotic BCL-2 proteins share similar conserved structural features, MCL-1 contains notable differences in its amino acid sequence and an unstructured amino-terminus core that provides a unique regulatory mechanism.<sup>29,30</sup> For example, studies have revealed that MCL-1 exhibits a more prominent mitochondrial localization than BCL-2 does. In cells undergoing differentiation, expression of MCL-1 increases rapidly, whereas that of BCL-2 decreases after complete differentiation.<sup>31</sup> Therefore, selective MCL-1 inhibitors may be applied at least as a supplement to current BCL-2 inhibitors to clinical cancer treatment.

In the past decade or so, a number of selective MCL-1 inhibitors have been developed by academic research groups and pharmaceutical companies.<sup>32,33</sup> Many current MCL-1

inhibitors share rather similar chemical fragments or certain structural features, such as a macrocyclic moiety. Although those MCL-1 inhibitors are often reported to achieve subnanomolar affinity in *in vitro* binding assay, only some of them, such as A1210477,<sup>34</sup> Fesik's compound 42,<sup>35</sup> and others,<sup>36–39</sup> have relatively clear mechanism of action in cells and also exhibit antitumor activity *in vivo* (Figure 1). Even fewer MCL-1 inhibitors (such as AMG176,<sup>40</sup> AMG397,<sup>41</sup> AZD5991,<sup>42</sup> and S64315<sup>43</sup>) have entered clinical trials. Unfortunately, some clinical trials have already been terminated, for example NCT03218683 and NCT03797261, due to side effects. To date, no MCL-1 inhibitor has successfully completed a phase II clinical trial. Apparently, a wider range of chemotypes still need to be explored in order to develop MCL-1 inhibitors successfully into effective and safe anticancer drugs.

In our previous work, we discovered a lead compound with a phenyltetrazole core moiety through docking-based virtual screening targeting the BH3-domain-binding pocket on MCL-1.<sup>44</sup> This lead compound was then optimized into a class of compound with a 3-phenylthiophene-2-sulfonamide core moiety, which exhibited micromolar binding affinity to MCL-1 and BCL-2. Later, we further optimized this class of compound and obtained new derivatives with submicromolar binding affinity and improved selectivity for MCL-1.<sup>45</sup> The representative compounds among them, such as FWJ-D4 as well as its precursor FWJ-DS, effectively induced mitochondrial apoptosis in a range of cancer cells. Treatment with FWJ-D5 on a RS4;11

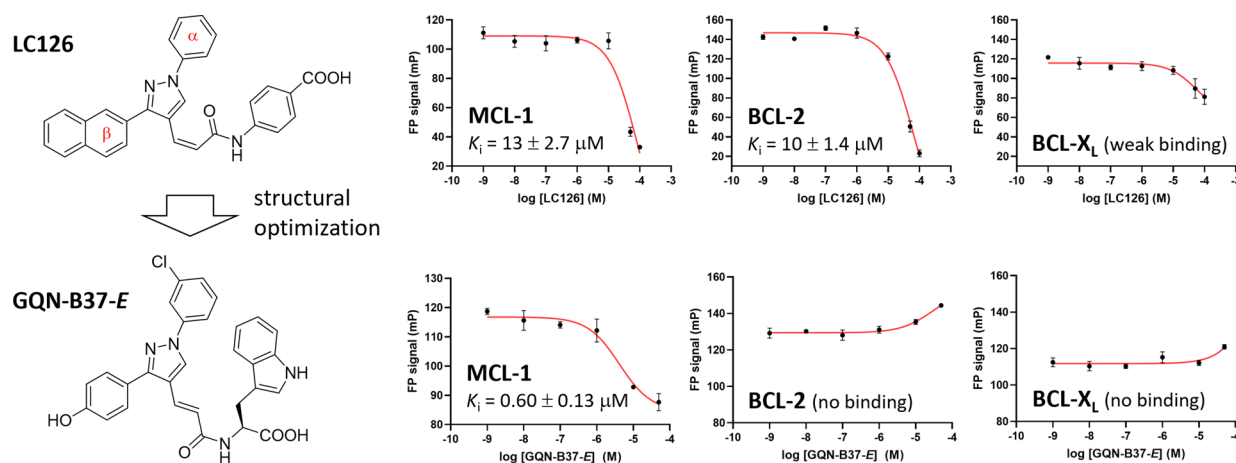


**Figure 2.** Structure of LC126 and a representative derivative GQN-B37-E as well as their dose-dependent binding to MCL-1, BCL-2, and BCL-X<sub>L</sub>. In each case, the given compound was tested up to 100  $\mu\text{M}$ . Mean values and standard deviations of FP signal were derived from three parallel measurements.

xenograft mouse leukemia model led to significant reduction in tumor volume.<sup>45</sup> This class of compound certainly needs further preclinical developments. Nevertheless, our previous work at least has demonstrated that docking-based virtual screening is useful for discovering new small-molecule MCL-1 inhibitors.

Recently, we developed another class of small-molecule MCL-1 inhibitors. The starting point, LC126, was also discovered through docking-based virtual screening targeting MCL-1. This compound exhibited binding affinity to MCL-1 and BCL-2 ( $K_i \sim 10 \mu\text{M}$ ). After three rounds of structural optimization, we obtained some compounds exhibiting selective binding to MCL-1 at submicromolar concentrations. Cellular studies indicated that those compounds disrupt the binding of BIM to MCL-1 in cells and induce mitochondrial apoptosis primarily in leukemia cell lines. Among them, compound GQN-B37-Me was selected for assessment in a MV-4–11 xenograft mouse leukemia model, and it led to significant reduction in tumor volume at doses ranging from 12.5 to 50 mg/kg without causing obvious body weight loss.

## 2. RESULTS AND DISCUSSION

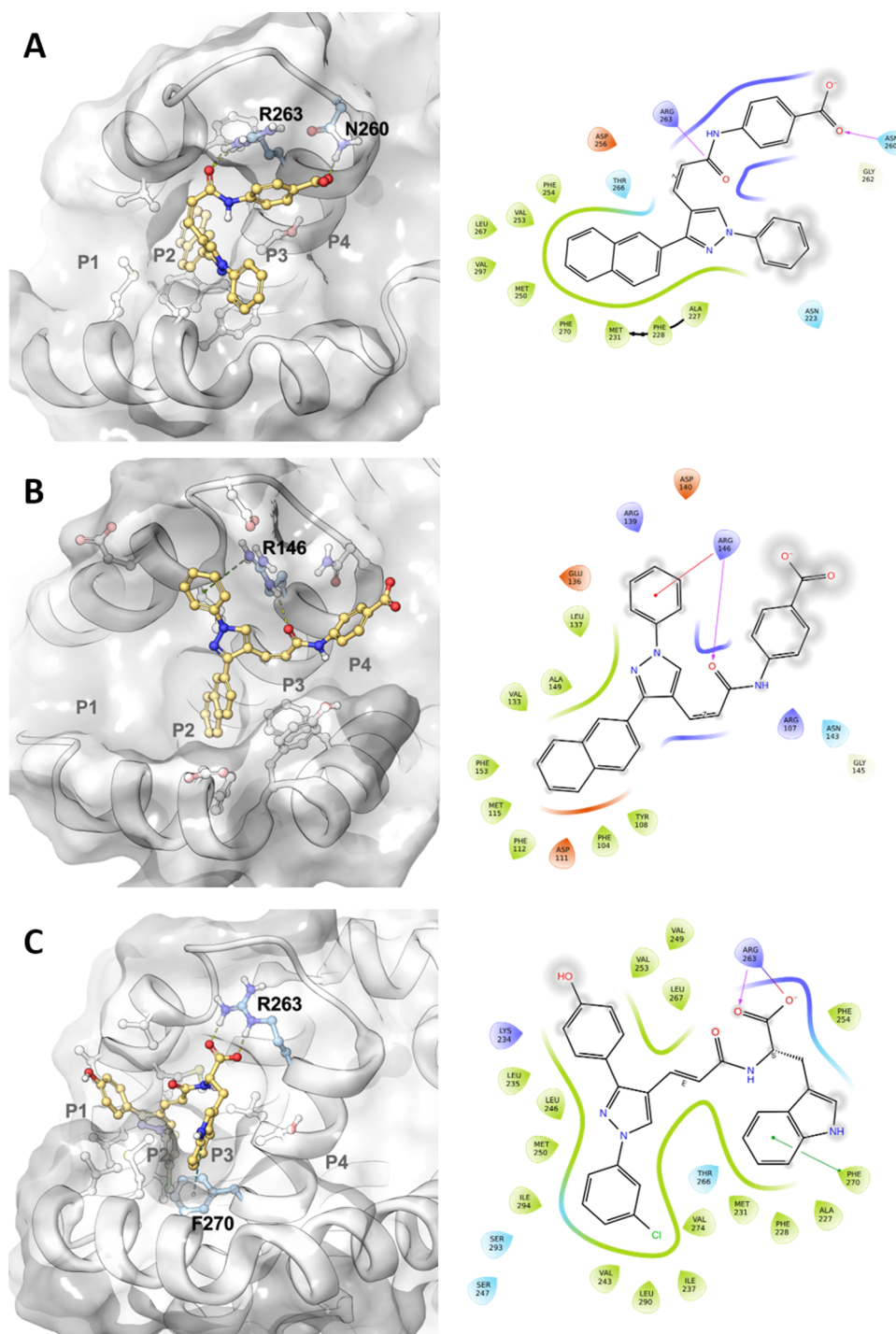
**2.1. Discovery of the Active Hit.** As described in Section 4, around 630,000 small molecules assembled from three commercial compound libraries (MayBridge, SPECS, and LifeChemicals) were examined through docking-based virtual screening by targeting the BH3-domain-binding pocket on MCL-1 or BCL-X<sub>L</sub>. Our initial objective was to identify new inhibitors for either MCL-1 or BCL-X<sub>L</sub>, as both are envisaged to be complementary to selective BCL-2 inhibitors. To account for the conformational flexibility inherent in the designated binding pocket, we considered three representative structures for MCL-1 and BCL-X<sub>L</sub>, respectively, for docking of each putative ligand molecule in parallel. Finally, we selected 349 molecules as potential inhibitors for MCL-1 and 317 for BCL-X<sub>L</sub> by considering their binding mode and ligand efficiency. Out of these selections, samples of 644 compounds were purchased from commercial suppliers (see the Supporting Information for more details).

All obtained compounds were tested in a fluorescence polarization (FP)-based binding assay, which was also employed in our previous work.<sup>44,45</sup> Unfortunately, we did not discover any noteworthy BCL-X<sub>L</sub> binder among these compounds. However, we did obtain one compound, i.e., LC126, that

exhibited clear, dose-dependent binding to MCL-1 with a  $K_i$  value of  $13 \pm 2.7 \mu\text{M}$ . Interestingly, it also bound to BCL-2 with a  $K_i$  value of  $10 \pm 1.4 \mu\text{M}$  (Figure 2). LC126 contains a phenylpyrazole core moiety that is not observed in other known MCL-1 inhibitors. By considering its binding affinity for the desired target as well as structural novelty, we selected LC126 as the lead compound to develop derivatives with the aim of achieving enhanced activity and selectivity.

In order to gain some insights for subsequent structural optimization, we then predicted the binding modes of LC126 to MCL-1 and BCL-2 through molecular modeling (Figure 3A,B). It is described in the literature<sup>29</sup> that the BH3-domain-binding pocket in MCL-1 and BCL-2 comprises four subpockets (i.e., P1–P4) and a conserved Arg residue (see Figure S2 in the Supporting Information). A noteworthy distinction here is that MCL-1 harbors hotspot residues at the P2 and P3 subpockets, whereas BCL-2 has hotspot residues at the P2 and P4 subpockets. As suggested by our predicted binding mode, the naphthyl group on LC126 becomes ensconced within the P2 subpocket in both MCL-1 and BCL-2, thereby establishing a key hydrophobic interaction for anchoring this ligand. Furthermore, the central amide group in LC126 forms a hydrogen bond with the conserved Arg residue on both MCL-1 and BCL-2. However, in the case of MCL-1, LC126 does not fully occupy the P3 subpocket; instead, the terminal phenyl group at one end points toward the bulk solvent, while the terminal benzoic acid moiety at the other end engages in a weak interaction with Asn260 within a nonhotspot region. In contrast, in the case of BCL-2, the terminal benzoic acid group of LC126 is oriented toward the P4 subpocket but fails to form any significant interactions. In summary, the predicted binding modes of LC126 with MCL-1 and BCL-2 share certain common features but also exhibit significant differences. It stands to reason that structural optimization of this lead compound, aimed at obtaining selective MCL-1 inhibitors, should amplify the distinctions discussed above.

**2.2. Structural Optimization.** The predicted binding mode of LC126 to MCL-1 suggests a need for structural modification to enhance access to the P3 subpocket. Consequently, our initial round of structural optimization for LC126 focused on replacing its benzoic acid moiety with other synthetically accessible moieties. To this end, we synthesized a series of compounds (GQN-A1 to GQN-A9) featuring diverse substitutions in place

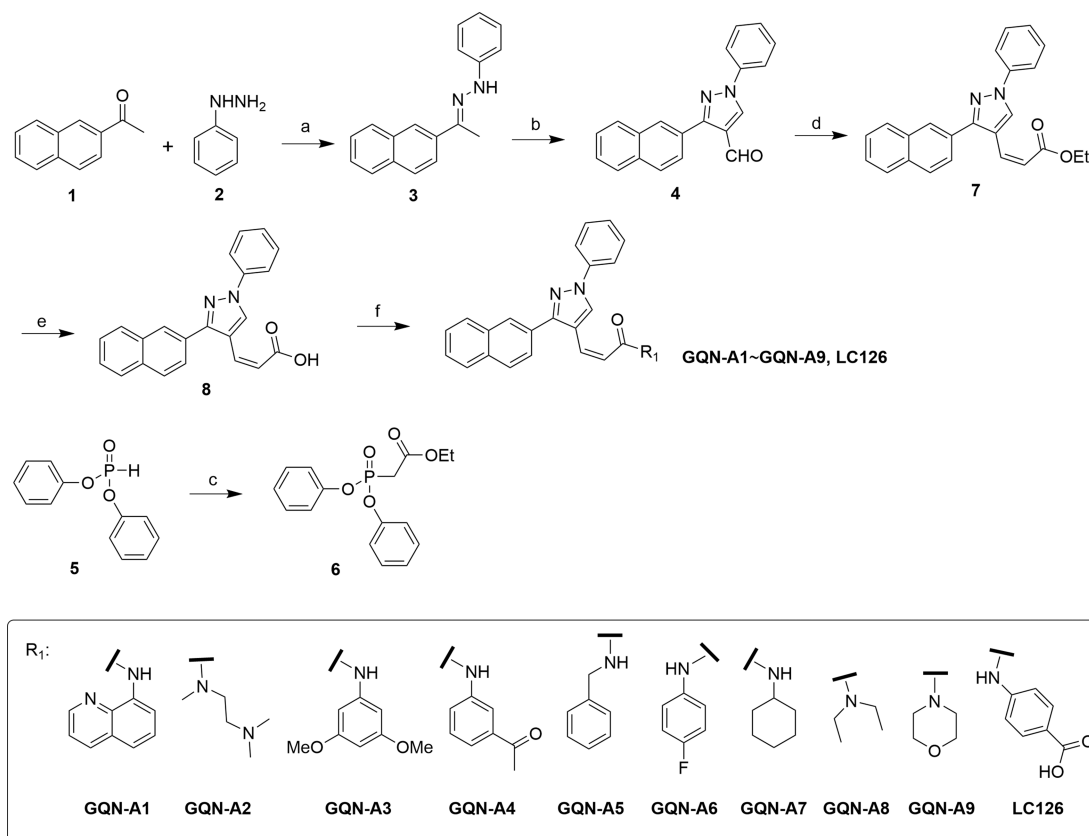


**Figure 3.** Predicted binding modes of (A) LC126 with MCL-1 based on PDB entry 5FDR; (B) LC126 with BCL-2 based on PDB entry 4LVT; and (C) GQN-B37-E with MCL-1 based on PDB entry 6U65. Here, the ligand molecule is shown in the stick-and-ball model, and the molecular surfaces of MCL-1 or BCL-2 is colored in gray. A two-dimensional schematic illustration generated by the Schrödinger software is also given in each case. The MD simulation trajectories for deriving these binding modes are given in Figure S4 in the Supporting Information.

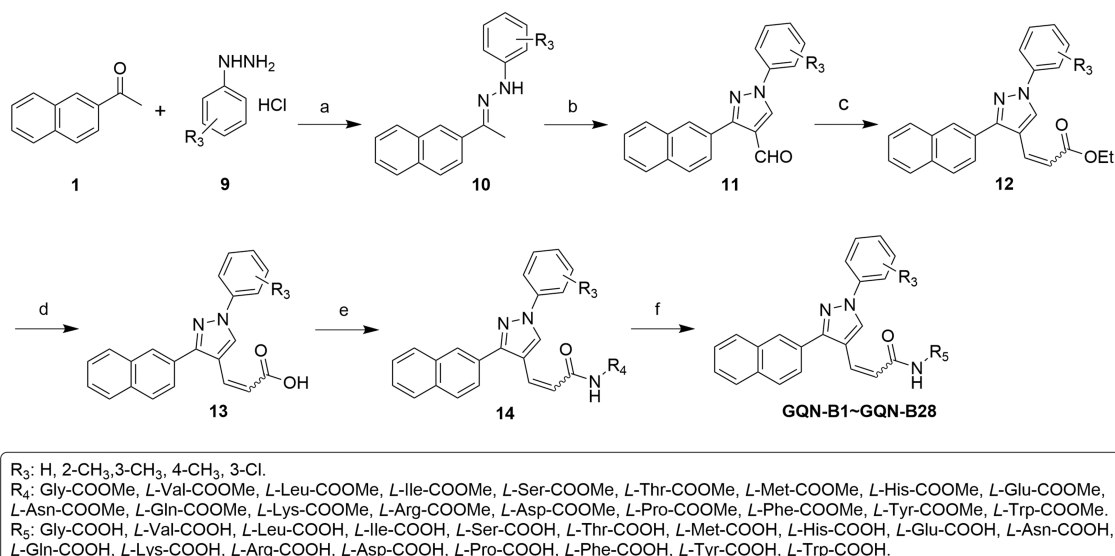
of the benzoic acid moiety, given that the synthetic methods were feasible and the required material were accessible to us. The synthetic methods and the chemical structures of the obtained compounds are outlined in Scheme 1. Binding affinities of these compounds for MCL-1, BCL-2, and BCL-X<sub>L</sub> were evaluated in our FP-based binding assay. However, none of these compounds exhibited any discernible binding to all three target proteins. It is worth noting that several newly synthesized compounds here (such as GQN-A3 to GQN-A6) actually have a

R<sub>1</sub> group similar in size and nature to the benzoic acid moiety on LC126. This set of results underscores the importance of the benzoic acid moiety, especially the carboxylic acid group, in binding to MCL-1, which is not evident in our predicted binding mode for LC126.

Based on this understanding, our second round of structural optimization aimed at substituting the terminal benzoic acid moiety. Here, we conceived the idea of introducing an  $\alpha$ -amino acid residue for several reasons: First, an amino acid also

Scheme 1. Synthesis of Compounds LC126 and GQN-A1 to GQN-A9<sup>a</sup>

<sup>a</sup>Reagents and conditions: (a) EtOH, AcOH, reflux; (b) DMF, POCl<sub>3</sub>, rt; (c) BrCH<sub>2</sub>COOEt, DCM, Et<sub>3</sub>N, rt; (d) 6, NaH, THF, rt; (e) 1.2 M KOH, MeOH, THF, 50 °C; 2.2 M HCl; (f) R<sup>1</sup>-NH<sub>2</sub>, HATU, DIPEA, DMF, rt. Overall yield of each final product can be found in Section 4.

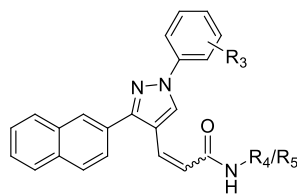
Scheme 2. Synthesis of Compounds GQN-B1 to GQN-B28<sup>a</sup>

<sup>a</sup>Reagents and conditions: (a) EtOH, AcOH, reflux; (b) DMF, POCl<sub>3</sub>, rt; (c) 6, NaH, THF, rt; (d) 1.2 M KOH, MeOH, THF, 50 °C; 2.2 M HCl; (e) L-amino acid methyl ester, HATU, DIPEA, DMF, rt; and (f) 1.2 M KOH, MeOH, THF, 50 °C; 2.2 M HCl. Overall yield of each final product can be found in Section 4.

possesses a carboxylic acid group; second, they offer diverse side chains with various sizes and properties; and third, introducing an amino acid residue as the substitute is synthetically feasible. As result, we synthesized compounds GQN-B1 to GQN-B18

with the methods outlined in Scheme 2. Of the 20 natural  $\alpha$ -amino acids, we successfully obtained corresponding products for all of them except Ala and Cys (Table 1). GQN-B1 to GQN-B18 were subsequently evaluated in our FP-based assay for

Table 1. Chemical Structures and Binding Data of Compounds GQN-B1 to GQN-B28

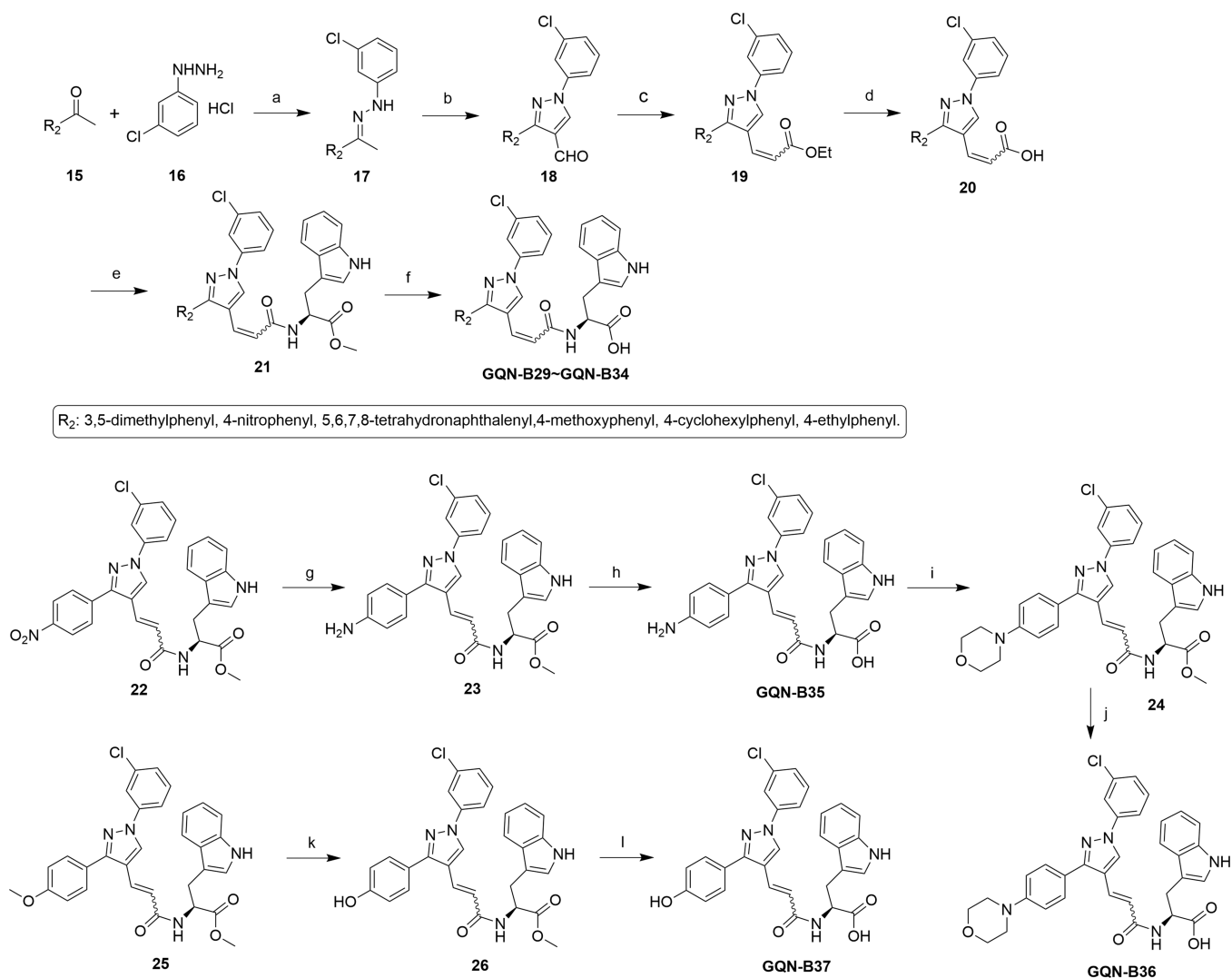


compd	Z/E	R <sub>3</sub>	R <sub>4</sub> /R <sub>5</sub>	inhibition constant ( $K_i$ , $\mu\text{M}$ ) <sup>a</sup>		
				BCL-x <sub>L</sub>	BCL-2	MCL-1
GQN-B1	Z/E	H	Gly-COOH	N.A.	N.A.	N.A.
GQN-B2	Z/E	H	L-Val-COOH	N.A.	N.A.	N.A.
GQN-B3	Z/E	H	L-Leu-COOH	N.A.	N.A.	N.A.
GQN-B4	Z/E	H	L-Ile-COOH	N.A.	N.A.	N.A.
GQN-B5	Z/E	H	L-Ser-COOH	N.A.	N.A.	N.A.
GQN-B6	Z/E	H	L-Thr-COOH	N.A.	N.A.	N.A.
GQN-B7	Z/E	H	L-Met-COOH	N.A.	N.A.	N.A.
GQN-B8	Z/E	H	L-His-COOH	N.A.	N.A.	N.A.
GQN-B9	Z/E	H	L-Asp-COOH	N.A.	N.A.	N.A.
GQN-B10	Z/E	H	L-Asn-COOH	N.A.	N.A.	N.A.
GQN-B11	Z/E	H	L-Glu-COOH	N.A.	N.A.	N.A.
GQN-B12	Z/E	H	L-Gln-COOH	N.A.	N.A.	N.A.
GQN-B13	Z/E	H	L-Lys-COOH	N.A.	N.A.	N.A.
GQN-B14	Z/E	H	L-Arg-COOH	N.A.	N.A.	N.A.
GQN-B15	Z/E	H	L-Pro-COOH	N.A.	N.A.	N.A.
GQN-B16-Z	Z	H	L-Phe-COOH	N.A.	N.A.	N.A.
GQN-B16-E	E	H	L-Phe-COOH	N.A.	weak	5.30 ± 3.80
GQN-B17-Z	Z	H	L-Tyr-COOH	N.A.	N.A.	N.A.
GQN-B17-E	E	H	L-Tyr-COOH	N.A.	N.A.	11.00 ± 3.90
GQN-B18-Z	Z	H	L-Trp-COOH	N.A.	N.A.	N.A.
GQN-B18-E	E	H	L-Trp-COOH	N.A.	5.60 ± 1.10	0.25 ± 0.10
GQN-B18-Me	E	H	L-Trp-COOMe	N.A.	N.A.	N.A.
GQN-B19-Z	Z	3-CH <sub>3</sub>	L-Trp-COOH	N.A.	N.A.	N.A.
GQN-B19-E	E	3-CH <sub>3</sub>	L-Trp-COOH	N.A.	N.A.	0.74 ± 0.09
GQN-B20-Z	Z	3-CH <sub>3</sub>	L-Tyr-COOH	N.A.	N.A.	N.A.
GQN-B20-E	E	3-CH <sub>3</sub>	L-Tyr-COOH	N.A.	16.01 ± 10.10	9.20 ± 2.50
GQN-B21-Z	Z	3-CH <sub>3</sub>	L-Phe-COOH	N.A.	N.A.	6.20 ± 0.58
GQN-B21-E	E	3-CH <sub>3</sub>	L-Phe-COOH	N.A.	N.A.	N.A.
GQN-B22-Z	Z	3-Cl	L-Trp-COOH	17.01 ± 7.20	7.60 ± 0.47	5.30 ± 0.15
GQN-B22-E	E	3-Cl	L-Trp-COOH	N.A.	8.60 ± 1.10	0.64 ± 0.10
GQN-B23-Z	Z	3-Cl	L-Tyr-COOH	N.A.	N.A.	N.A.
GQN-B23-E	E	3-Cl	L-Tyr-COOH	N.A.	8.70 ± 2.02	7.10 ± 0.53
GQN-B24-Z	Z	3-Cl	L-Phe-COOH	N.A.	N.A.	N.A.
GQN-B24-E	E	3-Cl	L-Phe-COOH	N.A.	N.A.	N.A.
GQN-B25-Z	Z	2-CH <sub>3</sub>	L-Trp-COOH	N.A.	N.A.	N.A.
GQN-B25-E	E	2-CH <sub>3</sub>	L-Trp-COOH	N.A.	N.A.	14.02 ± 7.70
GQN-B26-Z	Z	2-CH <sub>3</sub>	L-Tyr-COOH	N.A.	N.A.	N.A.
GQN-B26-E	E	2-CH <sub>3</sub>	L-Tyr-COOH	N.A.	N.A.	N.A.
GQN-B27-Z	Z	2-CH <sub>3</sub>	L-Phe-COOH	N.A.	N.A.	N.A.
GQN-B27-E	E	2-CH <sub>3</sub>	L-Phe-COOH	N.A.	N.A.	N.A.
GQN-B28-Z	Z	4-CH <sub>3</sub>	L-Trp-COOH	N.A.	11.02 ± 3.10	6.50 ± 1.20
GQN-B28-E	E	4-CH <sub>3</sub>	L-Trp-COOH	N.A.	7.51 ± 1.21	2.80 ± 0.62
ABT-199				<0.001	<1.0	N. A.
A1210477				N. A.	N. A.	<0.01

<sup>a</sup>Mean values and standard deviations of inhibition constant were derived from three parallel measurements. N.A., No obvious binding was observed at a dose up to 100  $\mu\text{M}$ .

binding affinity. Notably, the three compounds featuring aromatic amino acid residues (i.e., GQN-B16 to GQN-B18) exhibited binding to MCL-1 with  $K_i$  values below 11  $\mu\text{M}$ . We assume that the aromatic amino acid residues in these three compounds substitute for the benzoic acid moiety in LC126,

which is important for MCL-1 binding. In particular, GQN-B18 achieved a remarkable 50-fold enhancement in binding affinity for MCL-1 ( $K_i = 0.25 \mu\text{M}$ ) as compared to LC126. Furthermore, this compound demonstrated approximately 20-fold selectivity for BCL-2 ( $K_i = 0.25 \mu\text{M}$  versus  $K_i = 5.6 \mu\text{M}$ ). As demonstrated

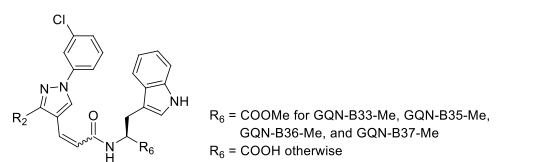
Scheme 3. Synthesis of Compounds GQN-B29 to GQN-B37<sup>a</sup>

<sup>a</sup>Reagents and conditions: (a) EtOH, AcOH, reflux; (b) DMF, POCl<sub>3</sub>, rt; (c) 6, NaH, THF, rt; (d) 1.2 M KOH, MeOH, THF, 50 °C; 2.2 M HCl; (e) *L*-amino acid methyl ester, HATU, DIPEA, DMF, rt; (f) 1.2 M KOH, MeOH, THF, 50 °C; 2.2 M HCl. (g) Fe, NH<sub>4</sub>Cl, MeOH, 80 °C; (h) 1.2 M KOH, MeOH, THF, 50 °C; 2.2 M HCl; (i) DIPEA, DMF, 1-bromo-2-(2-bromoethoxy)ethane, 75 °C; (j) 1.2 M KOH, MeOH, THF, 50 °C; 2.2 M HCl; (k) DCM, BBr<sub>3</sub>, 0 °C; (l) 1.2 M KOH, MeOH, THF, 50 °C; 2.2 M HCl. Overall yield of each final product can be found in Section 4.

in the case of GQN-B18-Me, binding to MCL-1 was totally abolished when the terminal carboxylic acid was esterified. This was consistent with our finding at the first-round optimization.

Note that both LC126 and the derivative compounds that we have synthesized feature a double bond in their chemical structures. Substitution of the double bond in LC126 was determined by our experimental analysis to be in the *cis*-configuration. However, as for GQN-B16 to GQN-B18, we observed binding to MCL-1 only in the case of the *trans*-isomers but not the *cis*-isomers (Table 1). This disparity suggests that the aromatic side chains in these three compounds probably bind within a constrained region in the MCL-1-binding pocket, and thus the double bond in their structure must adopt a certain configuration to maintain the optimal interactions with MCL-1. Moreover, usually the *trans*-isomer of a double bond-containing compound is thermodynamically more stable than the *cis*-isomer. Therefore, the observation that only the *trans*-isomers may be active represents a favorable result of our structural optimization.

The synthetic methods described in Scheme 2 also facilitate the introduction of simple substituents to the phenyl ring attached to the pyrazole core moiety in the LC126 structure. In this context, we selected active compounds discovered during the second-round optimization, namely those containing the Phe, Tyr, or Trp moieties, as templates for synthesis. We attempted to introduce methyl and chloro substituents at various positions on this phenyl ring, resulting in compounds GQN-B19 to GQN-B28 (Table 1). Our FP measurements revealed that when the R<sub>2</sub> group is at the *meta*- or *para*-position of this phenyl ring, such as in GQN-B19-*E*, GQN-B22-*E*, and GQN-B28-*E*, the resulting compounds are more likely to maintain binding to MCL-1 or BCL-2. Conversely, when the R<sub>2</sub> group is at the *ortho*-position, most of the resulting compounds lose their binding for MCL-1 or BCL-2. We postulate that the steric hindrance created by the R<sub>2</sub> group at the *ortho*-position influences the relative orientation of this phenyl ring required for binding. The most potent compound out of this round of synthesis was GQN-B22-*E* ( $K_i = 0.64 \mu\text{M}$  for MCL-1 and  $K_i =$

**Table 2. Chemical Structures and Binding Data of Compounds GQN-B29 to GQN-B37**


Compd	Z/E	R <sub>2</sub>	Inhibition constant ( $K_i$ , $\mu\text{M}$ ) <sup>a</sup>		
			BCL-X <sub>L</sub>	BCL-2	MCL-1
GQN-B29-Z	Z		N.A.	N.A.	N.A.
GQN-B29-E	E		N.A.	N.A.	4.80 ± 1.80
GQN-B30-Z	Z		N.A.	N.A.	13.01 ± 2.30
GQN-B30-E	E		N.A.	13.00 ± 1.20	3.30 ± 1.10
GQN-B31-Z	Z		8.60 ± 4.70	9.40 ± 1.60	3.40 ± 0.81
GQN-B31-E	E		N.A.	N.A.	N.A.
GQN-B32-Z	Z		N.A.	N.A.	N.A.
GQN-B32-E	E		N.A.	N.A.	0.70 ± 0.20
GQN-B33-Z	Z		0.85 ± 0.13	3.00 ± 0.25	1.30 ± 0.29
GQN-B33-E	E		N.A.	1.50 ± 0.21	0.41 ± 0.19
GQN-B33-Me	E		N.A.	N.A.	N.A.
GQN-B34-Z	Z		N.A.	N.A.	12.01 ± 4.20
GQN-B34-E	E		N.A.	5.70 ± 1.80	N.A.
GQN-B35-Z	Z		N.A.	N.A.	N.A.
GQN-B35-E	E		N.A.	N.A.	4.80 ± 3.80
GQN-B35-Me	E		N.A.	N.A.	N.A.
GQN-B36-Z	Z		N.A.	N.A.	N.A.
GQN-B36-E	E		N.A.	N.A.	1.60 ± 0.85
GQN-B36-Me	E		N.A.	N.A.	N.A.
GQN-B37-Z	Z		N.A.	N.A.	N.A.
GQN-B37-E	E		N.A.	N.A.	0.60 ± 0.13
GQN-B37-Me	E		N.A.	N.A.	N.A.

**Table 2. continued**

<sup>a</sup>Mean values and standard deviations of inhibition constant were derived from three parallel measurements. N.A., no obvious binding was observed at a dose up to 100  $\mu\text{M}$ .

8.60  $\mu\text{M}$  for BCL-2). Notably, its binding affinity for MCL-1 is rather close to that of GQN-B18-E ( $K_i = 0.25 \mu\text{M}$ ).

In our third round of structural optimization, our goal was to replace the naphthyl moiety in compound GQN-B22 with other cyclic moieties. By using the synthetic methods outlined in Scheme 3, we obtained compounds GQN-B29 to GQN-B37 (Table 2). Our FP measurements indicated that the introduced cyclic R<sub>2</sub> group in these compounds plays a more subtle role in influencing their binding affinity and selectivity. In comparison to the original naphthyl moiety, it appears that a bulkier group introduced here results in compounds that bind to both MCL-1 and BCL-2, such as GQN-B31 and GQN-B33. Conversely, a smaller group enhances selectivity for MCL-1, as observed in the cases of GQN-B29, GQN-B32, GQN-B35, and GQN-B37. In fact, these particular compounds exhibit binding exclusively to MCL-1, with no sign of binding to BCL-2 or BCL-X<sub>L</sub>.

A total of 73 new compounds were synthesized in our three rounds of structural optimization. In order to evaluate the drug-likeness of these compounds, we applied the pan-assay interference compounds (PAINS) filters proposed by Baell et al.<sup>46</sup> (as implemented in the RDKit software package, version 2020.09.05) to examine their structures. Our result indicate that none of them falls in the category of PAINS.

### 2.3. Derivation of the Binding Mode of GQN-B37-E.

Among the newly synthesized compounds, GQN-B37-E is the most potent selective binder to MCL-1 ( $K_i = 0.60 \mu\text{M}$ , Figure 2). To understand the interaction of this compound with MCL-1, we conducted 1  $\mu\text{s}$  long molecular dynamics (MD) simulations to elucidate its binding mode. This result is depicted in Figure 3C. A notable feature observed in this binding mode is the formation of chelated hydrogen bonds between the terminal carboxylic acid group on the tryptophan moiety of GQN-B37-E and the Arg263 residue on MCL-1. This interaction pattern is pivotal for maintaining the binding of GQN-B37-E, as well as other analogous compounds listed in Tables 1 and 2, because esterification of this carboxylic acid group leads to a complete loss of binding, such as in the cases of GQN-B18-Me and GQN-B37-Me. The carboxylic acid group in LC126 is also essential for its binding to MCL-1. However, a comparison of the binding modes of LC126 and GQN-B37-E (Figure 3A vs C) reveals that the carboxylic acid group in the latter case is positioned more optimally to interact with the Arg263 residue. The side chain of the tryptophan moiety on GQN-B37-E is nestled within the P3 subpocket, forming a potential  $\pi$ -stacking interaction with the adjacent Phe270 residue on MCL-1. In contrast, the P3 subpocket is largely vacant in the case of LC126. Notably, a significant disparity between the binding pockets of MCL-1 and BCL-2 is evident at the P3 subpocket (Figure S2 in the Supporting Information). This distinction may account for the selective binding of GQN-B37-E to MCL-1. Concerning the P2 subpocket, the 3-chlorophenyl moiety on GQN-B37-E occupies this cavity, resembling the role played by the naphthyl moiety on LC126. Importantly, the trans-configuration of the double bond in GQN-B37-E is essential for maintaining a suitable conformation to simultaneously accommodate the three features mentioned here.



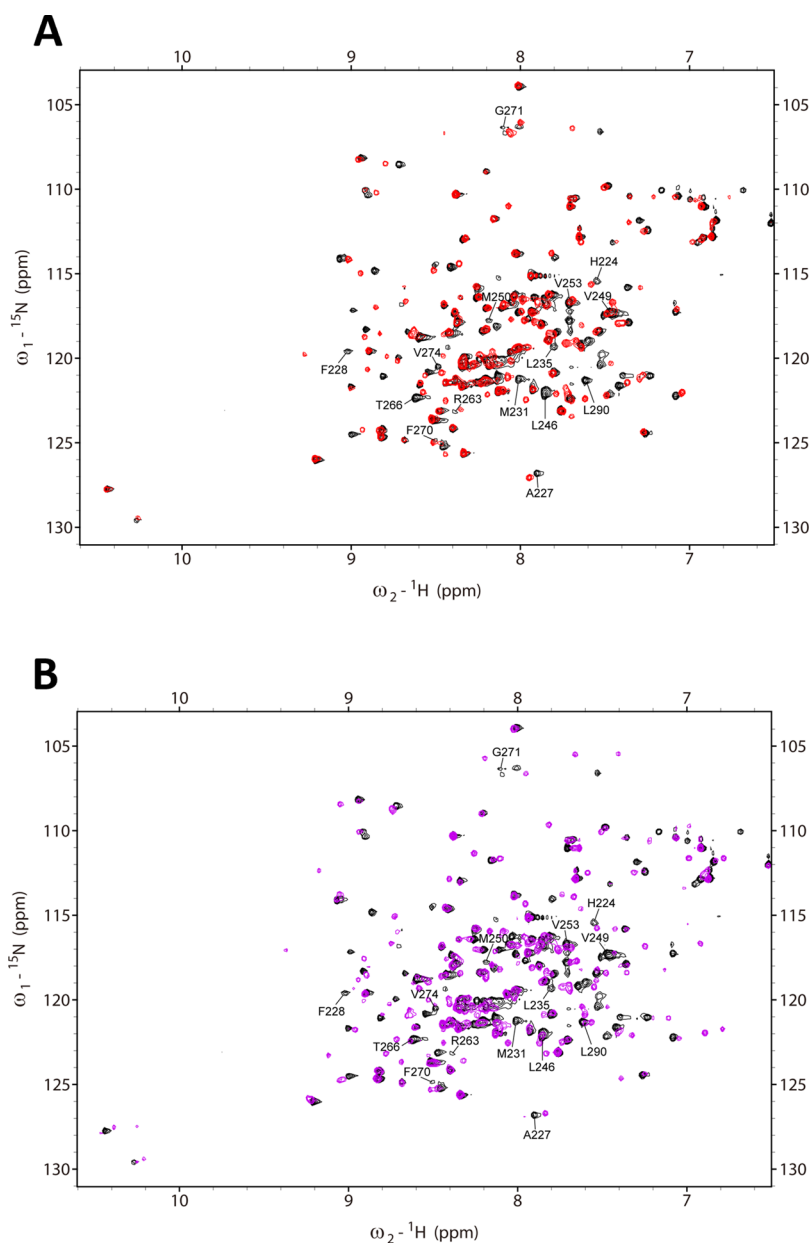


**Figure 4.**  $^{15}\text{N}$  HSQC spectra of free MCL-1 (in black) superimposed with that of MCL-1 in complex with (A) GQN-B37-*E* (in red) or (B) AZD5991 (in purple). The residues around the BH3-domain-binding pocket in MCL-1 that exhibits altered chemical shifts after ligand binding are explicitly labeled.

We also utilized  $^{15}\text{N}$ -heteronuclear single-quantum coherence (HSQC) spectroscopy to validate the predicted binding mode of GQN-B37-*E* discussed above. In addition to GQN-B37-*E*, a known selective MCL-1 inhibitor AZD5991 (Figure 1) was also tested in this experiment as the reference. The  $^1\text{H}$ - $^{15}\text{N}$  HSQC spectra of MCL-1 in complex with these two compounds are presented in Figure 4. First, it is evident that the overall HSQC spectrum of GQN-B37-*E* closely resembles that of AZD5991. Furthermore, the residues displaying significant changes in chemical shifts upon ligand binding are also remarkably similar in both cases. Among them include the crucial Arg263 residue, Leu235, Val249, Leu246 at the P1 subpocket, Met231, Met250, Val253, Phe270, Gly271, Val274, Leu290 at the P2 subpocket, and His224, Ala227, Phe228, Thr266 around the P3 subpocket (see Figure S2 in the Supporting Information for reference). While the outcomes of this  $^1\text{H}$ - $^{15}\text{N}$  HSQC experiment do not

reveal details at atomic resolution, they do confirm that GQN-B37-*E* binds to the BH3-domain-binding pocket in MCL-1 as anticipated. Consequently, its binding modes derived through meticulous molecular modeling is highly credible.

**2.4. Cytotoxicity on Cancer Cells.** We then selected several compounds with the highest binding affinity for MCL-1, including GQN-B18-*E*, GQN-B33-*E*, GQN-B35-*E*, GQN-B36-*E*, and GQN-B37-*E*. These compounds were tested for cytotoxicity in the range of cancer cell lines, including H929, MV-4-11, RS;411, HL-60, HeLa, and HEK293T, utilizing the CCK-8 cell viability assay. Here, AZD5991 and A1210477 served as the positive controls. Results are summarized in Table 3. It is evident that when the carboxyl acid group in their structure was masked through esterification, compounds such as GQN-B37-*Me* exhibited noteworthy cytotoxicity, particularly against H929 (plasmacytoma myeloma) or MV-4-11 (acute

Table 3. Cytotoxicity of Selected Compounds on Several Cancer Cell Lines

compd	cytotoxicity (IC <sub>50</sub> , μM) <sup>a</sup>					
	H929	MV-4–11	RS4;11	HL-60	HeLa	HEK293T
GQN-B18-Me	7.97 ± 1.01	>20	>20	>20	>20	>20
GQN-B18-E	>50	>50	>20	>20	>50	>20
GQN-B33-Me	4.64 ± 0.01	>20	>20	>50	>50	>20
GQN-B33-E	>50	>20	>20	>50	>50	>20
GQN-B35-Me	3.89 ± 0.07	20.52 ± 0.12	>20	>20	>50	>20
GQN-B35-E	>50	>50	>50	>50	>50	>20
GQN-B36-Me	>20	>20	>20	>20	>50	>20
GQN-B36-E	>50	>50	>50	>50	>50	>20
GQN-B37-Me	3.71 ± 0.33	5.57 ± 0.09	15.92 ± 0.98	>20	>20	>20
GQN-B37-E	>50	>50	>50	>50	>50	>20
A1210477	1.43 ± 0.06	0.34 ± 0.01	>20	2.46 ± 0.21	>20	>20
AZD5991	0.05 ± 0.01	<0.01				>20

<sup>a</sup>Mean values and standard deviations of IC<sub>50</sub> values were derived from three parallel measurements.

myeloid leukemia) cells, with an IC<sub>50</sub> value at the micromolar range. In contrast, cytotoxicity was basically diminished (IC<sub>50</sub> > 20 μM) when the carboxylic acid group was exposed. We hypothesize that the carboxylate form was not cell permeable but was important for maintaining the compounds' binding to MCL-1. The cytotoxic effect of these esterified compounds is likely achieved through ester hydrolysis after entering the cell, leading to the formation of the carboxylate form. This mechanism aligns with a common mechanism among some known prodrugs.

To verify this hypothesis, we selected GQN-B37-Me, the most potent compound identified in the cytotoxicity assay, and performed a kinetics assay to monitor its distribution in MV-4–11 cells over an 8 h period. The results are illustrated in Figure 5.

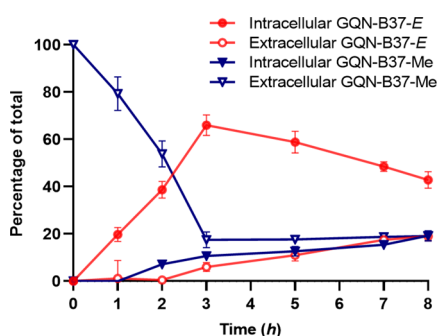


**Figure 5.** Partition of GQN-B37-Me and GQN-B37-E in cells measured by a kinetics assay. Here, GQN-B37-Me was given to MV-4–11 cell cultures in a total concentration of 40 μM. Then, the weight percentages of extracellular and intracellular GQN-B37-Me and GQN-B37-E were determined at a set of time points.

Initially, no GQN-B37-E, the bioactive form, was present. However, as the incubation of GQN-B37-Me with the cells continued, the amount of extracellular GQN-B37-Me diminished rapidly, while the amount of intracellular GQN-B37-E increased rapidly. Although a minor fraction of intracellular GQN-B37-Me was also observable, most GQN-B37-Me that entered the cells had been converted into GQN-B37-E. By the 3 h mark, the intracellular GQN-B37-E reached a peak because some cells had already undergone apoptosis. This explains the detection of extracellular GQN-B37-E at this point. These findings validate our hypothesis, emphasizing the importance of

considering our compounds in the esterified form for subsequent cellular and in vivo assays.

**2.5. Investigation of the Mechanism of Action for GQN-B37-Me.** Subsequently, we attempted to elucidate the mechanism of action for GQN-B37-Me in cells. First, we employed flow cytometry analysis with annexin V and propidium iodide (PI) double-staining to discern cell apoptosis induced by GQN-B37-Me. The results are illustrated in Figures 6 and S5 in the Supporting Information. The combination of annexin V and PI enables distinction between cells in early apoptosis [annexin V (+) and PI (–)] and late apoptosis [annexin V (+) and PI (+)], corresponding to the lower left and upper right regions in these two figures. Here, A1210477 and AZD5991 were tested as positive controls. At an equivalent dose of 1 μM, AZD5991 caused more late apoptosis (~75%) compared to A1210477 (~10%), which is consistent with the findings from our cytotoxicity assay. In this experiment, GQN-B37-Me was incubated with H929 cells at five different doses ranging from 1 to 40 μM. While GQN-B37-Me was less potent than AZD5991, it induced late apoptosis in a clear dose-dependent manner.

Then, we investigated the activation of poly-ADP-ribose polymerase protein (PARP) and caspase-3 in live cells induced by GQN-B37-Me. In this Western blot assay, H929 cells were incubated with GQN-B37-Me at four doses ranging from 5 to 40 μM, and the outcomes are shown in Figure 7. PARP, a principal substrate of activated caspases, undergoes cleavage as an indicative marker of caspase-dependent apoptosis. It is evident from our results that GQN-B37-Me induced a dose-dependent cleavage of full-length PARP (116 to 89 kDa). A similar pattern is also observed in the cleavage of full-length caspase-3 with the treatment of GQN-B37-Me. Complemented by the outcome from the flow cytometry analysis, our experimental findings affirm the efficacy of GQN-B37-Me in inducing caspase-dependent apoptosis.

To elucidate the potential molecular target of our compound in cells, we conducted a coimmunoprecipitation (co-IP) assay using H929 cells, which exhibit a high expression level of MCL-1. AZD5991 again served as the positive control in this assay, and the results are shown in Figure 8. Notably, at a dose of 10 μM, GQN-B37-Me already disrupts the MCL-1/BIM interaction considerably, with this effect becoming more pronounced at higher doses of GQN-B37-Me. Consequently, our experimental findings suggest that GQN-B37-Me is able to block the MCL-1/BIM interaction in cells and consequently induces

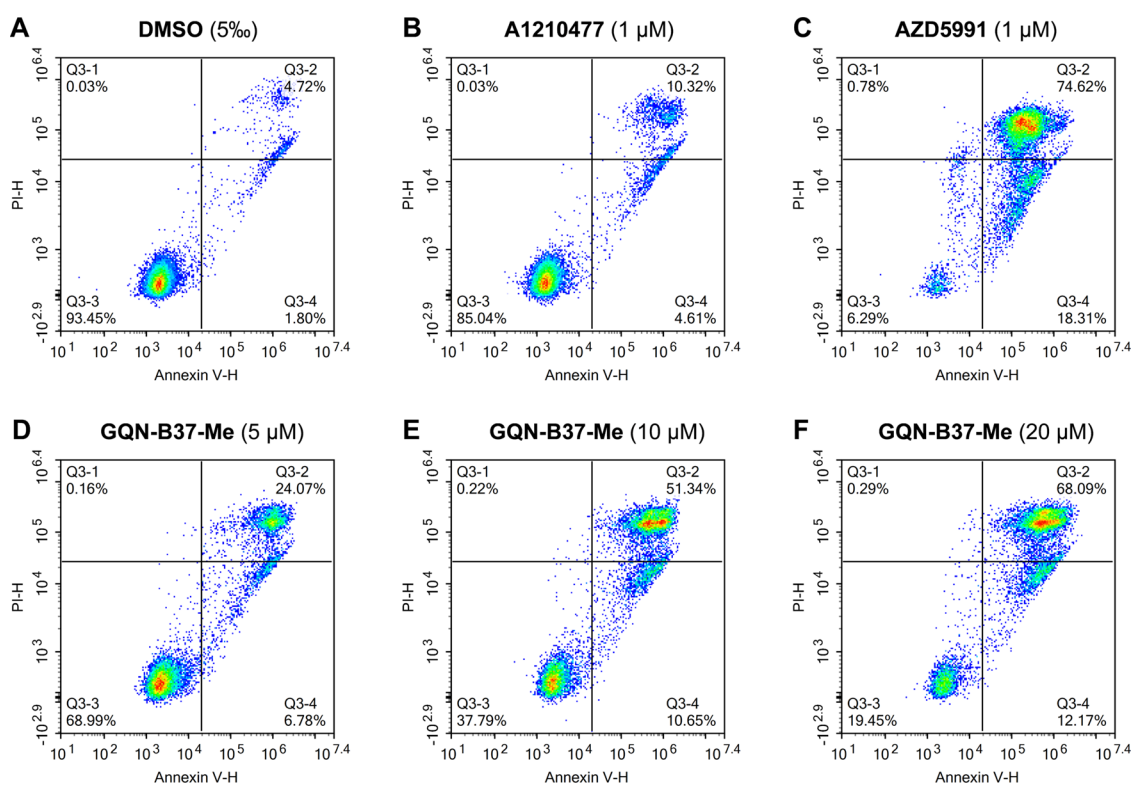


**Figure 6.** Results of the annexin V and PI double-staining flow cytometry experiment for (A) DMSO; (B) A1210477; (C) AZD5991; and (D)(E)(F) GQN-B37-Me. Here, MV-4-11 cells were incubated with the tested compounds for 24 h.

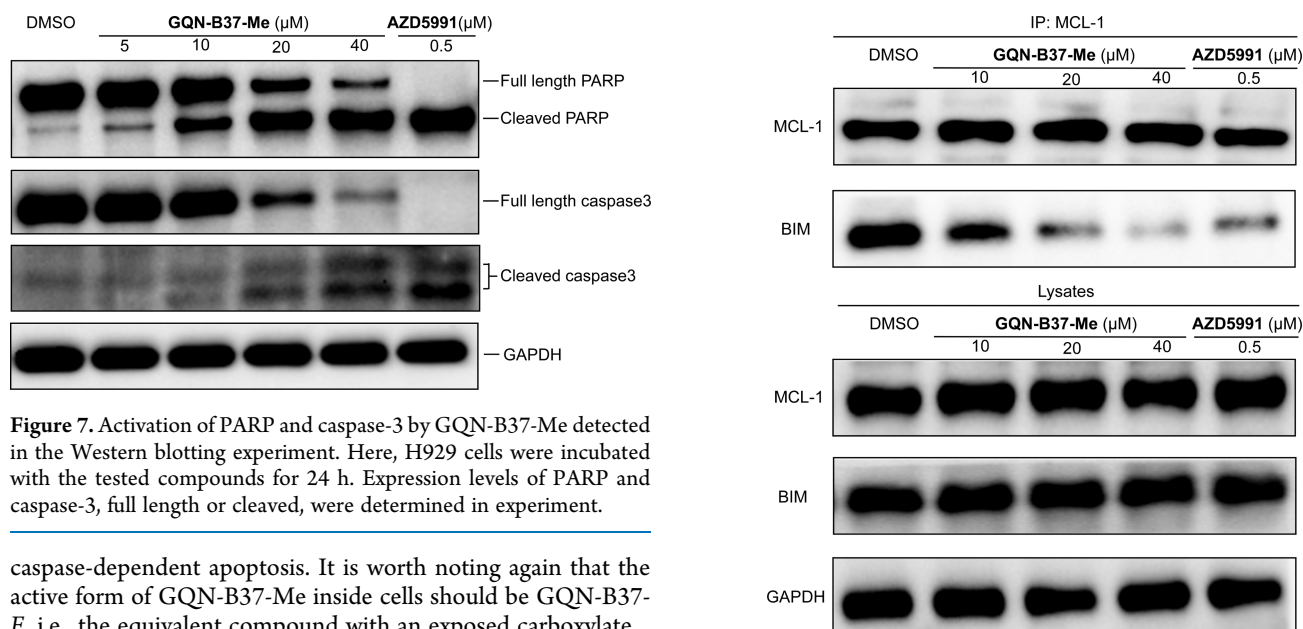


**Figure 7.** Activation of PARP and caspase-3 by GQN-B37-Me detected in the Western blotting experiment. Here, H929 cells were incubated with the tested compounds for 24 h. Expression levels of PARP and caspase-3, full length or cleaved, were determined in experiment.

caspase-dependent apoptosis. It is worth noting again that the active form of GQN-B37-Me inside cells should be GQN-B37-E, i.e., the equivalent compound with an exposed carboxylate.

**2.6. Antitumor Efficacy of GQN-B37-Me in a Xenograft Mouse Leukemia Model.** Our cellular assay indicated that MV-4-11 cells are responsive to GQN-B37-Me treatment. Additionally, MV-4-11 is a widely chosen model for evaluating antileukemia drug candidates. Consequently, we employed the MV-4-11 xenograft mouse model to assess the antitumor efficacy of GQN-B37-Me. The xenograft mice were treated with GQN-B37-Me at a low dose of 12.5 mg/kg and a high dose of 50 mg/kg, respectively, via intraperitoneal injection every 2 days over a 20 day period. In this experiment, we chose AZD5991, a selective MCL-1 inhibitor that has entered clinical trials, as the positive reference.

**Figure 8.** Result of the coimmunoprecipitation assay in cells for GQN-B37-Me. Here, H929 cells were incubated with the tested compounds for 10 h. The cell lysates were incubated with the MCL-1 antibody and protein A/G magnetic beads, and then the immunoprecipitated fractions of MCL-1 and BIM were analyzed by immunoblotting.

As depicted in Figure 9A, treatment with AZD5991 at 10 mg/kg caused 56% tumor growth inhibition on day 20. In the case of GQN-B37-Me, the low-dose group (12.5 mg/kg) caused 30% tumor growth inhibition on day 20, while the high-dose group (50 mg/kg) caused 43% tumor growth inhibition at the same

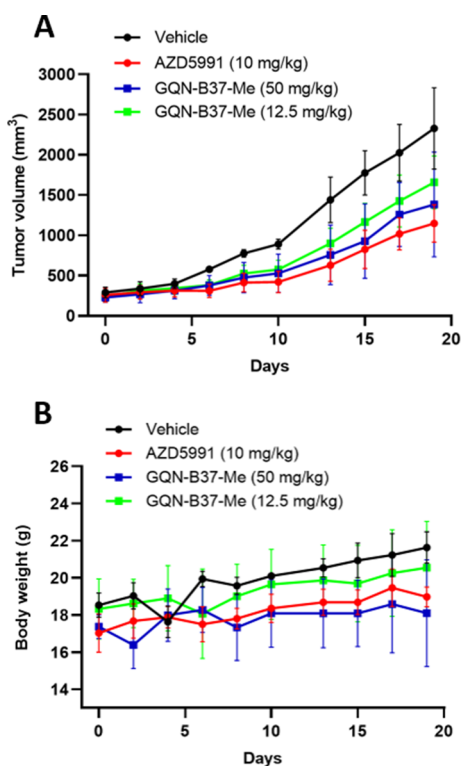


**Figure 9.** Evaluation of antitumor efficacy and weight change of GQN-B37-Me in the MV-4-11 xenograft mouse model. (A) Changes in the tumor volume. (B) Changes in body weight of the xenograft mice. Here, the xenograft mice were intraperitoneally treated with vehicle, AZD5991, or GQN-B37-Me at the indicated doses every 2 days for 20 days.

time point. We have computed the  $p$  value between the tumor volumes after 20 days' treatment for vehicle vs AZD5991, vehicle vs GQN-B37-Me (50 mg/kg), and vehicle vs GQN-B37-Me (12.5 mg/kg). The results are  $p = 0.004$  for vehicle vs AZD5991,  $p = 0.027$  for vehicle vs GQN-B37-Me (50 mg/kg), and  $p = 0.076$  vehicle vs GQN-B37-Me (12.5 mg/kg). Thus, significant difference is observed in all three pairs at the 90% confidence level. This analysis indicates that treatment of GQN-B37-Me led to significant reduction in tumor volume at the low dose as well as the high dose.

Furthermore, body weights of the xenograft mice were monitored over the period of 20 days (Figure 9B). We also computed the  $p$  value between the body weights after 20 days' treatment for vehicle vs AZD5991, vehicle vs GQN-B37-Me (50 mg/kg), and vehicle vs GQN-B37-Me (12.5 mg/kg). The results are  $p = 0.001$  for vehicle vs AZD5991,  $p = 0.090$  for vehicle vs GQN-B37-Me (50 mg/kg), and  $p = 0.492$  vehicle vs GQN-B37-Me (12.5 mg/kg). This analysis indicates that at the 90% confidence level, AZD5991 certainly caused significant body weight loss at the dose of 10 mg/kg, whereas GQN-B37-Me also affected body weight at the dose of 50 mg/kg, but it did not cause significant body weight loss at the dose of 12.5 mg/kg. Thus, it is fair to conclude that GQN-B37-Me is generally safer than AZD5991 in this test.

Next, we assessed the toxicity, antiproliferative effects, and apoptosis caused by GQN-B37-Me in MV-4-11 xenograft mice using histological and immunohistochemical staining. Hematoxylin-eosin (HE) staining revealed dose-dependent necrosis of tumor tissues by GQN-B37-Me, with no evidence of lesions in other organs such as the liver, kidney, and heart (Figure 10A).

The level of proliferation in tumor tissues, as indicated by the amount of the proliferation-associated antigen detected by the  $K_i$ -67 antibody, was significantly reduced following GQN-B37-Me treatment compared to the blank group (Figure 10B). The antitumor efficacy of GQN-B37-Me was directly associated with the level of cleaved PARP, indicating induced apoptosis in tumor cells (Figure 10C). These observations further affirm that GQN-B37-Me elicits in vivo antitumor effect by inducing apoptosis while still maintaining the desired level of safety.

**2.7. In Vitro Stability of GQN-B37-Me.** To evaluate the in vitro stability of GQN-B37-Me, we utilized a glutathione (GSH)-based assay, exposing GQN-B37-Me to GSH for up to 2 h. The results are presented in Figure S6 in the Supporting Information. One can see that GQN-B37-Me was basically intact following incubation with GSH. Furthermore, GQN-B37-Me was incubated with liver microsomes from humans (HLM), dogs (DLM), rats (RLM), and monkeys (MLM), respectively, for 1 h, and the residual amount was quantified through LC-MS/MS analysis. The results are presented in Figure S7 in the Supporting Information. Half-life times ( $T_{1/2}$ ) of GQN-B37-Me were determined to be 0.77, 1.93, 1.92, and 0.58 h in HLM, DLM, RLM, and MLM, respectively. Collectively, these results suggest that GQN-B37-Me has reasonable metabolic stability in vitro. We hope that this stability could translate into in vivo conditions, thereby enhancing the potential of GQN-B37-Me as a promising preclinical candidate.

### 3. CONCLUSIONS

Only a handful of MCL-1 inhibitors have entered clinical trial so far, but none of them has successfully passed the phase II trial. Therefore, a wider range of chemotypes still need to be explored to provide new candidates. In this study, we have developed a new class of MCL-1 inhibitors with in vivo antitumor activity. The starting point, LC126, was identified among over 600 compounds selected through virtual screening. This compound actually exhibited comparable binding affinity for MCL-1 ( $K_i = 13 \mu\text{M}$ ) and BCL-2 ( $K_i = 10 \mu\text{M}$ ). Guided by the predicted binding mode of LC126, our structural optimization underwent three rounds, in which a total of 73 new compounds were synthesized. A remarkable effort was to incorporate an amino acid moiety in order to disrupt the planar structural scaffold of LC126. Interestingly, this modification not only increased the binding affinity of the resulting compounds for MCL-1 but also resulted in a remarkable selectivity for MCL-1. For example, the representative compound GQN-B37-E exhibited a submicromolar affinity to MCL-1 ( $K_i = 0.6 \mu\text{M}$ ) without apparent binding to BCL-2 or BCL-X<sub>L</sub>. If computing the ligand efficiency (LE) value as binding energy divided by the number of heavy atoms, the LE value for LC126 is 0.19 kcal/mol, while the LE value for GQN-B37-E is 0.22 kcal/mol. One can see that our structural optimization of LC126 indeed resulted in an improved ligand efficiency.

We then conducted a set of cellular assays to explore the mechanism of action for GQN-B37-E and several other compounds. Our results revealed that GQN-B37-Me, the precursor of GQN-B37-E, is particularly effective on certain leukemia cells, such as H929 and MV-4-11. At micromolar concentration, GQN-B37-Me induced caspase-dependent apoptosis. Its interaction with MCL-1 in cells was confirmed by coimmunoprecipitation experiment. Administration of GQN-B37-Me to MV-4-11 xenograft mice at 12.5 and 50 mg/kg every 2 days for 20 days caused 30 to 43% tumor growth inhibition. HE staining revealed dose-dependent antiprolifera-

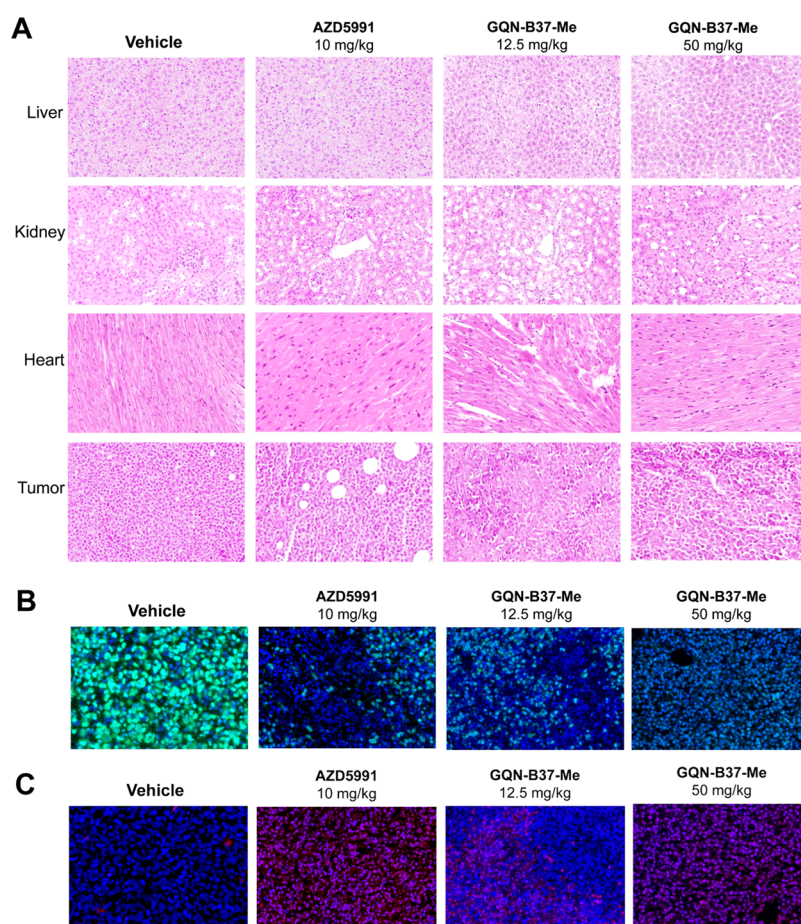


**Figure 10.** (A) HE staining images of the liver, kidney, heart, and tumor after treatment with AZD5991 or GQN-B37-Me after 20 days. (B) Staining images of K<sub>I</sub>-67 and (C) cleaved PARP of tumor tissues after treatment with AZD5991 or GQN-B37-Me for 20 days. Here, fluorescence signal is shown alone (blue), merged with the K<sub>I</sub>-67 stain (green), or merged with the cleaved PARP stain (red).

tion and apoptosis effects caused by GQN-B37-Me with no evidence of lesions in major organs such as the liver, kidney, and heart. Although these *in vivo* evaluations are still preliminary, our results affirm that GQN-B37-Me elicits antitumor activity while maintaining a good level of safety. We also demonstrated that GQN-B37-Me exhibits reasonable *in vitro* stability in GSH and liver microsomes from several species. Collectively, this class of MCL-1 inhibitors provides a new possibility for developing preclinical candidates for treating leukemia.

## 4. EXPERIMENTAL SECTION

**4.1. Chemistry General Procedures.** Synthesis of the new compounds described in this study is shown in Schemes 1–3. All reagents and starting materials used in our synthesis were purchased from commercial suppliers without further purification unless noted. Reactions were monitored by thin-layer chromatography (TLC) and analyzed by UV light and by LC–MS. The <sup>1</sup>H NMR and <sup>13</sup>C NMR spectra were recorded in CDCl<sub>3</sub>, Methanol-d<sub>4</sub> or DMSO-d<sub>6</sub> on a 400 or 600 MHz Ascend Bruker spectrometer in  $\delta$  values in parts per million (ppm) as chemical shifts reported. NMR data are reported as follows: chemical shift, multiplicity (*s* = singlet, *d* = doublet, *t* = triplet, *q* = quartet, *br* = broad, *m* = multiplet), integration, coupling constant (Hz). Low-resolution mass spectra were obtained on an Agilent 1200 series 6140 mass spectrometer with electrospray ionization. High-resolution mass spectrometry (HRMS) was performed on an AB SCIEX TripleTOF 5600+ mass

spectrometer or Micromass Ultra Q-TOF spectrometer. All final compounds were of  $\geq 95.0\%$  purity analyzed on the analytical Agilent 1260 series HPLC with an Agilent Zorbax Eclipse Plus-C18 (4.6  $\times$  150 mm, 5  $\mu$ M) reversed-phase column at 1 mL/min flow monitored by UV absorption at 254 nm using 0.1% trifluoroacetic acid in water (A) and 0.1% trifluoroacetic acid in methanol (B) as a mobile phase.

The synthetic methods shown in Scheme 1 are as follows: a mixture solution of 1-(naphthalen-2-yl)ethan-1-one **1** (3.54 g, 20.81 mmol) and phenylhydrazine **2** (2.7 g, 24.97 mmol) in EtOH (100 mL) containing 0.5 mL of AcOH were refluxed for 5 h to obtain product **3**. **3** (2.18 g, 8.39 mmol) was added with POCl<sub>3</sub> (2.34 mL, 25.17 mmol) to DMF (40 mL) in an ice-water bath, and then the mixture was stirred at room temperature overnight to obtain **4**. To obtain **6**, ethyl-2-bromoacetate (9.27 g, 55.54 mmol) was added dropwise to a mixture of **5** (10 g, 42.72 mmol), Et<sub>3</sub>N (7.72 mL, 55.54 mmol), and dry DCM (100 mL), and then was stirred at room temperature for 8 h. To a solution of **4** (2 g, 4.01 mmol) in dry THF (40 mL) at room temperature, sodium hydride (221.04 mg, 9.21 mmol) and **6** (1.92 g, 6.01 mmol) were added in turn and stirred overnight to obtain **7**. Two mL of NaOH (2 M) was added to a solution of **7** (471.23 mg, 1.28 mmol) in MeOH/THF (5 mL/5 mL) and was stirred at 50 °C for 2 h. After completion of the reaction, the mixture was quenched to pH 2 with 2 M hydrochloric acid to produce the hydrolysis product **8**. A mixture of **8** (67.34 mg, 0.198 mmol), 1.2 equiv of fatty amine

or aromatic amine, HATU (90.11 mg, 0.237 mmol), and DIPEA (90.71  $\mu$ L, 0.549 mmol) was stirred in DMF (10 mL) at room temperature overnight. The resulting mixture was extracted with EtOAc (3  $\times$  10 mL), dried over Na<sub>2</sub>SO<sub>4</sub>, filtered, and then concentrated under a reduced pressure. The residue was purified by flash silica chromatography (petroleum ether/ethyl acetate = 2:1 v/v) to obtain the final products, including LC126 and GQN-A1 to GQN-A9.

The synthetic methods shown in Scheme 2 are as follows: 1-(naphthalen-2-yl)ethan-1-one **1** (3.54 g, 20.81 mmol) and 1.2 equiv of phenylhydrazine derivatives **9** in EtOH (100 mL) containing 0.5 mL of AcOH were refluxed for 5 h to obtain **10**. Employing the same reaction conditions as Scheme 1, the residue was purified by flash silica chromatography (petroleum ether/ethyl acetate = 2:1 v/v) to obtain the final products, including GQN-B1 to GQN-B28.

The synthetic methods shown in Scheme 3 are as follows: (3-chlorophenyl)hydrazine hydrochloride **16** (4.7 g, 24.97 mmol) and 0.9 equiv of benzaldehyde derivatives **15** in EtOH (100 mL) containing 0.5 mL of AcOH were refluxed for 5 h to obtain **17**. Employing the same reaction conditions as in Schemes 1 and 2, the residue was purified by flash silica chromatography (petroleum ether/ethyl acetate = 2:1 v/v) to obtain the final products, including GQN-B29 to GQN-B34. Besides, a saturated solution of NH<sub>4</sub>Cl (8.02 mg, 0.15 mmol) was added to a mixture of **22** (28.26 mg, 0.05 mmol) and iron (14 mg, 0.25 mmol) in MeOH (8 mL) and heated to 80 °C for 5 h. Iron was then filtered out with diatomaceous earth. The resulting mixture was extracted with DCM (3  $\times$  10 mL), dried over Na<sub>2</sub>SO<sub>4</sub>, filtered, and concentrated under a reduced pressure. The residue was purified by flash silica chromatography (petroleum ether/ethyl acetate = 1:1 v/v) to obtain GQN-B35. 1-bromo-2-(2-bromoethoxy)ethane (30.15 mg, 0.13 mmol) was added to a mixture of **23** (53.92 mg, 0.1 mmol) and DIPEA (0.3 mmol) in dry DMF (8 mL) under Argon gas and heated to 75 °C for 6 h. The resulting mixture was extracted with EtOAc (3  $\times$  10 mL), dried over Na<sub>2</sub>SO<sub>4</sub>, filtered, and concentrated under a reduced pressure. The residue was purified by flash silica chromatography (petroleum ether/ethyl acetate = 1:1 v/v) to obtain GQN-B36. BBr<sub>3</sub> (5 mL) was added dropwise to a mixture of **25** (55.41 mg, 0.1 mmol) and DCM (5 mL) in an ice-water bath. The mixture was stirred for 5 h at room temperature. The mixture was then quenched with MeOH, and purified by flash silica chromatography (DMC/MeOH = 20:1 v/v) to obtain GQN-B37.

**4.1.1. (Z)-4-(3-(3-(Naphthalen-2-yl)-1-phenyl-1H-pyrazol-4-yl)acrylamido)benzoic Acid (LC126).** Yield: 80%, purity: 96%. <sup>1</sup>H NMR (400 MHz, acetone-*d*<sub>6</sub>)  $\delta$  9.80 (s, 1H), 9.65 (s, 1H), 8.18 (s, 1H), 8.04 (t, *J* = 8.3 Hz, 4H), 7.98 (d, *J* = 7.7 Hz, 3H), 7.92 (d, *J* = 8.7 Hz, 2H), 7.87 (dd, *J* = 8.4, 1.5 Hz, 1H), 7.59 (dd, *J* = 12.8, 6.4 Hz, 4H), 7.41 (t, *J* = 7.4 Hz, 1H), 6.99 (d, *J* = 12.5 Hz, 1H), 6.18 (d, *J* = 12.5 Hz, 1H). <sup>13</sup>C NMR (126 MHz, acetone-*d*<sub>6</sub>)  $\delta$  167.18, 165.71, 155.31, 144.60, 140.78, 134.26, 134.14, 132.51, 132.45, 131.56, 131.08, 130.54, 129.26, 129.18, 129.07, 128.61, 127.81, 127.74, 127.42, 127.38, 120.35, 119.94, 119.50, 117.37. ESI-MS: *m/z* 482.2 [M + Na]<sup>+</sup>, ESI-HRMS: calcd for C<sub>29</sub>H<sub>21</sub>N<sub>3</sub>NaO [M + Na]<sup>+</sup> 482.1472, found 482.1475.

**4.1.1.1. (Z)-3-(3-(Naphthalen-2-yl)-1-phenyl-1H-pyrazol-4-yl)-N-(quinolin-8-yl)acrylamide (GQN-A1).** Yield: 99%, purity: 99%. <sup>1</sup>H NMR (500 MHz, CDCl<sub>3</sub>)  $\delta$  10.04 (s, 1H), 9.50 (s, 1H), 8.96 (d, *J* = 7.4 Hz, 1H), 8.77 (dd, *J* = 4.2, 1.6 Hz, 1H), 8.18–8.11 (m, 2H), 7.97 (d, *J* = 8.5 Hz, 1H), 7.96–7.93 (m, 1H), 7.91 (d, *J* = 5.2 Hz, 1H), 7.90–7.85 (m, 3H), 7.59 (t, *J*

= 7.9 Hz, 1H), 7.55–7.53 (m, 2H), 7.52 (dd, *J* = 8.3, 1.1 Hz, 1H), 7.50–7.46 (m, 2H), 7.42 (dd, *J* = 8.2, 4.2 Hz, 1H), 7.33 (t, *J* = 7.4 Hz, 1H), 6.97 (d, *J* = 12.4 Hz, 1H), 6.16 (d, *J* = 12.5 Hz, 1H). <sup>13</sup>C NMR (126 MHz, CDCl<sub>3</sub>)  $\delta$  164.85, 154.94, 148.26, 139.95, 138.57, 136.45, 134.91, 133.39, 133.28, 131.86, 131.82, 130.10, 129.48, 128.71, 128.44, 128.36, 128.12, 127.87, 127.52, 127.11, 126.96, 126.51, 126.46, 121.74, 121.65, 119.78, 116.48, 116.41. ESI-MS: *m/z* 467.2 [M + H]<sup>+</sup>, ESI-HRMS: calcd for C<sub>31</sub>H<sub>23</sub>N<sub>4</sub>O [M + H]<sup>+</sup> 467.1866, found 467.1871.

**4.1.1.2. (Z)-N-(2-(Dimethylamino)ethyl)-N-methyl-3-(3-(naphthalen-2-yl)-1-phenyl-1H-pyrazol-4-yl)acrylamide (GQN-A2).** Yield: 83%, purity: 99%. <sup>1</sup>H NMR (500 MHz, CDCl<sub>3</sub>)  $\delta$  8.74 (d, *J* = 20.5 Hz, 1H), 8.12 (s, 1H), 7.94 (d, *J* = 8.5 Hz, 1H), 7.92–7.87 (m, 2H), 7.86 (d, *J* = 1.6 Hz, 1H), 7.85–7.80 (m, 2H), 7.54–7.49 (m, 2H), 7.47 (t, *J* = 7.9 Hz, 2H), 7.31 (t, *J* = 7.3 Hz, 1H), 6.78 (dd, *J* = 12.1, 11.0 Hz, 1H), 6.12 (dd, *J* = 24.9, 12.5 Hz, 1H), 3.61 (t, *J* = 6.8 Hz, 1H), 3.49 (t, *J* = 7.2 Hz, 1H), 3.08 (d, *J* = 13.1 Hz, 3H), 2.50 (t, *J* = 6.8 Hz, 1H), 2.43 (t, *J* = 7.2 Hz, 1H), 2.23 (d, *J* = 20.0 Hz, 6H). <sup>13</sup>C NMR (126 MHz, CDCl<sub>3</sub>)  $\delta$  168.50, 168.35, 153.41, 153.29, 139.95, 139.89, 133.38, 133.18, 130.28, 129.48, 129.47, 129.26, 129.14, 128.37, 128.34, 128.32, 128.12, 128.06, 127.84, 126.86, 126.83, 126.78, 126.75, 126.72, 126.41, 126.13, 120.57, 119.98, 119.61, 119.50, 116.69, 57.69, 56.76, 49.13, 45.89, 45.78, 45.21, 36.34, 33.60, 29.79. ESI-MS: *m/z* 425.2 [M + H]<sup>+</sup>, ESI-HRMS: calcd for C<sub>27</sub>H<sub>29</sub>N<sub>4</sub>O [M + H]<sup>+</sup> 425.2336, found 425.2337.

**4.1.1.3. (Z)-3-(3-(Naphthalen-2-yl)-1-phenyl-1H-pyrazol-4-yl)-N-(3,4,5-trimethoxyphenyl)acrylamide (GQN-A3).** Yield: 98%, purity: 98%. <sup>1</sup>H NMR (500 MHz, CDCl<sub>3</sub>)  $\delta$  9.30 (s, 1H), 8.08 (s, 1H), 7.93 (d, *J* = 8.5 Hz, 1H), 7.91–7.85 (m, 2H), 7.85–7.78 (m, 3H), 7.69 (s, 1H), 7.51 (dd, *J* = 6.2, 3.2 Hz, 2H), 7.45 (t, *J* = 8.0 Hz, 2H), 7.30 (t, *J* = 7.4 Hz, 1H), 6.86 (s, 2H), 5.85 (d, *J* = 12.5 Hz, 1H), 3.83 (s, 3H), 3.81 (s, 6H). <sup>13</sup>C NMR (126 MHz, CDCl<sub>3</sub>)  $\delta$  164.74, 154.91, 153.44, 139.78, 134.19, 133.31, 133.24, 131.80, 131.59, 129.88, 129.50, 128.64, 128.38, 128.35, 127.85, 127.11, 126.95, 126.57, 126.51, 119.78, 119.41, 119.01, 116.20, 98.17, 61.07, 56.21. ESI-MS: *m/z* 506.2 [M + H]<sup>+</sup>, ESI-HRMS: calcd for C<sub>31</sub>H<sub>28</sub>N<sub>3</sub>O<sub>4</sub> [M + H]<sup>+</sup> 506.2074, found 506.2076.

**4.1.1.4. (Z)-N-(3-Acetylphenyl)-3-(3-(naphthalen-2-yl)-1-phenyl-1H-pyrazol-4-yl)acrylamide (GQN-A4).** Yield: 92%, purity: 99%. <sup>1</sup>H NMR (500 MHz, CDCl<sub>3</sub>)  $\delta$  9.38 (s, 1H), 8.13 (s, 1H), 8.08 (d, *J* = 10.3 Hz, 2H), 7.99 (d, *J* = 7.5 Hz, 1H), 7.92 (d, *J* = 8.5 Hz, 1H), 7.91–7.85 (m, 2H), 7.85–7.81 (m, 2H), 7.79 (dd, *J* = 8.4, 1.6 Hz, 1H), 7.66 (d, *J* = 7.8 Hz, 1H), 7.55–7.48 (m, 2H), 7.47–7.39 (m, 3H), 7.29 (t, *J* = 7.4 Hz, 1H), 6.87 (d, *J* = 12.4 Hz, 1H), 5.89 (d, *J* = 12.5 Hz, 1H), 2.58 (s, 3H). <sup>13</sup>C NMR (126 MHz, CDCl<sub>3</sub>)  $\delta$  198.30, 139.76, 138.81, 137.80, 133.31, 133.24, 132.45, 131.79, 129.87, 129.50, 129.42, 128.72, 128.37, 127.85, 127.09, 127.02, 126.57, 126.49, 124.91, 124.32, 119.77, 119.63, 118.46, 116.24, 26.88. ESI-MS: *m/z* 458.2 [M + H]<sup>+</sup>, ESI-HRMS: calcd for C<sub>30</sub>H<sub>24</sub>N<sub>3</sub>O<sub>2</sub> [M + H]<sup>+</sup> 458.1863, found 458.1863.

**4.1.1.5. (Z)-N-Benzyl-3-(3-(naphthalen-2-yl)-1-phenyl-1H-pyrazol-4-yl)acrylamide (GQN-A5).** Yield: 70%, purity: 97%. <sup>1</sup>H NMR (500 MHz, CDCl<sub>3</sub>)  $\delta$  9.32 (s, 1H), 8.09 (s, 1H), 7.94 (d, *J* = 8.5 Hz, 1H), 7.90 (ddd, *J* = 9.8, 6.2, 3.5 Hz, 2H), 7.82 (dd, *J* = 11.6, 4.6 Hz, 3H), 7.52 (dd, *J* = 6.2, 3.3 Hz, 2H), 7.46 (t, *J* = 7.9 Hz, 2H), 7.32 (d, *J* = 6.3 Hz, 4H), 7.30–7.27 (m, 1H), 6.78 (d, *J* = 12.5 Hz, 1H), 6.12 (t, *J* = 5.5 Hz, 1H), 5.75 (d, *J* = 12.5 Hz, 1H), 4.53 (d, *J* = 5.8 Hz, 2H). <sup>13</sup>C NMR (126 MHz, CDCl<sub>3</sub>)  $\delta$  166.42, 154.61, 139.82, 138.22, 133.33, 133.21, 131.42, 130.46, 130.05, 129.46, 128.84, 128.56, 128.37, 128.32, 127.88,

127.84, 127.63, 126.99, 126.93, 126.49, 126.44, 119.69, 118.90, 116.29, 43.66. ESI-MS:  $m/z$  430.2  $[M + H]^+$ , ESI-HRMS: calcd for  $C_{29}H_{24}N_3O_2$   $[M + H]^+$  430.1914, found 430.1917.

**4.1.1.6. (Z)-N-(4-Fluorophenyl)-3-(3-(naphthalen-2-yl)-1-phenyl-1H-pyrazol-4-yl)acrylamide (GQN-A6).** Yield: 78%, purity: 98%.  $^1H$  NMR (500 MHz,  $CDCl_3$ )  $\delta$  9.34 (s, 1H), 8.07 (s, 1H), 7.92 (d,  $J$  = 8.4 Hz, 1H), 7.88 (dd,  $J$  = 9.0, 5.0 Hz, 2H), 7.82 (d,  $J$  = 7.9 Hz, 2H), 7.79 (d,  $J$  = 8.3 Hz, 1H), 7.62 (s, 1H), 7.54–7.47 (m, 4H), 7.44 (t,  $J$  = 7.9 Hz, 2H), 7.30 (t,  $J$  = 7.4 Hz, 1H), 7.01 (t,  $J$  = 8.6 Hz, 2H), 6.83 (d,  $J$  = 12.4 Hz, 1H), 5.79 (d,  $J$  = 12.4 Hz, 1H).  $^{13}C$  NMR (126 MHz,  $CDCl_3$ )  $\delta$  164.71, 155.00, 139.75, 133.32, 133.26, 132.07, 131.73, 129.88, 129.50, 128.69, 128.38, 128.37, 127.87, 127.10, 127.01, 126.58, 126.51, 122.24, 122.18, 119.77, 118.53, 116.22, 115.88, 115.71. ESI-MS:  $m/z$  434.2  $[M + H]^+$ , ESI-HRMS: calcd for  $C_{28}H_{21}FN_3O$   $[M + H]^+$  434.1663, found 434.1666.

**4.1.1.7. (Z)-N-Cyclohexyl-3-(3-(naphthalen-2-yl)-1-phenyl-1H-pyrazol-4-yl)acrylamide (GQN-A7).** Yield: 98%, purity: 96%.  $^1H$  NMR (500 MHz,  $CDCl_3$ )  $\delta$  9.35 (s, 1H), 8.09 (s, 1H), 7.93 (d,  $J$  = 8.5 Hz, 1H), 7.92–7.84 (m, 4H), 7.81 (dd,  $J$  = 8.4, 1.5 Hz, 1H), 7.54–7.49 (m, 2H), 7.46 (t,  $J$  = 7.9 Hz, 2H), 7.30 (t,  $J$  = 7.4 Hz, 1H), 6.74 (d,  $J$  = 12.5 Hz, 1H), 5.71 (d,  $J$  = 12.5 Hz, 1H), 5.65 (d,  $J$  = 8.1 Hz, 1H), 3.97–3.83 (m, 1H), 2.00–1.92 (m, 2H), 1.76–1.67 (m, 2H), 1.63 (dd,  $J$  = 9.4, 3.8 Hz, 1H), 1.46–1.35 (m, 2H), 1.19–1.09 (m, 3H).  $^{13}C$  NMR (126 MHz,  $CDCl_3$ )  $\delta$  165.67, 154.53, 139.88, 133.34, 133.19, 131.45, 130.14, 129.82, 129.43, 128.53, 128.36, 128.29, 127.83, 127.02, 126.88, 126.44, 126.41, 119.71, 119.68, 116.36, 48.26, 33.31, 25.62, 25.00. ESI-MS:  $m/z$  422.2  $[M + H]^+$ , ESI-HRMS: calcd for  $C_{28}H_{28}N_3O$   $[M + H]^+$  422.2230, found 422.2227.

**4.1.1.8. (Z)-N,N-Diethyl-3-(3-(naphthalen-2-yl)-1-phenyl-1H-pyrazol-4-yl)acrylamide (GQN-A8).** Yield: 99%, purity: 96%.  $^1H$  NMR (500 MHz,  $CDCl_3$ )  $\delta$  8.77 (s, 1H), 8.13 (s, 1H), 7.95 (d,  $J$  = 8.5 Hz, 1H), 7.92 (d,  $J$  = 5.2 Hz, 1H), 7.90–7.87 (m, 1H), 7.86 (d,  $J$  = 1.7 Hz, 1H), 7.84 (d,  $J$  = 1.7 Hz, 1H), 7.84–7.81 (m, 2H), 7.52 (ddd,  $J$  = 4.7, 2.2, 0.7 Hz, 2H), 7.49–7.44 (m, 2H), 7.31 (t,  $J$  = 7.4 Hz, 1H), 6.80–6.73 (m, 1H), 6.11 (d,  $J$  = 12.5 Hz, 1H), 3.51 (q,  $J$  = 7.1 Hz, 2H), 3.42 (q,  $J$  = 7.1 Hz, 2H), 1.22 (t,  $J$  = 7.1 Hz, 3H), 1.16 (t,  $J$  = 7.1 Hz, 3H).  $^{13}C$  NMR (126 MHz,  $CDCl_3$ )  $\delta$  167.71, 153.35, 139.90, 133.39, 133.18, 130.32, 129.49, 129.15, 128.37, 128.31, 128.10, 127.84, 126.79, 126.75, 126.40, 126.39, 126.19, 120.45, 119.43, 116.77, 43.03, 39.88, 14.51, 13.29. ESI-MS:  $m/z$  396.2  $[M + H]^+$ , ESI-HRMS: calcd for  $C_{26}H_{26}N_3O$   $[M + H]^+$  396.2070, found 396.2076.

**4.1.1.9. (Z)-1-Morpholino-3-(3-(naphthalen-2-yl)-1-phenyl-1H-pyrazol-4-yl)prop-2-en-1-one (GQN-A9).** Yield: 98%, purity: 96%.  $^1H$  NMR (500 MHz,  $CDCl_3$ )  $\delta$  8.67 (s, 1H), 8.11 (s, 1H), 7.94 (d,  $J$  = 8.5 Hz, 1H), 7.92 (dd,  $J$  = 5.2, 4.3 Hz, 1H), 7.90–7.87 (m, 1H), 7.85 (d,  $J$  = 1.6 Hz, 1H), 7.84–7.79 (m, 2H), 7.54–7.50 (m, 2H), 7.48 (dd,  $J$  = 8.3, 7.6 Hz, 2H), 7.32 (t,  $J$  = 7.4 Hz, 1H), 6.84 (d,  $J$  = 12.2 Hz, 1H), 6.06 (d,  $J$  = 12.4 Hz, 1H), 3.71 (dd,  $J$  = 19.0, 4.6 Hz, 4H), 3.57 (s, 4H).  $^{13}C$  NMR (126 MHz,  $CDCl_3$ )  $\delta$  167.07, 153.25, 139.79, 133.37, 133.20, 130.14, 129.57, 129.03, 128.39, 128.35, 127.97, 127.86, 127.42, 126.99, 126.58, 126.50, 126.48, 119.47, 119.30, 116.56, 66.89, 46.81, 41.86, 38.70. ESI-MS:  $m/z$  410.2  $[M + H]^+$ , ESI-HRMS: calcd for  $C_{26}H_{24}N_3O_2$   $[M + H]^+$  410.1863, found 410.1864.

**4.1.1.10. (E)-3-(3-(Naphthalen-2-yl)-1-phenyl-1H-pyrazol-4-yl)acryloyl)glycine (GQN-B1).** Yield: 33%, purity: 99%.  $^1H$  NMR (400 MHz,  $DMSO-d_6$ )  $\delta$  9.08 (s, 1H), 8.42 (s, 1H), 8.17 (s, 1H), 8.12–7.94 (m, 5H), 7.80 (dd,  $J$  = 8.4, 1.6 Hz, 1H), 7.66–7.47 (m, 5H), 7.40 (d,  $J$  = 7.4 Hz, 1H), 6.57 (d,  $J$  = 15.7 Hz, 1H), 3.85 (d,  $J$  = 5.9 Hz, 2H).  $^{13}C$  NMR (126 MHz,  $DMSO-$

$d_6$ )  $\delta$  171.4, 165.5, 151.7, 139.1, 132.9, 132.7, 129.8, 129.6, 129.5, 128.3, 128.2, 127.9, 127.7, 127.3, 126.9, 126.6, 126.2, 121.5, 118.7, 117.7, 40.8. ESI-MS:  $m/z$  398.2  $[M + H]^+$ , ESI-HRMS: calcd for  $C_{24}H_{20}N_3O_3$   $[M + H]^+$  398.1499, found 398.1498.

**4.1.1.11. (E)-3-(3-(Naphthalen-2-yl)-1-phenyl-1H-pyrazol-4-yl)acryloyl)-L-valine (GQN-B2).** Yield: 16%, purity: 96%.  $^1H$  NMR (400 MHz,  $Methanol-d_4$ )  $\delta$  8.73 (s, 1H), 8.16 (s, 1H), 8.02–7.88 (m, 5H), 7.85 (dd,  $J$  = 8.4, 1.7 Hz, 1H), 7.73 (d,  $J$  = 15.6 Hz, 1H), 7.58–7.53 (m, 5H), 7.43–7.37 (m, 1H), 6.69 (d,  $J$  = 15.7 Hz, 1H), 4.46 (d,  $J$  = 5.6 Hz, 1H), 2.23 (q,  $J$  = 6.6 Hz, 1H), 1.01 (dd,  $J$  = 6.8, 2.4 Hz, 6H).  $^{13}C$  NMR (126 MHz,  $DMSO-d_6$ )  $\delta$  173.2, 165.3, 151.7, 139.1, 132.9, 132.6, 129.8, 129.7, 129.3, 128.3, 128.2, 127.7, 127.6, 127.2, 126.9, 126.6, 126.1, 122.0, 118.7, 117.9, 57.6, 30.0, 29.9, 19.2, 18.2. ESI-MS:  $m/z$  440.2  $[M + H]^+$ , ESI-HRMS: calcd for  $C_{27}H_{26}N_3O_3$   $[M + H]^+$  440.1969, found 440.2004.

**4.1.1.12. (E)-3-(3-(Naphthalen-2-yl)-1-phenyl-1H-pyrazol-4-yl)acryloyl)-L-leucine (GQN-B3).** Yield: 19%, purity: 99%.  $^1H$  NMR (400 MHz,  $Methanol-d_4$ )  $\delta$  8.71 (s, 1H), 8.15 (d,  $J$  = 1.5 Hz, 1H), 8.02–7.96 (m, 2H), 7.95–7.87 (m, 3H), 7.84 (dd,  $J$  = 8.5, 1.6 Hz, 1H), 7.77–7.67 (m, 1H), 7.60–7.50 (m, 4H), 7.45–7.36 (m, 1H), 6.61 (d,  $J$  = 15.4 Hz, 1H), 4.66–4.49 (m, 1H), 1.81–1.64 (m, 3H), 0.99 (dd,  $J$  = 9.4, 5.5 Hz, 6H).  $^{13}C$  NMR (126 MHz,  $DMSO-d_6$ )  $\delta$  174.4, 165.1, 151.7, 139.1, 132.9, 132.6, 129.8, 129.6, 129.3, 128.3, 128.2, 127.7, 127.7, 127.2, 126.9, 126.6, 126.1, 121.9, 118.7, 117.8, 50.7, 40.1, 24.4, 22.9, 21.4. ESI-MS:  $m/z$  454.2  $[M + H]^+$ , ESI-HRMS: calcd for  $C_{28}H_{28}N_3O_3$   $[M + H]^+$  454.2125, found 454.2126.

**4.1.1.13. ((E)-3-(3-(Naphthalen-2-yl)-1-phenyl-1H-pyrazol-4-yl)acryloyl)-L-alloisoleucine (GQN-B4).** Yield: 17%, purity: 98%.  $^1H$  NMR (400 MHz,  $Methanol-d_4$ )  $\delta$  8.70 (s, 1H), 8.19–8.11 (m, 1H), 8.01–7.95 (m, 2H), 7.94–7.87 (m, 3H), 7.83 (dd,  $J$  = 8.5, 1.7 Hz, 1H), 7.71 (d,  $J$  = 15.6 Hz, 1H), 7.59–7.50 (m, 4H), 7.44–7.34 (m, 1H), 6.67 (d,  $J$  = 15.6 Hz, 1H), 4.55–4.44 (m, 1H), 2.00–1.87 (m, 1H), 1.62–1.51 (m, 1H), 1.33–1.29 (m, 1H), 1.02–0.92 (m, 6H).  $^{13}C$  NMR (126 MHz,  $DMSO-d_6$ )  $\delta$  173.3, 165.2, 151.7, 139.1, 132.9, 132.6, 129.8, 129.7, 129.3, 128.3, 128.2, 127.7, 127.6, 127.2, 126.9, 126.6, 126.1, 122.1, 118.7, 117.9, 56.7, 36.4, 24.8, 15.7, 11.3. ESI-MS:  $m/z$  434.2  $[M + H]^+$ , ESI-HRMS: calcd for  $C_{28}H_{28}N_3O_3$   $[M + H]^+$  454.2125, found 454.2130.

**4.1.1.14. (E)-3-(3-(Naphthalen-2-yl)-1-phenyl-1H-pyrazol-4-yl)acryloyl)-L-serine (GQN-B5).** Yield: 13%, purity: 96%.  $^1H$  NMR (400 MHz,  $Methanol-d_4$ )  $\delta$  8.74 (s, 1H), 8.15 (d,  $J$  = 1.7 Hz, 1H), 8.02–7.96 (m, 2H), 7.94–7.88 (m, 3H), 7.84 (dd,  $J$  = 8.5, 1.7 Hz, 1H), 7.73 (d,  $J$  = 15.7 Hz, 1H), 7.61–7.48 (m, 4H), 7.39 (t,  $J$  = 7.5 Hz, 1H), 6.67 (d,  $J$  = 15.7 Hz, 1H), 4.63 (t,  $J$  = 4.4 Hz, 1H), 3.99–3.83 (m, 2H).  $^{13}C$  NMR (126 MHz,  $DMSO-d_6$ )  $\delta$  172.2, 165.1, 151.7, 139.1, 132.9, 132.6, 129.8, 129.6, 129.3, 128.3, 128.2, 127.8, 127.7, 127.2, 126.9, 126.6, 126.1, 122.0, 118.7, 117.9, 61.5, 54.9. ESI-MS:  $m/z$  428.2  $[M + H]^+$ , ESI-HRMS: calcd for  $C_{25}H_{22}N_3O_4$   $[M + H]^+$  428.1605, found 428.1608.

**4.1.1.15. ((E)-3-(3-(Naphthalen-2-yl)-1-phenyl-1H-pyrazol-4-yl)acryloyl)-L-allothreonine (GQN-B6).** Yield: 18%, purity: 97%.  $^1H$  NMR (400 MHz,  $Methanol-d_4$ )  $\delta$  8.82 (s, 1H), 8.19–8.15 (m, 1H), 8.05–7.98 (m, 2H), 7.98–7.91 (m, 3H), 7.87 (dd,  $J$  = 8.5, 1.7 Hz, 1H), 7.74 (d,  $J$  = 15.6 Hz, 1H), 7.60–7.51 (m, 4H), 7.44–7.38 (m, 1H), 6.76 (d,  $J$  = 15.6 Hz, 1H), 4.54 (s, 1H), 4.36 (s, 1H), 1.23 (d,  $J$  = 5.7 Hz, 3H).  $^{13}C$  NMR (126 MHz,  $DMSO-d_6$ )  $\delta$  172.5, 165.2, 151.7, 139.1, 132.9, 132.7, 129.8, 129.7, 129.1, 128.3, 128.2, 127.7, 127.6, 127.2, 126.9,

126.6, 126.1, 122.3, 118.7, 118.0, 66.5, 58.0, 20.2. ESI-MS:  $m/z$  442.2  $[M + H]^+$ , ESI-HRMS: calcd for  $C_{26}H_{24}N_3O_4$   $[M + H]^+$  442.1761, found 442.1764.

4.1.1.16. (*E*)-(3-(3-(Naphthalen-2-yl)-1-phenyl-1H-pyrazol-4-yl)acryloyl)-L-methionine (**GQN-B7**). Yield: 13%, purity: 97%.  $^1H$  NMR (400 MHz, Methanol- $d_4$ )  $\delta$  8.71 (s, 1H), 8.18–8.11 (m, 1H), 8.02–7.95 (m, 2H), 7.95–7.87 (m, 3H), 7.84 (dd,  $J = 8.5, 1.7$  Hz, 1H), 7.72 (d,  $J = 15.7$  Hz, 1H), 7.62–7.49 (m, 4H), 7.42–7.34 (m, 1H), 6.59 (d,  $J = 15.6$  Hz, 1H), 4.68 (dd,  $J = 9.1, 4.6$  Hz, 1H), 2.69–2.50 (m, 2H), 2.24–2.12 (m, 1H), 2.10 (s, 3H), 2.03–1.91 (m, 1H).  $^{13}C$  NMR (126 MHz, DMSO- $d_6$ )  $\delta$  173.4, 165.3, 151.7, 139.1, 132.9, 132.7, 129.8, 129.7, 129.5, 128.3, 128.2, 127.9, 127.7, 127.3, 126.9, 126.6, 126.1, 121.6, 118.7, 117.8, 51.1, 30.6, 29.8, 14.5. ESI-MS:  $m/z$  472.2  $[M + H]^+$ , ESI-HRMS: calcd for  $C_{27}H_{26}N_3O_3S$   $[M + H]^+$  472.1689, found 472.1689.

4.1.1.17. (*E*)-(3-(3-(Naphthalen-2-yl)-1-phenyl-1H-pyrazol-4-yl)acryloyl)-L-histidine (**GQN-B8**). Yield: 27%, purity: 97%.  $^1H$  NMR (400 MHz, Methanol- $d_4$ )  $\delta$  8.77 (d,  $J = 1.3$  Hz, 1H), 8.72 (s, 1H), 8.12 (d,  $J = 1.6$  Hz, 1H), 8.02–7.86 (m, 5H), 7.81 (dd,  $J = 8.5, 1.7$  Hz, 1H), 7.69 (d,  $J = 15.7$  Hz, 1H), 7.59–7.51 (m, 4H), 7.40 (t,  $J = 7.4$  Hz, 1H), 7.32 (s, 1H), 6.55 (d,  $J = 15.7$  Hz, 1H), 4.88–4.86 (m, 1H), 3.37 (dd,  $J = 15.3, 5.2$  Hz, 1H), 3.16 (dd,  $J = 15.3, 8.7$  Hz, 1H).  $^{13}C$  NMR (126 MHz, DMSO- $d_6$ )  $\delta$  172.6, 165.2, 151.8, 139.1, 132.9, 132.7, 131.1, 129.8, 129.7, 128.4, 128.3, 127.9, 127.7, 127.3, 127.0, 126.7, 126.2, 121.5, 118.7, 117.8, 116.9, 51.9, 27.3. ESI-MS:  $m/z$  478.2  $[M + H]^+$ , ESI-HRMS: calcd for  $C_{28}H_{24}N_3O_3$   $[M + H]^+$  478.1874, found 478.1877.

4.1.1.18. (*E*)-(3-(3-(Naphthalen-2-yl)-1-phenyl-1H-pyrazol-4-yl)acryloyl)-L-aspartic acid (**GQN-B9**). Yield: 26%, purity: 98%.  $^1H$  NMR (400 MHz, Methanol- $d_4$ )  $\delta$  8.72 (s, 1H), 8.14 (s, 1H), 8.03–7.95 (m, 2H), 7.94–7.86 (m, 3H), 7.83 (dd,  $J = 8.5, 1.7$  Hz, 1H), 7.72 (d,  $J = 15.7$  Hz, 1H), 7.59–7.50 (m, 4H), 7.39 (t,  $J = 7.4$  Hz, 1H), 6.60 (d,  $J = 15.7$  Hz, 1H), 4.88–4.86 (m, 1H), 2.93–2.85 (m, 2H).  $^{13}C$  NMR (126 MHz, DMSO- $d_6$ )  $\delta$  172.6, 171.8, 164.9, 151.7, 139.1, 132.9, 132.7, 129.8, 129.7, 128.4, 128.3, 127.9, 127.7, 127.3, 127.0, 126.7, 126.2, 121.6, 118.7, 117.8, 48.9, 36.2. ESI-MS:  $m/z$  456.2  $[M + H]^+$ , ESI-HRMS: calcd for  $C_{26}H_{22}N_3O_5$   $[M + H]^+$  456.1554, found 456.1559.

4.1.1.19. (*E*)-(3-(3-(Naphthalen-2-yl)-1-phenyl-1H-pyrazol-4-yl)acryloyl)-L-asparagine (**GQN-B10**). Yield: 19%, purity: 98%.  $^1H$  NMR (400 MHz, Methanol- $d_4$ )  $\delta$  8.72 (s, 1H), 8.13 (s, 1H), 8.01–7.94 (m, 2H), 7.98–7.85 (m, 3H), 7.82 (dd,  $J = 8.4, 1.7$  Hz, 1H), 7.71 (d,  $J = 15.7$  Hz, 1H), 7.59–7.49 (m, 4H), 7.38 (t,  $J = 7.4$  Hz, 1H), 6.60 (d,  $J = 15.7$  Hz, 1H), 4.87–4.83 (m, 1H), 2.83 (d,  $J = 5.9$  Hz, 2H).  $^{13}C$  NMR (126 MHz, DMSO- $d_6$ )  $\delta$  172.9, 171.3, 164.8, 151.7, 139.1, 132.9, 132.7, 129.8, 129.7, 129.4, 128.4, 128.2, 127.8, 127.7, 127.2, 126.9, 126.6, 126.1, 121.8, 118.7, 117.8, 49.0, 36.7. ESI-MS:  $m/z$  455.2  $[M + H]^+$ , ESI-HRMS: calcd for  $C_{26}H_{23}N_4O_4$   $[M + H]^+$  455.1714, found 455.1738.

4.1.1.20. (*E*)-(3-(3-(Naphthalen-2-yl)-1-phenyl-1H-pyrazol-4-yl)acryloyl)-L-glutamic acid (**GQN-B11**). Yield: 14%, purity: 98%.  $^1H$  NMR (400 MHz, Methanol- $d_4$ )  $\delta$  8.73 (s, 1H), 8.15 (d,  $J = 1.6$  Hz, 1H), 8.02–7.96 (m, 2H), 7.94–7.87 (m, 3H), 7.84 (dd,  $J = 8.5, 1.7$  Hz, 1H), 7.72 (d,  $J = 15.7$  Hz, 1H), 7.58–7.51 (m, 4H), 7.43–7.37 (m, 1H), 6.60 (d,  $J = 15.6$  Hz, 1H), 4.57 (dd,  $J = 9.1, 5.1$  Hz, 1H), 2.47–2.40 (m, 2H), 2.29–2.19 (m, 1H), 2.06–1.95 (m, 1H).  $^{13}C$  NMR (126 MHz, DMSO- $d_6$ )  $\delta$  173.8, 173.4, 165.2, 151.7, 139.1, 132.9, 132.7, 129.8, 129.7, 129.5, 128.4, 128.2, 127.9, 127.7, 127.3, 126.9, 126.6, 126.1,

121.7, 118.7, 117.8, 51.5, 30.3, 26.5. ESI-MS:  $m/z$  470.2  $[M + H]^+$ , ESI-HRMS: calcd for  $C_{27}H_{24}N_3O_5$   $[M + H]^+$  470.171, found 470.1707.

4.1.1.21. (*E*)-(3-(3-(Naphthalen-2-yl)-1-phenyl-1H-pyrazol-4-yl)acryloyl)-L-glutamine (**GQN-B12**). Yield: 23%, purity: 96%.  $^1H$  NMR (400 MHz, DMSO- $d_6$ )  $\delta$  9.04 (s, 1H), 8.40 (d,  $J = 7.7$  Hz, 1H), 8.17 (s, 1H), 8.11–7.95 (m, 5H), 7.80 (dd,  $J = 8.4, 1.7$  Hz, 1H), 7.63–7.47 (m, 5H), 7.39 (t,  $J = 7.4$  Hz, 1H), 7.31 (s, 1H), 6.78 (s, 1H), 6.59 (d,  $J = 15.7$  Hz, 1H), 4.32–4.23 (m, 1H), 2.15 (t,  $J = 7.8$  Hz, 2H), 2.04–1.94 (m, 1H), 1.87–1.73 (m, 1H).  $^{13}C$  NMR (126 MHz, DMSO- $d_6$ )  $\delta$  173.5, 165.2, 151.7, 139.1, 132.9, 132.7, 129.8, 129.7, 129.4, 128.4, 128.3, 127.8, 127.7, 127.3, 126.9, 126.6, 126.1, 121.7, 118.7, 117.8, 51.9, 31.4, 26.9. ESI-MS:  $m/z$  469.2  $[M + H]^+$ , ESI-HRMS: calcd for  $C_{27}H_{25}N_4O_4$   $[M + H]^+$  469.1871, found 469.1892.

4.1.1.22. (*E*)-(3-(3-(Naphthalen-2-yl)-1-phenyl-1H-pyrazol-4-yl)acryloyl)-L-lysine (**GQN-B13**). Yield: 14%, purity: 95%.  $^1H$  NMR (400 MHz, Methanol- $d_4$ )  $\delta$  8.75 (s, 1H), 8.15 (d,  $J = 1.7$  Hz, 1H), 8.03–7.89 (m, 5H), 7.84 (dd,  $J = 8.5, 1.8$  Hz, 1H), 7.73 (d,  $J = 15.7$  Hz, 1H), 7.61–7.51 (m, 4H), 7.40 (t,  $J = 7.4$  Hz, 1H), 6.62 (d,  $J = 15.7$  Hz, 1H), 4.56 (dd,  $J = 9.1, 5.0$  Hz, 1H), 2.99–2.85 (m, 2H), 2.03–1.62 (m, 4H), 1.59–1.43 (m, 2H).  $^{13}C$  NMR (151 MHz, DMSO- $d_6$ )  $\delta$  173.6, 165.2, 151.7, 139.1, 132.9, 132.7, 129.8, 129.7, 129.4, 128.3, 128.2, 127.8, 127.7, 127.3, 126.9, 126.6, 126.1, 121.7, 118.7, 117.8, 51.9, 38.4, 30.4, 26.5, 22.5. ESI-MS:  $m/z$  469.2  $[M + H]^+$ , ESI-HRMS: calcd for  $C_{28}H_{29}N_4O_3$   $[M + H]^+$  469.2234, found 469.2236.

4.1.1.23. (*E*)-(3-(3-(Naphthalen-2-yl)-1-phenyl-1H-pyrazol-4-yl)acryloyl)-L-arginine (**GQN-B14**). Yield: 20%, purity: 98%.  $^1H$  NMR (400 MHz, Methanol- $d_4$ )  $\delta$  8.71 (s, 1H), 8.11 (d,  $J = 1.6$  Hz, 1H), 7.99–7.83 (m, 5H), 7.80 (dd,  $J = 8.5, 1.7$  Hz, 1H), 7.70 (d,  $J = 15.6$  Hz, 1H), 7.58–7.48 (m, 4H), 7.39–7.33 (m, 1H), 6.63 (d,  $J = 15.7$  Hz, 1H), 4.58–4.43 (m, 1H), 3.26–3.19 (m, 2H), 2.00–1.94 (m, 1H), 1.87–1.65 (m, 3H).  $^{13}C$  NMR (126 MHz, DMSO- $d_6$ )  $\delta$  174.7, 165.0, 157.1, 151.7, 139.1, 132.9, 132.6, 129.8, 129.6, 128.9, 128.3, 128.2, 127.7, 127.6, 127.2, 126.9, 126.6, 126.1, 122.1, 118.7, 117.9, 116.0, 52.6, 40.4, 28.7, 25.2. ESI-MS:  $m/z$  495.2  $[M - H]^+$ , ESI-HRMS: calcd for  $C_{28}H_{27}N_6O_3$   $[M - H]^+$  495.215, found 495.2152.

4.1.1.24. (*E*)-(3-(3-(Naphthalen-2-yl)-1-phenyl-1H-pyrazol-4-yl)acryloyl)-L-proline (**GQN-B15**). Yield: 13%, purity: 97%.  $^1H$  NMR (400 MHz, Methanol- $d_4$ )  $\delta$  8.92–8.76 (m, 1H), 8.14 (s, 1H), 8.01–7.71 (m, 7H), 7.59–7.50 (m, 4H), 7.43–7.35 (m, 1H), 6.96–6.70 (m, 1H), 4.66–4.45 (m, 1H), 3.81–3.62 (m, 2H), 2.30–2.17 (m, 1H), 2.09–1.90 (m, 3H).  $^{13}C$  NMR (126 MHz, DMSO- $d_6$ )  $\delta$  164.2, 163.7, 151.9, 151.7, 139.1, 132.9, 132.6, 131.0, 129.8, 129.7, 129.7, 129.6, 128.4, 128.3, 128.2, 127.7, 127.3, 127.2, 127.0, 126.8, 126.7, 126.1, 126.1, 119.2, 118.6, 118.2, 118.1, 59.2, 46.7, 46.1, 29.0, 28.8, 24.3. ESI-MS:  $m/z$  438.2  $[M + H]^+$ , ESI-HRMS: calcd for  $C_{27}H_{24}N_3O_3$   $[M + H]^+$  438.1812, found 438.1831.

4.1.1.25. (*Z*)-(3-(3-(Naphthalen-2-yl)-1-phenyl-1H-pyrazol-4-yl)acryloyl)-L-phenylalanine (**GQN-B16-Z**). Yield: 23%, purity: 98%.  $^1H$  NMR (400 MHz, DMSO- $d_6$ )  $\delta$  9.08 (s, 1H), 8.43 (d,  $J = 8.1$  Hz, 1H), 8.13 (d,  $J = 1.6$  Hz, 1H), 8.05–7.96 (m, 3H), 7.93–7.88 (m, 2H), 7.84 (dd,  $J = 8.4, 1.7$  Hz, 1H), 7.63–7.54 (m, 4H), 7.41 (t,  $J = 7.4$  Hz, 1H), 7.33–7.26 (m, 4H), 7.21–7.15 (m, 1H), 6.78 (d,  $J = 12.5$  Hz, 1H), 6.00 (d,  $J = 12.5$  Hz, 1H), 4.84–4.80 (m, 1H), 3.30–3.24 (m, 1H), 3.03 (dd,  $J = 13.9, 9.3$  Hz, 1H).  $^{13}C$  NMR (126 MHz, DMSO- $d_6$ )  $\delta$  173.3, 165.8, 152.1, 139.3, 137.8, 133.1, 132.7, 129.6, 129.6, 129.5, 129.1, 128.3, 128.2, 128.0, 127.8, 127.7, 127.3, 126.9, 126.8,



126.6, 126.3, 121.6, 118.9, 117.7, 53.8, 36.7. ESI-MS:  $m/z$  488.2  $[M + H]^+$ , ESI-HRMS: calcd for  $C_{31}H_{26}N_3O_3$   $[M + H]^+$  488.1969, found 488.1970.

4.1.1.26. (E)-(3-(3-(Naphthalen-2-yl)-1-phenyl-1H-pyrazol-4-yl)acryloyl)-L-phenylalanine (**GQN-B16-E**). Yield: 18%, purity: 96%.  $^1H$  NMR (400 MHz, Methanol- $d_4$ )  $\delta$  8.68 (s, 1H), 8.12 (d,  $J = 1.6$  Hz, 1H), 8.01–7.85 (m, 6H), 7.81 (dd,  $J = 8.5, 1.7$  Hz, 1H), 7.64 (d,  $J = 15.7$  Hz, 1H), 7.57–7.51 (m, 4H), 7.41–7.35 (m, 1H), 7.29–7.21 (m, 4H), 6.53 (d,  $J = 15.7$  Hz, 1H), 4.84–4.70 (m, 1H), 3.26 (dd,  $J = 14.1, 4.6$  Hz, 1H), 3.08–3.01 (m, 1H).  $^{13}C$  NMR (126 MHz, DMSO- $d_6$ )  $\delta$  173.2, 165.2, 151.7, 139.1, 137.9, 132.9, 132.6, 129.7, 129.6, 129.4, 129.1, 128.3, 128.2, 128.1, 127.8, 127.7, 127.3, 126.9, 126.6, 126.4, 126.1, 121.6, 118.7, 117.7, 53.9, 36.6. ESI-MS:  $m/z$  488.2  $[M + H]^+$ , ESI-HRMS: calcd for  $C_{31}H_{26}N_3O_3$   $[M + H]^+$  488.1969, found 488.1971.

4.1.1.27. (Z)-(3-(3-(Naphthalen-2-yl)-1-phenyl-1H-pyrazol-4-yl)acryloyl)-L-tyrosine (**GQN-B17-Z**). Yield: 32%, purity: 97%.  $^1H$  NMR (400 MHz, DMSO- $d_6$ )  $\delta$  9.32 (s, 1H), 9.20 (s, 1H), 8.47 (d,  $J = 7.8$  Hz, 1H), 8.13 (d,  $J = 1.7$  Hz, 1H), 8.08–8.03 (m, 2H), 7.99 (dd,  $J = 6.2, 3.4$  Hz, 1H), 7.87–7.83 (m, 2H), 7.79 (dd,  $J = 8.5, 1.7$  Hz, 1H), 7.61–7.55 (m, 4H), 7.39 (t,  $J = 7.4$  Hz, 1H), 7.12–7.02 (m, 2H), 6.74–6.59 (m, 3H), 6.02 (d,  $J = 12.6$  Hz, 1H), 4.52–4.39 (m, 1H), 3.01 (dd,  $J = 14.1, 4.8$  Hz, 1H), 2.80 (dd,  $J = 13.9, 9.6$  Hz, 1H).  $^{13}C$  NMR (126 MHz, DMSO- $d_6$ )  $\delta$  173.5, 165.2, 156.4, 151.0, 139.2, 133.2, 132.6, 130.0, 129.8, 129.5, 128.9, 128.3, 128.0, 127.9, 127.8, 127.7, 127.3, 126.8, 126.4, 125.9, 121.7, 118.7, 117.8, 114.9, 54.3, 36.1. ESI-MS:  $m/z$  504.2  $[M + H]^+$ , ESI-HRMS: calcd for  $C_{31}H_{26}N_3O_4$   $[M + H]^+$  504.1918, found 504.1920.

4.1.1.28. (E)-(3-(3-(Naphthalen-2-yl)-1-phenyl-1H-pyrazol-4-yl)acryloyl)-L-tyrosine (**GQN-B17-E**). Yield: 20%, purity: 97%.  $^1H$  NMR (400 MHz, Methanol- $d_4$ )  $\delta$  8.71–8.62 (m, 1H), 8.12 (s, 1H), 8.00–7.80 (m, 6H), 7.65 (d,  $J = 15.8$  Hz, 1H), 7.57–7.47 (m, 4H), 7.38 (t,  $J = 7.6$  Hz, 1H), 7.06 (d,  $J = 8.2$  Hz, 2H), 6.70 (d,  $J = 8.1$  Hz, 2H), 6.54 (d,  $J = 15.7$  Hz, 1H), 4.79–4.65 (m, 1H), 3.23–3.10 (m, 1H), 2.97–2.88 (m, 1H).  $^{13}C$  NMR (126 MHz, DMSO- $d_6$ )  $\delta$  173.4, 165.1, 155.9, 151.7, 139.1, 132.9, 132.6, 130.0, 129.8, 129.6, 129.3, 128.3, 128.2, 127.9, 127.8, 127.7, 127.3, 126.9, 126.6, 126.1, 121.7, 118.7, 117.8, 114.9, 54.3, 36.0. ESI-MS:  $m/z$  504.2  $[M + H]^+$ , ESI-HRMS: calcd for  $C_{31}H_{26}N_3O_4$   $[M + H]^+$  504.1918, found 504.1919.

4.1.1.29. (Z)-(3-(3-(Naphthalen-2-yl)-1-phenyl-1H-pyrazol-4-yl)acryloyl)-L-tryptophan (**GQN-B18-Z**). Yield: 18%, purity: 97%.  $^1H$  NMR (400 MHz, DMSO- $d_6$ )  $\delta$  10.70 (s, 1H), 9.44 (s, 1H), 8.12 (s, 1H), 8.04 (d,  $J = 8.1$  Hz, 2H), 8.00–7.97 (m, 1H), 7.88 (d,  $J = 8.1$  Hz, 2H), 7.79 (dd,  $J = 8.5, 1.8$  Hz, 2H), 7.59–7.52 (m, 6H), 7.37 (t,  $J = 7.4$  Hz, 1H), 7.31–7.23 (m, 1H), 7.10 (s, 1H), 6.99 (dd,  $J = 8.1, 6.9$  Hz, 1H), 6.88 (t,  $J = 7.4$  Hz, 1H), 6.57 (d,  $J = 12.5$  Hz, 1H), 6.00 (d,  $J = 12.6$  Hz, 1H), 4.34–4.27 (m, 1H), 3.16 (d,  $J = 4.7$  Hz, 1H), 3.02 (dd,  $J = 14.7, 7.4$  Hz, 1H).  $^{13}C$  NMR (126 MHz, DMSO- $d_6$ )  $\delta$  176.1, 165.3, 151.1, 139.1, 136.2, 132.8, 132.6, 129.8, 129.6, 129.0, 128.3, 128.1, 127.7, 127.3, 127.2, 126.8, 126.6, 126.2, 123.5, 122.1, 120.8, 118.7, 118.2, 117.8, 111.4, 110.3, 53.6, 27.3. ESI-MS:  $m/z$  527.2  $[M + H]^+$ , ESI-HRMS: calcd for  $C_{33}H_{27}N_4O_3$   $[M + H]^+$  527.2078, found 527.2081.

4.1.1.30. (E)-(3-(3-(Naphthalen-2-yl)-1-phenyl-1H-pyrazol-4-yl)acryloyl)-L-tryptophan (**GQN-B18-E**). Yield: 22%, purity: 98%.  $^1H$  NMR (400 MHz, Methanol- $d_4$ )  $\delta$  8.68 (s, 1H), 8.14 (d,  $J = 1.6$  Hz, 1H), 8.03–7.86 (m, 6H), 7.83 (dd,  $J = 8.5, 1.7$  Hz, 1H), 7.68 (d,  $J = 15.7$  Hz, 1H), 7.60 (d,  $J = 7.9$  Hz, 1H), 7.58–

7.53 (m, 4H), 7.40 (t,  $J = 7.4$  Hz, 1H), 7.33 (d,  $J = 8.1$  Hz, 1H), 7.12 (s, 1H), 7.09 (t,  $J = 7.5$  Hz, 1H), 7.04–6.95 (m, 1H), 6.55 (d,  $J = 15.7$  Hz, 1H), 4.87–4.83 (m, 4H), 3.44 (dd,  $J = 14.8, 4.5$  Hz, 1H), 3.26 (dd,  $J = 14.7, 7.3$  Hz, 1H).  $^{13}C$  NMR (126 MHz, DMSO- $d_6$ )  $\delta$  174.3, 164.9, 151.6, 139.1, 136.0, 132.9, 132.6, 129.8, 129.6, 129.0, 128.3, 128.2, 127.7, 127.3, 127.2, 126.9, 126.6, 126.1, 123.5, 122.0, 120.8, 118.7, 118.2, 117.8, 111.3, 110.3, 53.6, 27.2. ESI-MS:  $m/z$  527.2  $[M + H]^+$ , ESI-HRMS: calcd for  $C_{33}H_{27}N_4O_3$   $[M + H]^+$  527.2078, found 527.2082.

4.1.1.31. (Z)-(3-(3-(Naphthalen-2-yl)-1-(*m*-tolyl)-1H-pyrazol-4-yl)acryloyl)-L-tryptophan (**GQN-B19-Z**). Yield: 95%, purity: 98%.  $^1H$  NMR (600 MHz, DMSO- $d_6$ )  $\delta$  12.64 (s, 1H), 10.85 (d,  $J = 2.5$  Hz, 1H), 9.32 (s, 1H), 8.54 (d,  $J = 7.8$  Hz, 1H), 8.13 (d,  $J = 1.7$  Hz, 1H), 8.07–8.03 (m, 2H), 7.99 (dt,  $J = 6.9, 3.5$  Hz, 1H), 7.79 (dd,  $J = 8.4, 1.7$  Hz, 1H), 7.68 (d,  $J = 2.0$  Hz, 1H), 7.62 (dd,  $J = 8.1, 2.3$  Hz, 1H), 7.60–7.56 (m, 3H), 7.42 (t,  $J = 7.8$  Hz, 1H), 7.35–7.31 (m, 1H), 7.22–7.17 (m, 2H), 7.07 (ddd,  $J = 8.1, 7.0, 1.2$  Hz, 1H), 6.99 (ddd,  $J = 7.9, 6.9, 1.0$  Hz, 1H), 6.70 (d,  $J = 12.5$  Hz, 1H), 6.04 (d,  $J = 12.6$  Hz, 1H), 4.63 (ddd,  $J = 9.2, 7.8, 4.8$  Hz, 1H), 3.26 (dd,  $J = 14.7, 4.8$  Hz, 1H), 3.08 (dd,  $J = 14.7, 9.2$  Hz, 1H), 2.42 (s, 3H);  $^{13}C$  NMR (151 MHz, DMSO- $d_6$ )  $\delta$  174.09, 166.12, 153.66, 139.86, 139.65, 136.57, 133.28, 133.07, 131.58, 130.10, 130.03, 128.79, 128.77, 128.65, 128.33, 128.10, 128.06, 127.62, 127.08, 127.06, 127.02, 124.10, 121.42, 120.93, 119.74, 118.87, 118.65, 116.53, 116.47, 111.88, 110.49, 53.57, 27.58, 21.51; ESI-MS:  $m/z$  541.2  $[M + H]^+$ , ESI-HRMS: calcd for  $C_{34}H_{29}O_3N_4$   $[M + H]^+$  541.2234, found 541.2234.

4.1.1.32. (E)-(3-(3-(Naphthalen-2-yl)-1-(*m*-tolyl)-1H-pyrazol-4-yl)acryloyl)-L-tryptophan (**GQN-B19-E**). Yield: 99%, purity: 97%.  $^1H$  NMR (600 MHz, DMSO- $d_6$ )  $\delta$  12.48 (s, 1H), 10.85 (d,  $J = 2.4$  Hz, 1H), 8.98 (s, 1H), 8.39 (d,  $J = 7.9$  Hz, 1H), 8.16 (d,  $J = 1.7$  Hz, 1H), 8.09–7.97 (m, 3H), 7.84–7.74 (m, 3H), 7.61–7.54 (m, 3H), 7.48–7.42 (m, 2H), 7.34 (d,  $J = 8.1$  Hz, 1H), 7.20 (d,  $J = 7.5$  Hz, 1H), 7.16 (d,  $J = 2.4$  Hz, 1H), 7.06 (ddd,  $J = 8.2, 6.9, 1.2$  Hz, 1H), 6.97 (ddd,  $J = 8.0, 6.9, 1.0$  Hz, 1H), 6.58 (d,  $J = 15.7$  Hz, 1H), 4.60 (ddd,  $J = 9.2, 7.8, 4.8$  Hz, 1H), 3.23 (dd,  $J = 14.6, 4.8$  Hz, 1H), 3.08 (dd,  $J = 14.7, 9.2$  Hz, 1H), 2.42 (s, 3H);  $^{13}C$  NMR (151 MHz, DMSO- $d_6$ )  $\delta$  174.04, 172.48, 165.62, 152.08, 139.75, 139.56, 136.58, 133.37, 133.12, 130.27, 129.93, 129.87, 128.80, 128.73, 128.23, 128.14, 128.05, 127.71, 127.62, 127.10, 126.63, 124.05, 122.13, 121.41, 119.70, 118.86, 118.63, 118.16, 116.32, 111.86, 110.51, 53.64, 27.53, 21.54; ESI-MS:  $m/z$  541.2  $[M + H]^+$ , ESI-HRMS: calcd for  $C_{34}H_{29}O_3N_4$   $[M + H]^+$  541.2234, found 541.2235.

4.1.1.33. (Z)-(3-(3-(Naphthalen-2-yl)-1-(*m*-tolyl)-1H-pyrazol-4-yl)acryloyl)-L-tyrosine (**GQN-B20-Z**). Yield: 99%, purity: 98%.  $^1H$  NMR (600 MHz, DMSO- $d_6$ )  $\delta$  12.65 (s, 1H), 9.31 (s, 1H), 9.21 (s, 1H), 8.51 (d,  $J = 8.0$  Hz, 1H), 8.13 (d,  $J = 1.7$  Hz, 1H), 8.05 (dd,  $J = 7.2, 3.8$  Hz, 2H), 7.99 (dt,  $J = 7.1, 3.6$  Hz, 1H), 7.79 (dd,  $J = 8.5, 1.7$  Hz, 1H), 7.69 (d,  $J = 1.9$  Hz, 1H), 7.63 (dd,  $J = 8.0, 2.3$  Hz, 1H), 7.59 (dt,  $J = 6.2, 3.4$  Hz, 2H), 7.44 (t,  $J = 7.8$  Hz, 1H), 7.20 (d,  $J = 7.6$  Hz, 1H), 7.09–7.05 (m, 2H), 6.73–6.62 (m, 3H), 6.02 (d,  $J = 12.7$  Hz, 1H), 4.49 (ddd,  $J = 9.7, 8.0, 4.8$  Hz, 1H), 3.01 (dd,  $J = 14.0, 4.8$  Hz, 1H), 2.81 (dd,  $J = 14.0, 9.7$  Hz, 1H), 2.43 (s, 3H);  $^{13}C$  NMR (151 MHz, DMSO- $d_6$ )  $\delta$  173.82, 166.08, 156.41, 153.67, 139.87, 139.65, 133.29, 133.07, 131.56, 130.49 (2C), 130.10, 130.05, 128.86, 128.77, 128.66, 128.34, 128.21, 128.09, 128.07, 127.08, 127.07, 127.02, 120.86, 119.74, 116.53, 116.49, 115.47 (2C), 54.47, 36.49, 21.51; ESI-MS:  $m/z$  518.2  $[M + H]^+$ , ESI-HRMS: calcd for  $C_{32}H_{28}O_4N_3$   $[M + H]^+$  518.2074, found 518.2074.

4.1.1.34. (E)-(3-(3-(Naphthalen-2-yl)-1-(*m*-tolyl)-1H-pyrazol-4-yl)acryloyl)-L-tyrosine (**GQN-B20-E**). Yield: 99%, purity:

97%.  $^1\text{H}$  NMR (600 MHz, DMSO- $d_6$ )  $\delta$  12.61 (s, 1H), 9.20 (s, 1H), 9.01 (s, 1H), 8.37 (d,  $J$  = 8.1 Hz, 1H), 8.17 (d,  $J$  = 1.7 Hz, 1H), 8.09–8.03 (m, 2H), 8.02–7.98 (m, 1H), 7.83 (d,  $J$  = 2.0 Hz, 1H), 7.78 (ddd,  $J$  = 13.7, 8.3, 2.0 Hz, 2H), 7.62–7.55 (m, 2H), 7.4–7.40 (m, 2H), 7.23–7.18 (m, 1H), 7.07–7.03 (m, 2H), 6.65–6.63 (m, 2H), 6.56 (d,  $J$  = 15.8 Hz, 1H), 4.44 (ddd,  $J$  = 9.9, 8.1, 4.7 Hz, 1H), 2.98 (dd,  $J$  = 13.9, 4.6 Hz, 1H), 2.81 (dd,  $J$  = 13.9, 9.9 Hz, 1H), 2.43 (s, 3H);  $^{13}\text{C}$  NMR (151 MHz, DMSO- $d_6$ )  $\delta$  173.79, 170.81, 165.67, 156.36, 152.08, 139.75, 139.56, 133.38, 133.12, 130.48 (2C), 130.26, 129.93, 129.87, 128.80, 128.72, 128.27, 128.24, 128.15, 128.05, 127.72, 127.10, 126.63, 122.07, 119.69, 118.12, 116.32, 115.44 (2C), 60.23, 54.63, 21.54; ESI-MS:  $m/z$  518.2  $[\text{M} + \text{H}]^+$ , ESI-HRMS: calcd for  $\text{C}_{32}\text{H}_{28}\text{O}_4\text{N}_3$   $[\text{M} + \text{H}]^+$  518.2074, found 518.2076.

4.1.1.35. (Z)-(3-(3-(Naphthalen-2-yl)-1-(*m*-tolyl)-1H-pyrazol-4-yl)acryloyl)-L-phenylalanine (GQN-B21-Z). Yield: 99%, purity: 98%.  $^1\text{H}$  NMR (600 MHz, DMSO- $d_6$ )  $\delta$  12.77 (s, 1H), 9.27 (s, 1H), 8.58 (d,  $J$  = 8.1 Hz, 1H), 8.13 (d,  $J$  = 1.7 Hz, 1H), 8.07–8.03 (m, 2H), 7.99 (dt,  $J$  = 7.0, 3.6 Hz, 1H), 7.79 (dd,  $J$  = 8.5, 1.7 Hz, 1H), 7.68 (t,  $J$  = 2.0 Hz, 1H), 7.60 (ddd,  $J$  = 23.6, 7.1, 2.7 Hz, 3H), 7.44 (t,  $J$  = 7.8 Hz, 1H), 7.31–7.24 (m, 4H), 7.23–7.16 (m, 2H), 6.71 (d,  $J$  = 12.5 Hz, 1H), 6.01 (d,  $J$  = 12.6 Hz, 1H), 4.59 (ddd,  $J$  = 9.9, 8.1, 4.7 Hz, 1H), 3.14 (dd,  $J$  = 13.9, 4.7 Hz, 1H), 2.92 (dd,  $J$  = 13.9, 9.9 Hz, 1H), 2.43 (s, 3H);  $^{13}\text{C}$  NMR (151 MHz, DMSO- $d_6$ )  $\delta$  173.68, 166.11, 153.64, 139.87, 139.64, 138.25, 133.28, 133.07, 131.51, 130.09, 130.04, 129.58 (2C), 128.89, 128.77, 128.67 (2C), 128.66, 128.32, 128.09 (2C), 127.08, 127.05, 127.02, 126.91, 120.81, 119.74, 116.51, 116.49, 54.10, 37.23, 21.52; ESI-MS:  $m/z$  502.2  $[\text{M} + \text{H}]^+$ , ESI-HRMS: calcd for  $\text{C}_{32}\text{H}_{28}\text{O}_3\text{N}_3$   $[\text{M} + \text{H}]^+$  502.2125, found 502.2123.

4.1.1.36. (E)-(3-(3-(Naphthalen-2-yl)-1-(*m*-tolyl)-1H-pyrazol-4-yl)acryloyl)-L-phenylalanine (GQN-B21-E). Yield: 99%, purity: 99%.  $^1\text{H}$  NMR (600 MHz, DMSO- $d_6$ )  $\delta$  12.65 (s, 1H), 9.01 (s, 1H), 8.45 (d,  $J$  = 8.1 Hz, 1H), 8.16 (s, 1H), 8.09–7.97 (m, 3H), 7.83 (d,  $J$  = 2.2 Hz, 1H), 7.78 (ddd,  $J$  = 11.1, 8.4, 2.0 Hz, 2H), 7.62–7.55 (m, 2H), 7.47–7.41 (m, 2H), 7.30–7.22 (m, 4H), 7.22–7.16 (m, 2H), 6.54 (d,  $J$  = 15.7 Hz, 1H), 4.52 (ddd,  $J$  = 10.1, 8.1, 4.6 Hz, 1H), 3.11 (dd,  $J$  = 13.8, 4.6 Hz, 1H), 2.93 (dd,  $J$  = 13.8, 10.0 Hz, 1H), 2.42 (s, 3H);  $^{13}\text{C}$  NMR (151 MHz, DMSO- $d_6$ )  $\delta$  173.66, 165.71, 152.10, 139.75, 139.55, 138.29, 133.37, 133.12, 130.25, 129.93, 129.55 (2C), 128.80 (2C), 128.71, 128.65 (2C), 128.25, 128.15, 128.05, 127.73, 127.09 (2C), 126.88, 126.64, 121.97, 119.69, 118.09, 116.31, 54.27, 37.09, 21.53; ESI-MS:  $m/z$  502.2  $[\text{M} + \text{H}]^+$ , ESI-HRMS: calcd for  $\text{C}_{32}\text{H}_{28}\text{O}_3\text{N}_3$   $[\text{M} + \text{H}]^+$  502.2125, found 502.2124.

4.1.1.37. (Z)-(3-(1-(3-Chlorophenyl)-3-(naphthalen-2-yl)-1H-pyrazol-4-yl)acryloyl)-L-tryptophan (GQN-B22-Z). Yield: 97%, purity: 96%.  $^1\text{H}$  NMR (600 MHz, DMSO- $d_6$ )  $\delta$  12.59 (s, 1H), 10.85 (d,  $J$  = 2.4 Hz, 1H), 9.33 (s, 1H), 8.56 (d,  $J$  = 7.8 Hz, 1H), 8.15 (d,  $J$  = 1.7 Hz, 1H), 8.07–8.04 (m, 2H), 8.02–7.97 (m, 1H), 7.95 (t,  $J$  = 2.1 Hz, 1H), 7.80 (dt,  $J$  = 8.4, 1.7 Hz, 2H), 7.61–7.55 (m, 4H), 7.44 (ddd,  $J$  = 8.1, 2.1, 0.9 Hz, 1H), 7.34–7.32 (m, 1H), 7.19 (d,  $J$  = 2.4 Hz, 1H), 7.06 (ddd,  $J$  = 8.1, 6.9, 1.2 Hz, 1H), 6.99 (ddd,  $J$  = 8.0, 7.0, 1.1 Hz, 1H), 6.71 (d,  $J$  = 12.5 Hz, 1H), 6.07 (d,  $J$  = 12.7 Hz, 1H), 4.63 (ddd,  $J$  = 9.1, 7.7, 4.8 Hz, 1H), 3.26 (dd,  $J$  = 14.7, 4.8 Hz, 1H), 3.08 (dd,  $J$  = 14.7, 9.2 Hz, 1H);  $^{13}\text{C}$  NMR (151 MHz, DMSO- $d_6$ )  $\delta$  174.08, 166.00, 153.99, 140.76, 136.57, 134.59, 133.27, 133.14, 131.97, 131.83, 129.82, 128.80, 128.71, 128.51, 128.37, 128.10, 127.63, 127.17, 127.08, 127.05, 126.94, 124.11, 121.64, 121.41, 119.06, 118.87, 118.65, 117.73, 117.00, 111.87, 110.46, 53.58, 27.58; ESI-MS:

$m/z$  561.2  $[\text{M} + \text{H}]^+$ , ESI-HRMS: calcd for  $\text{C}_{33}\text{H}_{26}\text{O}_3\text{N}_4\text{Cl}$   $[\text{M} + \text{H}]^+$  561.1688, found 561.1689.

4.1.1.38. (E)-(3-(1-(3-Chlorophenyl)-3-(naphthalen-2-yl)-1H-pyrazol-4-yl)acryloyl)-L-tryptophan (GQN-B22-E). Yield: 95%, purity: 99%.  $^1\text{H}$  NMR (600 MHz, DMSO- $d_6$ )  $\delta$  12.54 (s, 1H), 10.85 (d,  $J$  = 2.4 Hz, 1H), 9.11 (s, 1H), 8.45 (d,  $J$  = 7.9 Hz, 1H), 8.17 (d,  $J$  = 1.7 Hz, 1H), 8.10 (t,  $J$  = 2.1 Hz, 1H), 8.08–7.95 (m, 4H), 7.79 (dd,  $J$  = 8.4, 1.7 Hz, 1H), 7.62–7.50 (m, 4H), 7.49–7.42 (m, 2H), 7.34 (dt,  $J$  = 8.1, 1.0 Hz, 1H), 7.16 (d,  $J$  = 2.3 Hz, 1H), 7.06 (ddd,  $J$  = 8.1, 6.9, 1.2 Hz, 1H), 6.97 (ddd,  $J$  = 7.9, 6.9, 1.0 Hz, 1H), 6.58 (d,  $J$  = 15.7 Hz, 1H), 4.59 (ddd,  $J$  = 9.2, 7.8, 4.8 Hz, 1H), 3.23 (dd,  $J$  = 14.7, 4.7 Hz, 1H), 3.08 (dd,  $J$  = 14.7, 9.3 Hz, 1H);  $^{13}\text{C}$  NMR (151 MHz, DMSO- $d_6$ )  $\delta$  174.03, 165.52, 152.56, 140.70, 136.57, 134.58, 133.35, 133.20, 131.86, 129.95, 129.63, 128.86, 128.76, 128.70, 128.15, 127.83, 127.61, 127.20, 127.14, 127.08, 126.55, 124.05, 122.57, 121.41, 118.88, 118.86, 118.67, 118.62, 117.68, 111.87, 110.52, 53.67, 27.51; ESI-MS:  $m/z$  561.2  $[\text{M} + \text{H}]^+$ , ESI-HRMS: calcd for  $\text{C}_{33}\text{H}_{26}\text{O}_3\text{N}_4\text{Cl}$   $[\text{M} + \text{H}]^+$  561.1688, found 561.1686.

4.1.1.39. (Z)-(3-(1-(3-Chlorophenyl)-3-(naphthalen-2-yl)-1H-pyrazol-4-yl)acryloyl)-L-tyrosine (GQN-B23-Z). Yield: 99%, purity: 99%.  $^1\text{H}$  NMR (600 MHz, DMSO- $d_6$ )  $\delta$  12.53 (s, 1H), 9.32 (s, 1H), 9.20 (s, 1H), 8.52 (d,  $J$  = 8.0 Hz, 1H), 8.17–8.14 (m, 1H), 8.06 (dd,  $J$  = 9.0, 2.4 Hz, 2H), 8.00 (dt,  $J$  = 6.2, 3.6 Hz, 1H), 7.95 (t,  $J$  = 2.1 Hz, 1H), 7.85–7.78 (m, 2H), 7.60–7.57 (m, 3H), 7.45 (ddd,  $J$  = 8.0, 2.0, 0.9 Hz, 1H), 7.09–7.04 (m, 2H), 6.71 (d,  $J$  = 12.5 Hz, 1H), 6.68–6.65 (m, 2H), 6.05 (d,  $J$  = 12.6 Hz, 1H), 4.50 (ddd,  $J$  = 9.6, 8.0, 4.8 Hz, 1H), 3.01 (dd,  $J$  = 14.0, 4.8 Hz, 1H), 2.81 (dd,  $J$  = 14.0, 9.6 Hz, 1H);  $^{13}\text{C}$  NMR (151 MHz, DMSO- $d_6$ )  $\delta$  173.80, 165.97, 156.40, 154.01, 140.77, 134.59, 133.27, 133.14, 131.99, 131.82, 130.50 (2C), 129.81, 128.81, 128.71, 128.57, 128.38, 128.18, 128.10, 127.17, 127.10, 127.05, 126.94, 121.57, 119.06, 117.75, 117.00, 115.46 (2C), 54.47, 36.49; ESI-MS:  $m/z$  538.2  $[\text{M} + \text{H}]^+$ , ESI-HRMS: calcd for  $\text{C}_{31}\text{H}_{25}\text{O}_4\text{N}_3\text{Cl}$   $[\text{M} + \text{H}]^+$  538.1528, found 538.1527.

4.1.1.40. (E)-(3-(1-(3-Chlorophenyl)-3-(naphthalen-2-yl)-1H-pyrazol-4-yl)acryloyl)-L-tyrosine (GQN-B23-E). Yield: 98%, purity: 96%.  $^1\text{H}$  NMR (600 MHz, DMSO- $d_6$ )  $\delta$  12.61 (s, 1H), 9.20 (s, 1H), 9.14 (s, 1H), 8.42 (d,  $J$  = 8.1 Hz, 1H), 8.18 (d,  $J$  = 1.7 Hz, 1H), 8.11 (t,  $J$  = 2.1 Hz, 1H), 8.09–8.04 (m, 2H), 8.00 (ddd,  $J$  = 12.3, 7.1, 2.8 Hz, 2H), 7.80 (dd,  $J$  = 8.4, 1.7 Hz, 1H), 7.62–7.57 (m, 3H), 7.47–7.42 (m, 2H), 7.07–7.03 (m, 2H), 6.65–6.63 (m, 2H), 6.55 (d,  $J$  = 15.7 Hz, 1H), 4.44 (ddd,  $J$  = 9.9, 8.0, 4.6 Hz, 1H), 2.99 (dd,  $J$  = 13.9, 4.6 Hz, 1H), 2.81 (dd,  $J$  = 13.9, 9.9 Hz, 1H);  $^{13}\text{C}$  NMR (151 MHz, DMSO- $d_6$ )  $\delta$  173.78, 165.56, 156.36, 152.57, 140.70, 134.58, 133.35, 133.20, 131.86, 130.48 (2C), 129.94, 129.63, 128.86, 128.75, 128.71, 128.27, 128.16, 127.84, 127.20, 127.13, 127.08, 126.55, 122.51, 118.87, 118.63, 117.67, 115.44 (2C), 54.65, 36.36; ESI-MS:  $m/z$  538.2  $[\text{M} + \text{H}]^+$ , ESI-HRMS: calcd for  $\text{C}_{31}\text{H}_{25}\text{O}_4\text{N}_3\text{Cl}$   $[\text{M} + \text{H}]^+$  538.1528, found 538.1528.

4.1.1.41. (Z)-(3-(1-(3-Chlorophenyl)-3-(naphthalen-2-yl)-1H-pyrazol-4-yl)acryloyl)-L-phenylalanine (GQN-B24-Z). Yield: 99%, purity: 98%.  $^1\text{H}$  NMR (600 MHz, DMSO- $d_6$ )  $\delta$  12.72 (s, 1H), 9.27 (s, 1H), 8.59 (d,  $J$  = 8.1 Hz, 1H), 8.15 (d,  $J$  = 1.7 Hz, 1H), 8.08–8.03 (m, 2H), 8.00 (dt,  $J$  = 6.2, 3.5 Hz, 1H), 7.94 (t,  $J$  = 2.1 Hz, 1H), 7.81 (ddd,  $J$  = 10.2, 7.8, 1.8 Hz, 2H), 7.62–7.56 (m, 3H), 7.48–7.43 (m, 1H), 7.30–7.24 (m, 4H), 7.18 (tt,  $J$  = 5.8, 3.0 Hz, 1H), 6.71 (d,  $J$  = 12.5 Hz, 1H), 6.04 (d,  $J$  = 12.6 Hz, 1H), 4.59 (ddd,  $J$  = 9.9, 8.0, 4.7 Hz, 1H), 3.14 (dd,  $J$  = 13.9, 4.7 Hz, 1H), 2.92 (dd,  $J$  = 13.9, 9.9 Hz, 1H);  $^{13}\text{C}$  NMR (151 MHz, DMSO- $d_6$ )  $\delta$  173.66, 165.99, 153.98, 140.75, 138.23, 134.59, 133.27, 133.14, 131.99, 131.75, 129.81, 129.58

(2C), 128.80, 128.71, 128.67 (2C), 128.60, 128.36, 128.10, 127.17, 127.10, 127.06, 126.93, 126.90, 121.55, 119.04, 117.76, 116.98, 54.11, 37.24; ESI-MS:  $m/z$  522.2  $[M + H]^+$ , ESI-HRMS: calcd for  $C_{31}H_{25}O_3N_3Cl$   $[M + H]^+$  522.1579, found 522.1580.

4.1.1.42. (*E*)-(3-(1-(3-Chlorophenyl)-3-(naphthalen-2-yl)-1H-pyrazol-4-yl)acryloyl)-L-phenylalanine (**GQN-B24-E**). Yield: 99%, purity: 97%.  $^1H$  NMR (600 MHz, DMSO- $d_6$ )  $\delta$  12.63 (s, 1H), 9.14 (s, 1H), 8.50 (d,  $J = 8.1$  Hz, 1H), 8.18 (d,  $J = 1.7$  Hz, 1H), 8.11 (t,  $J = 2.1$  Hz, 1H), 8.09–8.03 (m, 2H), 8.02–7.97 (m, 2H), 7.79 (dd,  $J = 8.4, 1.7$  Hz, 1H), 7.62–7.57 (m, 3H), 7.47–7.42 (m, 2H), 7.29–7.24 (m, 4H), 7.19 (ddt,  $J = 8.6, 6.2, 2.0$  Hz, 1H), 6.55 (d,  $J = 15.7$  Hz, 1H), 4.53 (ddd,  $J = 10.1, 8.1, 4.6$  Hz, 1H), 3.12 (dd,  $J = 13.8, 4.6$  Hz, 1H), 2.93 (dd,  $J = 13.9, 10.1$  Hz, 1H);  $^{13}C$  NMR (151 MHz, DMSO- $d_6$ )  $\delta$  173.65, 165.61, 152.59, 140.70, 138.30, 134.58, 133.35, 133.20, 131.86, 129.94, 129.70, 129.55 (2C), 128.85, 128.74, 128.72, 128.65 (2C), 128.16, 127.85, 127.20, 127.13, 127.08, 126.88, 126.56, 122.41, 118.86, 118.60, 117.66, 54.30, 37.08; ESI-MS:  $m/z$  522.2  $[M + H]^+$ , ESI-HRMS: calcd for  $C_{31}H_{25}O_3N_3Cl$   $[M + H]^+$  522.1579, found 522.1578.

4.1.1.43. (*Z*)-(3-(3-(Naphthalen-2-yl)-1-(*o*-tolyl)-1H-pyrazol-4-yl)acryloyl)-L-tryptophan (**GQN-B25-Z**). Yield: 99%, purity: 97%.  $^1H$  NMR (600 MHz, DMSO- $d_6$ )  $\delta$  12.49 (s, 1H), 10.84 (d,  $J = 2.4$  Hz, 1H), 8.98 (d,  $J = 0.5$  Hz, 1H), 8.49 (d,  $J = 7.8$  Hz, 1H), 8.15–8.09 (m, 1H), 8.05–8.01 (m, 2H), 8.00–7.95 (m, 1H), 7.76 (dd,  $J = 8.5, 1.7$  Hz, 1H), 7.60–7.53 (m, 3H), 7.48–7.36 (m, 4H), 7.32 (dt,  $J = 8.1, 0.9$  Hz, 1H), 7.17 (d,  $J = 2.4$  Hz, 1H), 7.05 (ddd,  $J = 8.1, 6.9, 1.2$  Hz, 1H), 6.97 (ddd,  $J = 8.0, 7.0, 1.1$  Hz, 1H), 6.76–6.71 (m, 1H), 6.01 (d,  $J = 12.7$  Hz, 1H), 4.58 (ddd,  $J = 9.2, 7.8, 4.9$  Hz, 1H), 3.24 (dd,  $J = 14.7, 4.5$  Hz, 1H), 3.06 (dd,  $J = 14.7, 9.1$  Hz, 1H), 2.30 (s, 3H);  $^{13}C$  NMR (151 MHz, DMSO- $d_6$ )  $\delta$  174.05, 172.49, 166.19, 153.03, 139.62, 136.56, 135.67, 133.31, 133.22, 132.98, 131.93, 130.27, 129.08, 129.02, 128.73, 128.63, 128.31, 128.07, 127.61, 127.36, 127.15, 126.98, 126.09, 124.07, 121.40, 120.29, 118.85, 118.62, 115.31, 111.86, 110.48, 53.51, 27.55, 18.45; ESI-MS:  $m/z$  541.2  $[M + H]^+$ , ESI-HRMS: calcd for  $C_{34}H_{29}O_3N_3$   $[M + H]^+$  541.2234, found 541.2234.

4.1.1.44. (*E*)-(3-(3-(Naphthalen-2-yl)-1-(*o*-tolyl)-1H-pyrazol-4-yl)acryloyl)-L-tryptophan (**GQN-B25-E**). Yield: 99%, purity: 98%.  $^1H$  NMR (600 MHz, DMSO- $d_6$ )  $\delta$  12.45 (s, 1H), 10.84 (d,  $J = 2.5$  Hz, 1H), 8.54 (s, 1H), 8.36 (d,  $J = 7.9$  Hz, 1H), 8.15–8.12 (m, 1H), 8.05 (d,  $J = 8.5$  Hz, 1H), 8.00 (ddd,  $J = 22.0, 6.1, 3.3$  Hz, 2H), 7.76 (dd,  $J = 8.4, 1.7$  Hz, 1H), 7.59–7.52 (m, 4H), 7.52–7.48 (m, 1H), 7.47–7.38 (m, 3H), 7.34 (dt,  $J = 8.1, 0.9$  Hz, 1H), 7.15 (d,  $J = 2.4$  Hz, 1H), 7.06 (ddd,  $J = 8.1, 6.9, 1.2$  Hz, 1H), 6.97 (ddd,  $J = 8.0, 7.0, 1.0$  Hz, 1H), 6.54 (d,  $J = 15.7$  Hz, 1H), 4.60 (ddd,  $J = 9.1, 7.9, 4.9$  Hz, 1H), 3.22 (dd,  $J = 14.7, 4.8$  Hz, 1H), 3.07 (dd,  $J = 14.7, 9.1$  Hz, 1H), 2.35 (s, 3H);  $^{13}C$  NMR (151 MHz, DMSO- $d_6$ )  $\delta$  174.04, 172.49, 165.67, 151.47, 139.62, 136.57, 133.40, 133.21, 133.03, 132.03, 131.90, 130.45, 130.07, 129.13, 128.77, 128.69, 128.12, 127.65, 127.32, 127.05, 127.01, 126.69, 126.26, 124.03, 121.75, 121.40, 118.85, 118.63, 116.89, 111.86, 110.49, 53.59, 27.57, 18.49; ESI-MS:  $m/z$  541.2  $[M + H]^+$ , ESI-HRMS: calcd for  $C_{34}H_{29}O_3N_3$   $[M + H]^+$  541.2234, found 541.2234.

4.1.1.45. (*Z*)-(3-(3-(Naphthalen-2-yl)-1-(*o*-tolyl)-1H-pyrazol-4-yl)acryloyl)-L-tyrosine (**GQN-B26-Z**). Yield: 95%, purity: 97%.  $^1H$  NMR (600 MHz, DMSO- $d_6$ )  $\delta$  12.50 (s, 1H), 9.21 (s, 1H), 8.99 (s, 1H), 8.46 (d,  $J = 8.0$  Hz, 1H), 8.13–8.10 (m, 1H), 8.04 (dd,  $J = 9.0, 4.1$  Hz, 2H), 8.01–7.95 (m, 1H), 7.76 (dd,  $J = 8.4, 1.7$  Hz, 1H), 7.59–7.56 (m, 2H), 7.48 (dd,  $J = 7.6, 1.5$  Hz,

1H), 7.46–7.36 (m, 3H), 7.07–7.03 (m, 2H), 6.74 (d,  $J = 12.6$  Hz, 1H), 6.68–6.63 (m, 2H), 5.99 (d,  $J = 12.7$  Hz, 1H), 4.44 (ddd,  $J = 9.6, 7.9, 4.8$  Hz, 1H), 2.99 (dd,  $J = 14.0, 4.8$  Hz, 1H), 2.79 (dd,  $J = 14.0, 9.7$  Hz, 1H), 2.31 (s, 3H);  $^{13}C$  NMR (151 MHz, DMSO- $d_6$ )  $\delta$  173.79, 172.49, 166.18, 156.39, 153.07, 139.62, 135.68, 133.32, 133.25, 132.99, 131.93, 130.46 (2C), 130.26, 129.11, 129.09, 128.74, 128.63, 128.33, 128.20, 128.07, 127.37, 127.16, 126.98, 126.10, 120.19, 115.46 (2C), 115.31, 54.43, 36.43, 18.46; ESI-MS:  $m/z$  518.2  $[M + H]^+$ , ESI-HRMS: calcd for  $C_{32}H_{28}O_4N_3$   $[M + H]^+$  518.2074, found 518.2074.

4.1.1.46. (*E*)-(3-(3-(Naphthalen-2-yl)-1-(*o*-tolyl)-1H-pyrazol-4-yl)acryloyl)-L-tyrosine (**GQN-B26-E**). Yield: 99%, purity: 98%.  $^1H$  NMR (600 MHz, DMSO- $d_6$ )  $\delta$  12.64 (s, 1H), 9.20 (s, 1H), 8.56 (s, 1H), 8.32 (d,  $J = 8.1$  Hz, 1H), 8.14 (d,  $J = 1.7$  Hz, 1H), 8.07–7.96 (m, 3H), 7.76 (dd,  $J = 8.4, 1.7$  Hz, 1H), 7.61–7.55 (m, 2H), 7.54 (dd,  $J = 7.5, 1.6$  Hz, 1H), 7.50–7.37 (m, 4H), 7.06–7.02 (m, 2H), 6.66–6.62 (m, 2H), 6.52 (d,  $J = 15.7$  Hz, 1H), 4.44 (ddd,  $J = 9.7, 8.1, 4.7$  Hz, 1H), 2.97 (dd,  $J = 13.9, 4.7$  Hz, 1H), 2.80 (dd,  $J = 13.9, 9.7$  Hz, 1H), 2.35 (s, 3H);  $^{13}C$  NMR (151 MHz, DMSO- $d_6$ )  $\delta$  173.78, 170.81, 165.69, 156.36, 151.48, 139.63, 133.40, 133.22, 133.04, 132.06, 131.90, 130.47, 130.44, 130.07, 129.13, 128.76, 128.68, 128.24, 128.12, 127.66, 127.32, 127.05, 127.02, 126.70, 126.26, 121.70, 116.85, 115.44 (2C), 54.57, 36.42, 18.50; ESI-MS:  $m/z$  518.2  $[M + H]^+$ , ESI-HRMS: calcd for  $C_{32}H_{28}O_4N_3$   $[M + H]^+$  518.2074, found 518.2073.

4.1.1.47. (*Z*)-(3-(3-(Naphthalen-2-yl)-1-(*o*-tolyl)-1H-pyrazol-4-yl)acryloyl)-L-phenylalanine (**GQN-B27-Z**). Yield: 99%, purity: 96%.  $^1H$  NMR (600 MHz, DMSO- $d_6$ )  $\delta$  12.66 (s, 1H), 8.91 (s, 1H), 8.53 (d,  $J = 8.0$  Hz, 1H), 8.11 (d,  $J = 1.7$  Hz, 1H), 8.06–8.01 (m, 2H), 8.00–7.95 (m, 1H), 7.76 (dd,  $J = 8.4, 1.7$  Hz, 1H), 7.60–7.54 (m, 2H), 7.49–7.36 (m, 4H), 7.29–7.22 (m, 4H), 7.16 (tt,  $J = 6.1, 2.3$  Hz, 1H), 6.73 (d,  $J = 12.5$  Hz, 1H), 5.98 (d,  $J = 12.6$  Hz, 1H), 4.54 (ddd,  $J = 9.9, 8.0, 4.7$  Hz, 1H), 3.12 (dd,  $J = 13.9, 4.7$  Hz, 1H), 2.90 (dd,  $J = 13.9, 9.9$  Hz, 1H), 2.30 (s, 3H);  $^{13}C$  NMR (151 MHz, DMSO- $d_6$ )  $\delta$  173.66, 166.19, 153.01, 139.62, 138.26, 135.59, 133.31, 133.25, 132.98, 131.92, 130.25, 129.55 (2C), 129.12, 129.09, 128.73, 128.65 (2C), 128.63, 128.30, 128.07, 127.36, 127.13, 127.00, 126.98, 126.86, 126.11, 120.17, 115.28, 54.05, 37.21, 18.44; ESI-MS:  $m/z$  502.2  $[M + H]^+$ , ESI-HRMS: calcd for  $C_{32}H_{28}O_3N_3$   $[M + H]^+$  502.2125, found 502.2124.

4.1.1.48. (*E*)-(3-(3-(Naphthalen-2-yl)-1-(*o*-tolyl)-1H-pyrazol-4-yl)acryloyl)-L-phenylalanine (**GQN-B27-E**). Yield: 99%, purity: 99%.  $^1H$  NMR (600 MHz, DMSO- $d_6$ )  $\delta$  12.55 (s, 1H), 8.57 (s, 1H), 8.40 (d,  $J = 8.1$  Hz, 1H), 8.15–8.12 (m, 1H), 8.05 (d,  $J = 8.5$  Hz, 1H), 8.04–7.97 (m, 2H), 7.76 (dd,  $J = 8.5, 1.7$  Hz, 1H), 7.59–7.56 (m, 2H), 7.54 (dd,  $J = 7.6, 1.6$  Hz, 1H), 7.51–7.37 (m, 4H), 7.27–7.24 (m, 4H), 7.19 (ddd,  $J = 8.7, 5.0, 3.8$  Hz, 1H), 6.51 (d,  $J = 15.7$  Hz, 1H), 4.53 (ddd,  $J = 9.9, 8.1, 4.7$  Hz, 1H), 3.10 (dd,  $J = 13.9, 4.7$  Hz, 1H), 2.92 (dd,  $J = 13.9, 9.9$  Hz, 1H), 2.35 (s, 3H);  $^{13}C$  NMR (151 MHz, DMSO- $d_6$ )  $\delta$  173.65, 165.74, 151.50, 139.62, 138.28, 133.40, 133.22, 133.04, 132.08, 131.89, 130.44, 130.16, 129.54 (2C), 129.13, 128.76, 128.67, 128.65 (2C), 128.13, 127.67, 127.32, 127.05, 127.02, 126.87, 126.70, 126.27, 121.60, 116.82, 54.21, 37.13, 18.49; ESI-MS:  $m/z$  502.2  $[M + H]^+$ , ESI-HRMS: calcd for  $C_{32}H_{28}O_3N_3$   $[M + H]^+$  502.2125, found 502.2126.

4.1.1.49. (*Z*)-(3-(3-(Naphthalen-2-yl)-1-(*p*-tolyl)-1H-pyrazol-4-yl)acryloyl)-L-tryptophan (**GQN-B28-Z**). Yield: 99%, purity: 96%.  $^1H$  NMR (600 MHz, DMSO- $d_6$ )  $\delta$  12.68 (s, 1H), 10.86 (d,  $J = 2.4$  Hz, 1H), 9.29 (s, 1H), 8.53 (d,  $J = 7.8$  Hz, 1H), 8.12 (d,  $J = 1.7$  Hz, 1H), 8.09–8.02 (m, 2H), 7.99 (dt,  $J = 7.1, 3.6$

Hz, 1H), 7.79 (dd,  $J = 8.4, 1.7$  Hz, 1H), 7.74–7.70 (m, 2H), 7.63–7.56 (m, 3H), 7.34 (dd,  $J = 8.2, 6.2$  Hz, 3H), 7.19 (d,  $J = 2.2$  Hz, 1H), 7.07 (t,  $J = 7.3$  Hz, 1H), 7.00 (t,  $J = 7.4$  Hz, 1H), 6.70 (d,  $J = 12.6$  Hz, 1H), 6.03 (d,  $J = 12.6$  Hz, 1H), 4.66–4.61 (m, 1H), 3.27 (dd,  $J = 14.7, 4.8$  Hz, 1H), 3.09 (dd,  $J = 14.7, 9.2$  Hz, 1H), 2.37 (s, 3H);  $^{13}\text{C}$  NMR (151 MHz, DMSO- $d_6$ )  $\delta$  174.09, 166.15, 153.49, 137.45, 136.74, 136.58, 133.29, 133.05, 131.38, 130.58 (2C), 130.15, 128.76, 128.65, 128.29, 128.09, 127.63, 127.60, 127.06 (2C), 127.02, 124.10, 121.42, 120.83, 119.20 (2C), 118.88, 118.65, 116.44, 111.89, 110.50, 53.57, 27.57, 20.98; ESI-MS:  $m/z$  541.2 [M + H] $^+$ , ESI-HRMS: calcd for  $\text{C}_{34}\text{H}_{29}\text{O}_3\text{N}_4$  [M + H] $^+$  541.2234, found 541.2233.

**4.1.1.50. (E)-(3-(3-(Naphthalen-2-yl)-1-(p-tolyl)-1H-pyrazol-4-yl)acryloyl)-L-tryptophan (GQN-B28-E).** Yield: 98%, purity: 97%.  $^1\text{H}$  NMR (600 MHz, DMSO- $d_6$ )  $\delta$  12.67 (s, 1H), 10.85 (d,  $J = 2.5$  Hz, 1H), 8.95 (s, 1H), 8.40 (d,  $J = 7.9$  Hz, 1H), 8.15 (d,  $J = 1.7$  Hz, 1H), 8.06 (d,  $J = 8.5$  Hz, 1H), 8.01 (ddd,  $J = 24.2, 6.2, 3.4$  Hz, 2H), 7.88–7.84 (m, 2H), 7.78 (dd,  $J = 8.4, 1.7$  Hz, 1H), 7.60–7.54 (m, 3H), 7.47 (d,  $J = 15.7$  Hz, 1H), 7.35 (dd,  $J = 15.7, 8.1$  Hz, 3H), 7.16 (d,  $J = 2.2$  Hz, 1H), 7.09–7.03 (m, 1H), 6.97 (t,  $J = 7.4$  Hz, 1H), 6.57 (d,  $J = 15.7$  Hz, 1H), 4.63–4.56 (m, 1H), 3.23 (dd,  $J = 14.7, 4.8$  Hz, 1H), 3.08 (dd,  $J = 14.7, 9.2$  Hz, 1H), 2.37 (s, 3H);  $^{13}\text{C}$  NMR (151 MHz, DMSO- $d_6$ )  $\delta$  174.02, 165.64, 151.93, 137.40, 136.82, 136.57, 133.37, 133.10, 130.49 (2C), 130.31, 129.91, 128.79, 128.72, 128.14, 128.05, 127.68, 127.62, 127.09 (2C), 126.63, 124.04, 122.00, 121.41, 119.12 (2C), 118.86, 118.63, 118.03, 111.86, 110.52, 53.64, 26.81, 20.98; ESI-MS:  $m/z$  541.2 [M + H] $^+$ , ESI-HRMS: calcd for  $\text{C}_{34}\text{H}_{29}\text{O}_3\text{N}_4$  [M + H] $^+$  541.2234, found 541.2231.

**4.1.1.51. (Z)-(3-(1-(3-Chlorophenyl)-3-(3,5-dimethylphenyl)-1H-pyrazol-4-yl)acryloyl)-L-tryptophan (GQN-B29-Z).** Yield: 99%, purity: 98%.  $^1\text{H}$  NMR (600 MHz, DMSO- $d_6$ )  $\delta$  10.78 (s, 1H), 9.34 (s, 1H), 8.24 (d,  $J = 7.8$  Hz, 1H), 7.90 (d,  $J = 2.2$  Hz, 1H), 7.78 (dd,  $J = 8.2, 2.2$  Hz, 1H), 7.58–7.50 (m, 2H), 7.39 (dd,  $J = 8.1, 2.1$  Hz, 1H), 7.29 (d,  $J = 8.0$  Hz, 1H), 7.19 (s, 2H), 7.15 (d,  $J = 2.1$  Hz, 1H), 7.09 (s, 1H), 7.02 (t,  $J = 7.5$  Hz, 1H), 6.93 (t,  $J = 7.4$  Hz, 1H), 6.50 (d,  $J = 12.6$  Hz, 1H), 5.99 (d,  $J = 12.6$  Hz, 1H), 4.51 (dt,  $J = 12.2, 5.8$  Hz, 1H), 3.29 (dd,  $J = 14.7, 4.6$  Hz, 1H), 3.05 (dd,  $J = 14.7, 8.6$  Hz, 1H), 2.34 (s, 6H);  $^{13}\text{C}$  NMR (151 MHz, DMSO- $d_6$ )  $\delta$  174.34, 165.61, 154.28, 140.80, 138.17 (2C), 136.49, 134.50, 132.26, 131.92, 131.55, 130.39, 128.01, 127.47, 126.97 (2C), 126.83, 123.88, 123.72, 121.15, 118.89, 118.85, 118.61, 117.61, 116.80, 111.69, 111.41, 60.23, 27.91, 21.40 (2C); ESI-MS:  $m/z$  539.2 [M + H] $^+$ , ESI-HRMS: calcd for  $\text{C}_{31}\text{H}_{28}\text{O}_3\text{N}_4\text{Cl}$  [M + H] $^+$  539.1844, found 539.1838.

**4.1.1.52. (E)-(3-(1-(3-Chlorophenyl)-3-(3,5-dimethylphenyl)-1H-pyrazol-4-yl)acryloyl)-L-tryptophan (GQN-B29-E).** Yield: 91%, purity: 99%.  $^1\text{H}$  NMR (600 MHz, DMSO- $d_6$ )  $\delta$  12.62 (s, 1H), 10.85 (s, 1H), 9.04 (s, 1H), 8.42 (d,  $J = 7.8$  Hz, 1H), 8.05 (t,  $J = 2.1$  Hz, 1H), 7.93 (dd,  $J = 8.1, 2.2$  Hz, 1H), 7.60–7.54 (m, 2H), 7.43 (dd,  $J = 8.0, 2.1$  Hz, 1H), 7.38–7.32 (m, 2H), 7.22 (s, 2H), 7.17 (d,  $J = 2.2$  Hz, 1H), 7.12 (s, 1H), 7.07 (t,  $J = 7.5$  Hz, 1H), 6.98 (t,  $J = 7.5$  Hz, 1H), 6.53 (d,  $J = 15.7$  Hz, 1H), 4.59 (td,  $J = 8.2, 4.7$  Hz, 1H), 3.24 (dd,  $J = 14.7, 4.7$  Hz, 1H), 3.09 (dd,  $J = 14.7, 9.3$  Hz, 1H), 2.35 (s, 6H);  $^{13}\text{C}$  NMR (151 MHz, DMSO- $d_6$ )  $\delta$  174.04, 165.55, 152.96, 140.69, 138.33 (2C), 136.57, 134.54, 132.32, 131.82, 130.57, 129.70, 128.31, 127.60, 126.96, 126.54 (2C), 124.04, 122.13, 121.41, 118.86, 118.79, 118.61, 118.38, 117.60, 111.87, 110.53, 53.68, 27.48, 21.43 (2C); ESI-MS:  $m/z$  539.2 [M + H] $^+$ , ESI-HRMS: calcd for  $\text{C}_{31}\text{H}_{28}\text{O}_3\text{N}_4\text{Cl}$  [M + H] $^+$  539.1844, found 539.1833.

**4.1.1.53. (Z)-(3-(1-(3-Chlorophenyl)-3-(4-nitrophenyl)-1H-pyrazol-4-yl)acryloyl)-L-tryptophan (GQN-B30-Z).** Yield:

97%, purity: 96%.  $^1\text{H}$  NMR (600 MHz, DMSO- $d_6$ )  $\delta$  12.52 (s, 1H), 10.84 (s, 1H), 9.23 (s, 1H), 8.57 (d,  $J = 7.8$  Hz, 1H), 8.38–8.30 (m, 2H), 7.98–7.88 (m, 3H), 7.79 (ddd,  $J = 8.2, 2.2, 0.9$  Hz, 1H), 7.56 (t,  $J = 8.0$  Hz, 2H), 7.46 (ddd,  $J = 8.1, 2.0, 0.9$  Hz, 1H), 7.32 (dd,  $J = 8.0, 1.0$  Hz, 1H), 7.17 (d,  $J = 2.2$  Hz, 1H), 7.05 (ddd,  $J = 8.1, 7.0, 1.2$  Hz, 1H), 6.98 (ddd,  $J = 7.9, 6.9, 1.0$  Hz, 1H), 6.65 (d,  $J = 12.5$  Hz, 1H), 6.11 (d,  $J = 12.5$  Hz, 1H), 4.63–4.56 (m, 1H), 3.24 (dd,  $J = 14.7, 4.8$  Hz, 1H), 3.07 (dd,  $J = 14.7, 9.1$  Hz, 1H);  $^{13}\text{C}$  NMR (151 MHz, DMSO- $d_6$ )  $\delta$  173.96, 165.63, 151.46, 147.64, 140.53, 138.89, 136.56, 134.61, 132.10, 131.98, 130.06 (2C), 127.81, 127.61, 127.42, 124.38 (2C), 124.11, 122.82, 121.41, 119.23, 118.86, 118.64, 117.90, 117.35, 111.86, 110.39, 53.56, 27.58; ESI-MS:  $m/z$  556.1 [M + H] $^+$ , ESI-HRMS: calcd for  $\text{C}_{29}\text{H}_{23}\text{O}_3\text{N}_4\text{Cl}$  [M + H] $^+$  556.1382, found 556.1381.

**4.1.1.54. (E)-(3-(1-(3-Chlorophenyl)-3-(4-nitrophenyl)-1H-pyrazol-4-yl)acryloyl)-L-tryptophan (GQN-B30-E).** Yield: 94%, purity: 99%.  $^1\text{H}$  NMR (600 MHz, DMSO- $d_6$ )  $\delta$  12.71 (s, 1H), 10.86 (s, 1H), 9.12 (s, 1H), 8.48 (d,  $J = 7.8$  Hz, 1H), 8.38 (d,  $J = 8.4$  Hz, 2H), 8.08 (s, 1H), 7.94 (dd,  $J = 14.1, 8.2$  Hz, 3H), 7.62–7.54 (m, 2H), 7.46 (d,  $J = 8.0$  Hz, 1H), 7.38 (d,  $J = 15.6$  Hz, 1H), 7.34 (d,  $J = 8.1$  Hz, 1H), 7.17 (s, 1H), 7.07 (t,  $J = 7.5$  Hz, 1H), 6.98 (t,  $J = 7.5$  Hz, 1H), 6.57 (d,  $J = 15.7$  Hz, 1H), 4.62 (dt,  $J = 12.5, 6.2$  Hz, 1H), 3.25 (dd,  $J = 14.8, 4.8$  Hz, 1H), 3.09 (dd,  $J = 14.7, 9.3$  Hz, 1H);  $^{13}\text{C}$  NMR (151 MHz, DMSO- $d_6$ )  $\delta$  173.98, 165.29, 150.22, 147.77, 140.46, 138.91, 136.58, 134.61, 131.90, 129.75 (2C), 129.31, 128.88, 127.61, 127.46, 124.58 (2C), 124.07, 123.46, 121.42, 119.07, 119.02, 118.87, 118.63, 117.83, 111.87, 110.47, 53.69, 27.54; ESI-MS:  $m/z$  556.1 [M + H] $^+$ , ESI-HRMS: calcd for  $\text{C}_{29}\text{H}_{23}\text{O}_3\text{N}_4\text{Cl}$  [M + H] $^+$  556.1382, found 556.1384.

**4.1.1.55. (Z)-(3-(1-(3-Chlorophenyl)-3-(5,6,7,8-tetrahydronaphthalen-2-yl)-1H-pyrazol-4-yl)acryloyl)-L-tryptophan (GQN-B31-Z).** Yield: 99%, purity: 97%.  $^1\text{H}$  NMR (600 MHz, DMSO- $d_6$ )  $\delta$  12.62 (s, 1H), 10.84 (d,  $J = 2.4$  Hz, 1H), 9.26 (s, 1H), 8.51 (d,  $J = 7.8$  Hz, 1H), 7.88 (t,  $J = 2.1$  Hz, 1H), 7.77–7.72 (m, 1H), 7.59–7.49 (m, 2H), 7.41 (dd,  $J = 8.2, 2.1$  Hz, 1H), 7.32 (d,  $J = 8.1$  Hz, 1H), 7.30–7.26 (m, 2H), 7.20–7.16 (m, 2H), 7.06 (ddd,  $J = 8.1, 6.9, 1.2$  Hz, 1H), 7.01–6.96 (m, 1H), 6.57 (d,  $J = 12.6$  Hz, 1H), 6.00 (d,  $J = 12.6$  Hz, 1H), 4.61 (ddt,  $J = 9.2, 4.9, 3.2$  Hz, 1H), 3.25 (dd,  $J = 14.7, 4.8$  Hz, 1H), 3.07 (dd,  $J = 14.7, 9.1$  Hz, 1H), 2.79 (dt,  $J = 10.8, 4.9$  Hz, 4H), 1.77 (h,  $J = 4.5, 3.9$  Hz, 4H);  $^{13}\text{C}$  NMR (151 MHz, DMSO- $d_6$ )  $\delta$  174.04, 166.02, 154.41, 140.78, 137.70, 137.47, 136.56, 134.53, 131.93, 131.59, 129.64 (2C), 129.43, 128.61, 127.61, 126.92, 126.40, 124.10, 121.41, 121.16, 118.93, 118.86, 118.64, 117.63, 116.66, 111.87, 110.45, 53.55, 29.24, 29.11, 27.56, 23.13 (2C); ESI-MS:  $m/z$  565.2 [M + H] $^+$ , ESI-HRMS: calcd for  $\text{C}_{33}\text{H}_{30}\text{O}_3\text{N}_4\text{Cl}$  [M + H] $^+$  565.2001, found 565.2005.

**4.1.1.56. (E)-(3-(1-(3-Chlorophenyl)-3-(5,6,7,8-tetrahydronaphthalen-2-yl)-1H-pyrazol-4-yl)acryloyl)-L-tryptophan (GQN-B31-E).** Yield: 92%, purity: 99%.  $^1\text{H}$  NMR (600 MHz, DMSO- $d_6$ )  $\delta$  12.52 (s, 1H), 10.85 (d,  $J = 2.5$  Hz, 1H), 9.02 (s, 1H), 8.42 (d,  $J = 7.9$  Hz, 1H), 8.04 (t,  $J = 2.1$  Hz, 1H), 7.92 (dd,  $J = 8.1, 2.2$  Hz, 1H), 7.60–7.53 (m, 2H), 7.42 (dd,  $J = 8.0, 2.0$  Hz, 1H), 7.38–7.31 (m, 3H), 7.29 (dd,  $J = 7.7, 1.9$  Hz, 1H), 7.19 (d,  $J = 7.9$  Hz, 1H), 7.16 (d,  $J = 2.1$  Hz, 1H), 7.09–7.04 (m, 1H), 6.98 (t,  $J = 7.2$  Hz, 1H), 6.53 (d,  $J = 15.7$  Hz, 1H), 4.59 (ddt,  $J = 9.4, 4.9, 3.1$  Hz, 1H), 3.23 (dd,  $J = 14.7, 4.8$  Hz, 1H), 3.08 (dd,  $J = 14.7, 9.3$  Hz, 1H), 2.78 (t,  $J = 6.3$  Hz, 4H), 1.77 (h,  $J = 4.6, 3.9$  Hz, 4H);  $^{13}\text{C}$  NMR (151 MHz, DMSO- $d_6$ )  $\delta$  174.02, 165.57, 152.91, 140.72, 137.82, 137.59, 136.58, 134.53, 131.81, 129.76 (2C), 129.55, 129.15, 128.31, 127.60, 126.91, 125.95, 124.04,

122.10, 121.41, 118.86, 118.76, 118.62, 118.32, 117.57, 111.87, 110.52, 53.65, 29.28, 29.12, 27.49, 23.12 (2C); ESI-MS:  $m/z$  565.2  $[M + H]^+$ , ESI-HRMS: calcd for  $C_{33}H_{30}O_3N_4Cl$   $[M + H]^+$  565.2001, found 565.2004.

4.1.1.57. (Z)-3-(1-(3-Chlorophenyl)-3-(4-methoxyphenyl)-1H-pyrazol-4-yl)acryloyl-L-tryptophan (**GQN-B32-Z**). Yield: 98%, purity: 96%.  $^1H$  NMR (600 MHz, DMSO- $d_6$ )  $\delta$  12.71 (s, 1H), 10.84 (d,  $J = 2.4$  Hz, 1H), 9.26 (s, 1H), 8.51 (d,  $J = 7.8$  Hz, 1H), 7.88 (t,  $J = 2.1$  Hz, 1H), 7.75 (ddd,  $J = 8.2, 2.2, 0.9$  Hz, 1H), 7.58–7.51 (m, 4H), 7.41 (ddd,  $J = 8.0, 2.1, 0.9$  Hz, 1H), 7.32 (d,  $J = 8.0$  Hz, 1H), 7.17 (d,  $J = 2.1$  Hz, 1H), 7.09–7.04 (m, 3H), 6.99 (ddd,  $J = 8.0, 7.0, 1.0$  Hz, 1H), 6.56 (d,  $J = 12.6$  Hz, 1H), 6.01 (d,  $J = 12.6$  Hz, 1H), 4.61 (ddt,  $J = 9.2, 4.9, 3.1$  Hz, 1H), 3.82 (s, 3H), 3.25 (dd,  $J = 14.7, 4.8$  Hz, 1H), 3.07 (dd,  $J = 14.7, 9.1$  Hz, 1H);  $^{13}C$  NMR (151 MHz, DMSO- $d_6$ )  $\delta$  174.05, 166.01, 160.03, 154.05, 140.78, 136.56, 134.54, 131.92, 131.57, 130.54 (2C), 128.59, 127.62, 126.88, 124.62, 124.10, 121.41, 121.17, 118.90, 118.86, 118.65, 117.58, 116.54, 114.62 (2C), 111.86, 110.46, 60.23, 55.70, 27.57; ESI-MS:  $m/z$  541.2  $[M + H]^+$ , ESI-HRMS: calcd for  $C_{30}H_{26}O_4N_4Cl$   $[M + H]^+$  541.1637, found 541.1637.

4.1.1.58. (E)-3-(1-(3-Chlorophenyl)-3-(4-methoxyphenyl)-1H-pyrazol-4-yl)acryloyl-L-tryptophan (**GQN-B32-E**). Yield: 92%, purity: 95%.  $^1H$  NMR (600 MHz, DMSO- $d_6$ )  $\delta$  12.69 (s, 1H), 10.85 (d,  $J = 2.4$  Hz, 1H), 9.02 (s, 1H), 8.42 (d,  $J = 7.9$  Hz, 1H), 8.04 (t,  $J = 2.1$  Hz, 1H), 7.92 (ddd,  $J = 8.2, 2.2, 0.9$  Hz, 1H), 7.58–7.53 (m, 4H), 7.41 (ddd,  $J = 8.0, 2.1, 0.9$  Hz, 1H), 7.37–7.32 (m, 2H), 7.16 (d,  $J = 2.1$  Hz, 1H), 7.10–7.05 (m, 3H), 6.98 (ddd,  $J = 7.9, 7.0, 1.0$  Hz, 1H), 6.53 (d,  $J = 15.7$  Hz, 1H), 4.59 (ddt,  $J = 9.4, 4.9, 3.1$  Hz, 1H), 3.82 (s, 3H), 3.24 (dd,  $J = 14.7, 4.8$  Hz, 1H), 3.09 (dd,  $J = 14.7, 9.3$  Hz, 1H);  $^{13}C$  NMR (151 MHz, DMSO- $d_6$ )  $\delta$  174.02, 165.54, 160.09, 152.55, 140.72, 136.57, 134.53, 131.80, 130.06 (2C), 129.79, 128.31, 127.62, 126.86, 124.74, 124.05, 122.14, 121.41, 118.86, 118.72, 118.63, 118.18, 117.51, 114.75 (2C), 111.86, 110.53, 60.23, 55.71, 27.51; ESI-MS:  $m/z$  541.2  $[M + H]^+$ , ESI-HRMS: calcd for  $C_{30}H_{26}O_4N_4Cl$   $[M + H]^+$  541.1637, found 541.1629.

4.1.1.59. (Z)-3-(1-(3-Chlorophenyl)-3-(4-cyclohexylphenyl)-1H-pyrazol-4-yl)acryloyl-L-tryptophan (**GQN-B33-Z**). Yield: 95%, purity: 98%.  $^1H$  NMR (600 MHz, DMSO- $d_6$ )  $\delta$  12.69 (s, 1H), 10.84 (d,  $J = 2.4$  Hz, 1H), 9.28 (s, 1H), 8.52 (d,  $J = 7.8$  Hz, 1H), 7.88 (t,  $J = 2.1$  Hz, 1H), 7.75 (ddd,  $J = 8.2, 2.2, 0.9$  Hz, 1H), 7.59–7.48 (m, 4H), 7.42 (ddd,  $J = 8.0, 2.1, 0.9$  Hz, 1H), 7.38–7.34 (m, 2H), 7.34–7.31 (m, 1H), 7.17 (d,  $J = 2.1$  Hz, 1H), 7.06 (ddd,  $J = 8.0, 6.9, 1.2$  Hz, 1H), 6.98 (ddd,  $J = 8.0, 7.0, 1.0$  Hz, 1H), 6.58 (d,  $J = 12.6$  Hz, 1H), 6.02 (d,  $J = 12.7$  Hz, 1H), 4.61 (ddt,  $J = 9.2, 4.9, 3.2$  Hz, 1H), 3.25 (dd,  $J = 14.7, 4.8$  Hz, 1H), 3.07 (dd,  $J = 14.7, 9.2$  Hz, 1H), 2.57 (tt,  $J = 11.8, 3.3$  Hz, 1H), 1.82 (td,  $J = 10.4, 9.9, 5.1$  Hz, 4H), 1.75–1.69 (m, 1H), 1.50–1.34 (m, 4H), 1.31–1.22 (m, 1H);  $^{13}C$  NMR (151 MHz, DMSO- $d_6$ )  $\delta$  174.04, 166.01, 154.24, 148.51, 140.77, 136.56, 134.54, 131.94, 131.63, 129.87, 129.21 (2C), 128.56, 127.61, 127.47 (2C), 126.94, 124.10, 121.41, 121.25, 118.93, 118.86, 118.64, 117.60, 116.65, 111.87, 110.45, 60.23, 44.06, 34.34 (2C), 27.56, 26.81 (2C), 26.06; ESI-MS:  $m/z$  593.2  $[M + H]^+$ , ESI-HRMS: calcd for  $C_{35}H_{34}O_3N_4Cl$   $[M + H]^+$  593.2314, found 593.2313.

4.1.1.60. (E)-3-(1-(3-Chlorophenyl)-3-(4-cyclohexylphenyl)-1H-pyrazol-4-yl)acryloyl-L-tryptophan (**GQN-B33-E**). Yield: 96%, purity: 97%.  $^1H$  NMR (600 MHz, DMSO- $d_6$ )  $\delta$  12.67 (s, 1H), 10.86 (s, 1H), 9.05 (s, 1H), 8.44 (d,  $J = 7.8$  Hz, 1H), 8.05 (s, 1H), 7.93 (d,  $J = 8.3$  Hz, 1H), 7.55 (dd,  $J = 23.6, 7.9$  Hz, 4H), 7.44–7.32 (m, 5H), 7.18 (s, 1H), 7.07 (t,  $J = 7.5$  Hz,

1H), 6.99 (t,  $J = 7.5$  Hz, 1H), 6.56 (d,  $J = 15.6$  Hz, 1H), 4.62–4.59 (m, 1H), 3.25 (dd,  $J = 15.1, 4.7$  Hz, 1H), 3.10 (dd,  $J = 14.7, 9.3$  Hz, 1H), 2.57 (t,  $J = 12.1$  Hz, 1H), 1.82 (t,  $J = 13.8$  Hz, 4H), 1.72 (d,  $J = 13.0$  Hz, 1H), 1.43 (dq,  $J = 25.5, 12.7$  Hz, 4H), 1.28–1.21 (m, 1H);  $^{13}C$  NMR (151 MHz, DMSO- $d_6$ )  $\delta$  174.04, 165.56, 152.79, 148.62, 140.72, 136.58, 134.54, 131.81, 129.93, 129.73, 128.72 (2C), 128.20, 127.63, 127.59 (2C), 126.93, 124.04, 122.25, 121.41, 118.86, 118.76, 118.64, 118.32, 117.53, 111.86, 110.54, 53.71, 44.07, 34.31 (2C), 27.52, 26.80 (2C), 26.05; ESI-MS:  $m/z$  593.2  $[M + H]^+$ , ESI-HRMS: calcd for  $C_{35}H_{34}O_3N_4Cl$   $[M + H]^+$  593.2314, found 593.2323.

4.1.1.61. (Z)-3-(1-(3-Chlorophenyl)-3-(4-ethylphenyl)-1H-pyrazol-4-yl)acryloyl-L-tryptophan (**GQN-B34-Z**). Yield: 96%, purity: 95%.  $^1H$  NMR (600 MHz, DMSO- $d_6$ )  $\delta$  12.72 (s, 1H), 10.84 (d,  $J = 2.4$  Hz, 1H), 9.29–9.26 (m, 1H), 8.52 (d,  $J = 7.8$  Hz, 1H), 7.89 (t,  $J = 2.1$  Hz, 1H), 7.75 (ddd,  $J = 8.2, 2.2, 0.9$  Hz, 1H), 7.58–7.50 (m, 4H), 7.42 (ddd,  $J = 8.0, 2.1, 0.9$  Hz, 1H), 7.37–7.31 (m, 3H), 7.18 (d,  $J = 2.1$  Hz, 1H), 7.06 (ddd,  $J = 8.1, 6.9, 1.2$  Hz, 1H), 6.99 (ddd,  $J = 8.0, 7.0, 1.0$  Hz, 1H), 6.58 (dd,  $J = 12.5, 0.7$  Hz, 1H), 6.02 (d,  $J = 12.6$  Hz, 1H), 4.61 (tdd,  $J = 6.5, 5.5, 3.2$  Hz, 1H), 3.28–3.22 (m, 1H), 3.07 (dd,  $J = 14.7, 9.2$  Hz, 1H), 2.68 (q,  $J = 7.6$  Hz, 2H), 1.23 (t,  $J = 7.6$  Hz, 3H);  $^{13}C$  NMR (151 MHz, DMSO- $d_6$ )  $\delta$  174.06, 166.00, 154.23, 144.76, 140.77, 136.56, 134.54, 131.94, 131.64, 129.71, 129.22 (2C), 128.56 (2C), 128.52, 127.62, 126.95, 124.10, 121.40, 121.29, 118.95, 118.86, 118.65, 117.62, 116.67, 111.86, 110.48, 60.23, 28.45, 27.57, 16.00; ESI-MS:  $m/z$  539.2  $[M + H]^+$ , ESI-HRMS: calcd for  $C_{31}H_{28}O_3N_4Cl$   $[M + H]^+$  539.1844, found 539.1854.

4.1.1.62. (E)-3-(1-(3-Chlorophenyl)-3-(4-ethylphenyl)-1H-pyrazol-4-yl)acryloyl-L-tryptophan (**GQN-B34-E**). Yield: 97%, purity: 96%.  $^1H$  NMR (600 MHz, DMSO- $d_6$ )  $\delta$  12.67 (s, 1H), 10.85 (d,  $J = 2.4$  Hz, 1H), 9.04 (s, 1H), 8.43 (d,  $J = 7.9$  Hz, 1H), 8.05 (t,  $J = 2.1$  Hz, 1H), 7.93 (ddd,  $J = 8.3, 2.2, 0.9$  Hz, 1H), 7.59–7.52 (m, 4H), 7.42 (ddd,  $J = 8.0, 2.1, 0.9$  Hz, 1H), 7.39–7.33 (m, 4H), 7.17 (d,  $J = 2.2$  Hz, 1H), 7.07 (ddd,  $J = 8.1, 7.0, 1.2$  Hz, 1H), 6.98 (td,  $J = 7.4, 6.9, 1.0$  Hz, 1H), 6.54 (d,  $J = 15.7$  Hz, 1H), 4.59 (ddt,  $J = 9.4, 4.9, 3.1$  Hz, 1H), 3.24 (dd,  $J = 14.7, 4.8$  Hz, 1H), 3.09 (dd,  $J = 14.7, 9.3$  Hz, 1H), 2.68 (q,  $J = 7.6$  Hz, 2H), 1.23 (t,  $J = 7.6$  Hz, 3H);  $^{13}C$  NMR (151 MHz, DMSO- $d_6$ )  $\delta$  174.02, 165.54, 152.77, 144.87, 140.71, 136.58, 134.54, 131.81, 129.80, 129.72, 128.74 (2C), 128.68 (2C), 128.30, 127.62, 126.94, 124.04, 122.24, 121.41, 118.86, 118.78, 118.63, 118.33, 117.56, 111.86, 110.53, 53.68, 28.47, 26.81, 15.98; ESI-MS:  $m/z$  539.2  $[M + H]^+$ , ESI-HRMS: calcd for  $C_{31}H_{28}O_3N_4Cl$   $[M + H]^+$  539.1844, found 539.1849.

4.1.1.63. Methyl-(E)-3-(3-(naphthalen-2-yl)-1-phenyl-1H-pyrazol-4-yl)acryloyl-L-tryptophanate (**GQN-B18-Me**). Yield: 67%, purity: 97%.  $^1H$  NMR (600 MHz, DMSO- $d_6$ )  $\delta$  10.88 (s, 1H), 9.03 (s, 1H), 8.57 (d,  $J = 7.6$  Hz, 1H), 8.18–8.15 (m, 1H), 8.07 (d,  $J = 8.5$  Hz, 1H), 8.05–7.97 (m, 4H), 7.79 (dd,  $J = 8.4, 1.7$  Hz, 1H), 7.62–7.47 (m, 6H), 7.42–7.37 (m, 1H), 7.35 (d,  $J = 8.1$  Hz, 1H), 7.18 (d,  $J = 2.4$  Hz, 1H), 7.07 (ddd,  $J = 8.1, 6.9, 1.1$  Hz, 1H), 6.99 (td,  $J = 7.4, 6.9, 1.0$  Hz, 1H), 6.58 (d,  $J = 15.7$  Hz, 1H), 4.64 (ddd,  $J = 8.9, 7.6, 5.5$  Hz, 1H), 3.61 (s, 3H), 3.20 (td,  $J = 14.3, 5.3$  Hz, 1H), 3.11 (dd,  $J = 14.6, 8.9$  Hz, 1H).  $^{13}C$  NMR (151 MHz, DMSO- $d_6$ )  $\delta$  172.42, 165.06, 151.60, 138.95, 135.96, 132.73, 132.51, 129.59, 129.53, 129.50 (2C), 128.19, 128.09, 127.71, 127.52, 127.12, 126.87, 126.79, 126.49 (2C), 125.98, 123.52, 121.19, 120.84, 118.58 (2C), 118.29, 117.83, 117.56, 111.30, 109.44, 53.16, 51.71, 26.87. ESI-MS:  $m/z$  541.2  $[M + H]^+$ , ESI-HRMS: calcd for  $C_{34}H_{28}N_4O_3$   $[M + H]^+$  541.2234, found 541.2224.

4.1.1.64. *Methyl-(E)-(3-(1-(3-chlorophenyl)-3-(4-cyclohexylphenyl)-1H-pyrazol-4-yl)acryloyl)-L-tryptophanate (GQN-B33-Me)*. Yield: 69%, purity: 98%.  $^1\text{H}$  NMR (600 MHz, DMSO- $d_6$ )  $\delta$  10.88 (d,  $J$  = 2.5 Hz, 1H), 9.07 (s, 1H), 8.59 (d,  $J$  = 7.5 Hz, 1H), 8.05 (t,  $J$  = 2.1 Hz, 1H), 7.95–7.90 (m, 1H), 7.57 (t,  $J$  = 8.1 Hz, 1H), 7.53 (dd,  $J$  = 8.0, 3.5 Hz, 3H), 7.44–7.41 (m, 1H), 7.39–7.33 (m, 4H), 7.17 (d,  $J$  = 2.1 Hz, 1H), 7.09–7.05 (m, 1H), 7.01–6.97 (m, 1H), 6.54 (d,  $J$  = 15.7 Hz, 1H), 4.66–4.59 (m, 1H), 3.62 (s, 3H), 3.21 (dd,  $J$  = 14.6, 5.4 Hz, 1H), 3.11 (dd,  $J$  = 14.6, 9.0 Hz, 1H), 2.57 (tt,  $J$  = 11.8, 3.3 Hz, 1H), 1.86–1.79 (m, 4H), 1.72 (dd,  $J$  = 13.0, 4.0 Hz, 1H), 1.50–1.34 (m, 4H), 1.26 (dddd,  $J$  = 15.9, 12.6, 8.2, 3.7 Hz, 1H);  $^{13}\text{C}$  NMR (151 MHz, DMSO- $d_6$ )  $\delta$  173.06, 165.64, 152.84, 148.65, 140.71, 136.59, 134.54, 131.83, 130.05, 129.91, 128.74 (2C), 128.29, 127.60 (2C), 127.49, 126.96, 124.15, 121.86, 121.47, 118.92, 118.78, 118.47, 118.25, 117.56, 111.93, 110.07, 53.82, 52.35, 44.06, 34.32 (2C), 27.47, 26.80 (2C), 26.05; ESI-MS:  $m/z$  607.2  $[\text{M} + \text{H}]^+$ , ESI-HRMS: calcd for  $\text{C}_{36}\text{H}_{36}\text{O}_3\text{N}_4\text{Cl}$   $[\text{M} + \text{H}]^+$  607.2470, found 607.2478.

4.1.1.65. *(Z)-(3-(3-(4-Aminophenyl)-1-(3-chlorophenyl)-1H-pyrazol-4-yl)acryloyl)-L-tryptophan (GQN-B35-Z)*. Yield: 91%, purity: 98%.  $^1\text{H}$  NMR (600 MHz, DMSO- $d_6$ )  $\delta$  10.85 (s, 1H), 9.23 (s, 1H), 8.48 (d,  $J$  = 7.8 Hz, 1H), 7.86 (s, 1H), 7.72 (d,  $J$  = 8.2 Hz, 1H), 7.57 (d,  $J$  = 7.9 Hz, 1H), 7.53 (t,  $J$  = 8.1 Hz, 1H), 7.39 (dd,  $J$  = 8.0, 2.0 Hz, 1H), 7.33 (d,  $J$  = 8.1 Hz, 1H), 7.28 (d,  $J$  = 8.2 Hz, 2H), 7.18 (s, 1H), 7.06 (t,  $J$  = 7.5 Hz, 1H), 6.99 (t,  $J$  = 7.4 Hz, 1H), 6.68 (d,  $J$  = 8.2 Hz, 2H), 6.57 (d,  $J$  = 12.6 Hz, 1H), 5.98 (d,  $J$  = 12.6 Hz, 1H), 4.61 (td,  $J$  = 8.4, 4.8 Hz, 1H), 3.25 (dd,  $J$  = 14.7, 4.8 Hz, 1H), 3.08 (dd,  $J$  = 14.7, 9.1 Hz, 1H).  $^{13}\text{C}$  NMR (151 MHz, DMSO- $d_6$ )  $\delta$  173.46, 165.49, 154.44, 149.04, 140.24, 135.93, 133.87, 131.25, 130.71, 129.44 (2C), 128.47, 126.99, 125.96, 123.46, 120.77, 119.88, 118.74, 118.23, 118.08, 118.01, 116.73, 115.62, 113.53 (2C), 111.23, 109.84, 52.92, 26.94. ESI-MS:  $m/z$  526.2  $[\text{M} + \text{H}]^+$ , ESI-HRMS: calcd for  $\text{C}_{29}\text{H}_{24}\text{ClN}_5\text{O}_3$   $[\text{M} + \text{H}]^+$  526.1640, found 526.1627.

4.1.1.66. *(E)-(3-(3-(4-Aminophenyl)-1-(3-chlorophenyl)-1H-pyrazol-4-yl)acryloyl)-L-tryptophan (GQN-B35-E)*. Yield: 98%, purity: 95%.  $^1\text{H}$  NMR (600 MHz, DMSO- $d_6$ )  $\delta$  10.85 (s, 1H), 8.96 (s, 1H), 8.40 (d,  $J$  = 7.8 Hz, 1H), 8.02 (s, 1H), 7.90 (d,  $J$  = 8.2 Hz, 1H), 7.59–7.53 (m, 2H), 7.41–7.36 (m, 2H), 7.36–7.32 (m, 2H), 7.30 (d,  $J$  = 8.0 Hz, 2H), 7.17 (s, 1H), 7.07 (t,  $J$  = 7.5 Hz, 1H), 6.99 (t,  $J$  = 7.5 Hz, 1H), 6.69 (d,  $J$  = 8.0 Hz, 2H), 6.52 (d,  $J$  = 15.7 Hz, 1H), 4.60 (td,  $J$  = 8.5, 4.8 Hz, 1H), 3.24 (dd,  $J$  = 14.7, 4.9 Hz, 1H), 3.09 (dd,  $J$  = 14.6, 9.5 Hz, 1H).  $^{13}\text{C}$  NMR (151 MHz, DMSO- $d_6$ )  $\delta$  173.43, 165.04, 152.89, 149.17, 140.18, 135.94, 133.86, 131.12, 129.67, 128.93 (2C), 127.31, 126.98, 125.93, 123.41, 120.94, 120.78, 118.85, 118.23, 118.00, 117.90, 117.23, 116.68, 113.59 (2C), 111.23, 109.90, 53.02, 26.89. ESI-MS:  $m/z$  526.2  $[\text{M} + \text{H}]^+$ , ESI-HRMS: calcd for  $\text{C}_{29}\text{H}_{24}\text{ClN}_5\text{O}_3$   $[\text{M} + \text{H}]^+$  526.1640, found 526.1632.

4.1.1.67. *Methyl-(E)-(3-(3-(4-aminophenyl)-1-(3-chlorophenyl)-1H-pyrazol-4-yl)acryloyl)-L-tryptophanate (GQN-B35-Me)*. Yield: 25%, purity: 96%.  $^1\text{H}$  NMR (600 MHz, DMSO- $d_6$ )  $\delta$  10.88 (s, 1H), 8.98 (s, 1H), 8.56 (d,  $J$  = 7.5 Hz, 1H), 8.03 (d,  $J$  = 2.5 Hz, 1H), 7.91 (d,  $J$  = 8.2 Hz, 1H), 7.57–7.51 (m, 2H), 7.40 (d,  $J$  = 7.4 Hz, 2H), 7.37–7.33 (m, 1H), 7.32–7.28 (m, 2H), 7.18 (s, 1H), 7.08 (t,  $J$  = 7.5 Hz, 1H), 7.00 (t,  $J$  = 7.6 Hz, 1H), 6.69 (d,  $J$  = 8.0 Hz, 2H), 6.51 (dd,  $J$  = 15.7, 2.0 Hz, 1H), 5.42 (s, 2H), 4.64 (q,  $J$  = 7.5 Hz, 1H), 3.62 (s, 3H), 3.22 (dd,  $J$  = 14.8, 5.4 Hz, 1H), 3.12 (dd,  $J$  = 14.6, 8.5 Hz, 1H).  $^{13}\text{C}$  NMR (151 MHz, DMSO- $d_6$ )  $\delta$  172.46, 165.13, 152.92, 149.15, 140.18, 135.96, 133.87, 131.13, 129.99, 128.94 (2C), 127.41, 126.87, 125.96, 123.52, 120.84, 120.59, 118.86, 118.29,

117.91, 117.84, 117.18, 116.70, 113.62 (2C), 111.30, 109.46, 53.17, 51.71, 26.86. ESI-MS:  $m/z$  540.2  $[\text{M} + \text{H}]^+$ , ESI-HRMS: calcd for  $\text{C}_{30}\text{H}_{26}\text{ClN}_5\text{O}_3$   $[\text{M} + \text{H}]^+$  540.1797, found 540.1790.

4.1.1.68. *(Z)-(3-(1-(3-Chlorophenyl)-3-(4-morpholinophenyl)-1H-pyrazol-4-yl)acryloyl)-L-tryptophan (GQN-B36-Z)*. Yield: 98%, purity: 99%.  $^1\text{H}$  NMR (600 MHz, DMSO- $d_6$ )  $\delta$  12.74 (s, 1H), 10.85 (s, 1H), 9.27–9.24 (m, 1H), 8.50 (d,  $J$  = 7.6 Hz, 1H), 7.88 (s, 1H), 7.77–7.72 (m, 1H), 7.58 (dd,  $J$  = 8.2, 2.9 Hz, 1H), 7.54 (t,  $J$  = 8.1 Hz, 1H), 7.48 (d,  $J$  = 8.4 Hz, 2H), 7.41 (d,  $J$  = 7.9 Hz, 1H), 7.33 (d,  $J$  = 8.0 Hz, 1H), 7.19 (s, 1H), 7.08–7.04 (m, 3H), 6.99 (t,  $J$  = 7.5 Hz, 1H), 6.58 (d,  $J$  = 12.5 Hz, 1H), 6.04–5.99 (m, 1H), 4.62 (dd,  $J$  = 8.5, 5.0 Hz, 1H), 3.77 (t,  $J$  = 4.6 Hz, 3H), 3.26 (dd,  $J$  = 14.7, 4.8 Hz, 1H), 3.21–3.17 (m, 4H), 3.08 (ddd,  $J$  = 14.8, 9.5, 3.6 Hz, 1H).  $^{13}\text{C}$  NMR (151 MHz, DMSO- $d_6$ )  $\delta$  173.48, 165.42, 153.67, 150.90, 140.19, 135.93, 133.90, 131.27, 130.88, 129.33 (2C), 128.13, 127.01, 126.14, 123.46, 122.04, 120.77, 120.35, 118.22, 118.21, 118.02, 116.86, 115.86, 114.56 (2C), 111.23, 109.87, 65.87 (2C), 52.97, 47.78 (2C), 26.96. ESI-MS:  $m/z$  596.2  $[\text{M} + \text{H}]^+$ , ESI-HRMS: calcd for  $\text{C}_{33}\text{H}_{30}\text{ClN}_5\text{O}_4$   $[\text{M} + \text{H}]^+$  596.2059, found 596.2044.

4.1.1.69. *(E)-(3-(1-(3-Chlorophenyl)-3-(4-morpholinophenyl)-1H-pyrazol-4-yl)acryloyl)-L-tryptophan (GQN-B36-E)*. Yield: 97%, purity: 99%.  $^1\text{H}$  NMR (600 MHz, DMSO- $d_6$ )  $\delta$  10.85 (s, 1H), 9.00 (s, 1H), 8.38 (d,  $J$  = 7.8 Hz, 1H), 8.04 (s, 1H), 7.91 (d,  $J$  = 8.2 Hz, 1H), 7.59–7.47 (m, 4H), 7.43–7.36 (m, 1H), 7.36–7.32 (m, 2H), 7.17 (s, 1H), 7.10–7.04 (m, 3H), 6.98 (t,  $J$  = 7.5 Hz, 1H), 6.54 (d,  $J$  = 15.7 Hz, 1H), 4.59 (dt,  $J$  = 8.9, 4.8 Hz, 1H), 3.76 (t,  $J$  = 4.8 Hz, 4H), 3.25 (dd,  $J$  = 14.7, 4.5 Hz, 1H), 3.19 (t,  $J$  = 4.9 Hz, 4H), 3.15–3.06 (m, 1H).  $^{13}\text{C}$  NMR (151 MHz, DMSO- $d_6$ )  $\delta$  173.54, 164.90, 152.15, 150.95, 140.13, 135.93, 133.88, 131.15, 129.27, 128.82 (2C), 127.51, 127.05, 126.11, 123.38, 122.13, 121.46, 120.74, 118.20, 118.02, 117.52, 116.80, 114.65 (2C), 114.47, 111.20, 110.02, 65.86 (2C), 53.20, 47.74 (2C), 26.93. ESI-MS:  $m/z$  596.2  $[\text{M} + \text{H}]^+$ , ESI-HRMS: calcd for  $\text{C}_{33}\text{H}_{30}\text{ClN}_5\text{O}_4$   $[\text{M} + \text{H}]^+$  596.2059, found 596.2041.

4.1.1.70. *Methyl-(E)-(3-(1-(3-chlorophenyl)-3-(4-morpholinophenyl)-1H-pyrazol-4-yl)acryloyl)-L-tryptophanate (GQN-B36-Me)*. Yield: 21%, purity: 97%.  $^1\text{H}$  NMR (600 MHz,  $\text{CDCl}_3$ )  $\delta$  8.09 (s, 1H), 7.79 (s, 1H), 7.68–7.56 (m, 4H), 7.56–7.48 (m, 2H), 7.44–7.35 (m, 2H), 7.28 (s, 2H), 7.21–7.15 (m, 2H), 7.14–7.06 (m, 2H), 7.05–6.94 (m, 1H), 6.16 (s, 1H), 5.10 (s, 1H), 3.97 (s, 4H), 3.73 (s, 3H), 3.40 (s, 2H), 3.26 (s, 4H).  $^{13}\text{C}$  NMR (151 MHz,  $\text{CDCl}_3$ )  $\delta$  172.51, 165.42, 140.38, 136.18, 135.39, 130.62 (2C), 129.75 (2C), 127.75, 126.90 (2C), 123.07, 122.23 (3C), 119.69 (2C), 119.50 (2C), 118.67 (2C), 118.09, 117.04, 111.42 (2C), 109.99, 72.14, 70.92, 61.73, 53.00, 52.54, 29.70, 27.76. ESI-MS:  $m/z$  610.2  $[\text{M} + \text{H}]^+$ , ESI-HRMS: calcd for  $\text{C}_{34}\text{H}_{32}\text{ClN}_5\text{O}_4$   $[\text{M} + \text{H}]^+$  610.2216, found 610.2188.

4.1.1.71. *(Z)-(3-(1-(3-Chlorophenyl)-3-(4-hydroxyphenyl)-1H-pyrazol-4-yl)acryloyl)-L-tryptophan (GQN-B37-Z)*. Yield: 98%, purity: 99%.  $^1\text{H}$  NMR (600 MHz, DMSO- $d_6$ )  $\delta$  12.68 (s, 1H), 10.84 (s, 1H), 9.74 (s, 1H), 9.26 (s, 1H), 8.50 (d,  $J$  = 7.7 Hz, 1H), 7.88 (d,  $J$  = 2.2 Hz, 1H), 7.74 (d,  $J$  = 8.3 Hz, 1H), 7.63–7.50 (m, 2H), 7.47–7.39 (m, 3H), 7.33 (d,  $J$  = 8.4 Hz, 1H), 7.18 (s, 1H), 7.10–7.04 (m, 1H), 7.04–6.97 (m, 1H), 6.90 (d,  $J$  = 8.0 Hz, 2H), 6.57 (d,  $J$  = 12.6 Hz, 1H), 6.01 (d,  $J$  = 12.6 Hz, 1H), 4.62 (td,  $J$  = 8.8, 5.1 Hz, 1H), 3.26 (dd,  $J$  = 14.8, 5.1 Hz, 1H), 3.08 (dd,  $J$  = 14.8, 9.0 Hz, 1H).  $^{13}\text{C}$  NMR (151 MHz, DMSO- $d_6$ )  $\delta$  173.45, 165.43, 157.74, 153.83, 140.18, 135.93, 133.90, 131.27, 130.85, 129.94 (2C), 129.44, 128.13, 127.00, 126.15, 123.46, 122.36, 120.77, 120.31, 118.22, 118.01, 116.86, 115.80, 115.32 (2C), 111.23, 109.84, 52.93, 26.94. ESI-MS:  $m/z$  527.2

[M + H]<sup>+</sup>, ESI-HRMS: calcd for C<sub>29</sub>H<sub>23</sub>ClN<sub>4</sub>O<sub>4</sub> [M + H]<sup>+</sup> 527.1481, found 527.1460.

4.1.1.72. (E)-3-(1-(3-Chlorophenyl)-3-(4-hydroxyphenyl)-1H-pyrazol-4-yl)acryloyl-L-tryptophan (**GQN-B37-E**). Yield: 96%, purity: 96%. <sup>1</sup>H NMR (600 MHz, DMSO-*d*<sub>6</sub>) δ 12.60 (s, 1H), 10.85 (d, *J* = 2.4 Hz, 1H), 9.76 (s, 1H), 9.00 (s, 1H), 8.42 (d, *J* = 7.9 Hz, 1H), 8.04 (s, 1H), 7.92 (d, *J* = 8.3 Hz, 1H), 7.59–7.51 (m, 2H), 7.47–7.43 (m, 2H), 7.41 (dd, *J* = 7.9, 1.9 Hz, 1H), 7.38–7.32 (m, 2H), 7.17 (d, *J* = 2.5 Hz, 1H), 7.07 (t, *J* = 7.5 Hz, 1H), 6.99 (t, *J* = 7.5 Hz, 1H), 6.94–6.89 (m, 2H), 6.53 (d, *J* = 15.7 Hz, 1H), 4.60 (tt, *J* = 8.3, 3.8 Hz, 1H), 3.24 (dd, *J* = 14.7, 4.7 Hz, 1H), 3.09 (dd, *J* = 15.0, 9.6 Hz, 1H). <sup>13</sup>C NMR (151 MHz, DMSO-*d*<sub>6</sub>) δ 173.42, 164.96, 157.81, 152.29, 140.12, 135.95, 133.89, 131.15, 129.44 (2C), 129.34, 127.55, 126.98, 126.13, 123.41, 122.49, 121.29, 120.78, 118.23, 118.03, 118.00, 117.43, 116.81, 115.44 (2C), 111.24, 109.90, 53.04, 26.89. ESI-MS: *m/z* 527.2 [M + H]<sup>+</sup>, ESI-HRMS: calcd for C<sub>29</sub>H<sub>23</sub>ClN<sub>4</sub>O<sub>4</sub> [M + H]<sup>+</sup> 527.1481, found 527.1464.

4.1.1.73. Methyl-(E)-3-(1-(3-chlorophenyl)-3-(4-hydroxyphenyl)-1H-pyrazol-4-yl)acryloyl-L-tryptophanate (**GQN-B37-Me**). Yield: 33%, purity: 99%. <sup>1</sup>H NMR (600 MHz, DMSO-*d*<sub>6</sub>) δ 10.99 (s, 1H), 9.90 (s, 1H), 9.03 (s, 1H), 8.63 (d, *J* = 7.5 Hz, 1H), 8.04 (s, 1H), 7.92 (d, *J* = 8.2 Hz, 1H), 7.58–7.50 (m, 2H), 7.44 (d, *J* = 7.9 Hz, 2H), 7.40 (d, *J* = 8.0 Hz, 1H), 7.38–7.33 (m, 2H), 7.20 (s, 1H), 7.07 (t, *J* = 7.6 Hz, 1H), 6.99 (t, *J* = 7.5 Hz, 1H), 6.94 (d, *J* = 7.9 Hz, 2H), 6.55 (d, *J* = 15.7 Hz, 1H), 4.63 (q, *J* = 7.3 Hz, 1H), 3.62 (s, 3H), 3.22 (dd, *J* = 14.7, 5.2 Hz, 1H), 3.13 (dd, *J* = 14.6, 9.3 Hz, 1H). <sup>13</sup>C NMR (151 MHz, DMSO-*d*<sub>6</sub>) δ 172.44, 165.10, 157.90, 152.35, 140.10, 135.96, 133.89, 131.16, 129.62, 129.42 (2C), 127.64, 126.84, 126.15, 123.60, 122.40, 120.97, 120.80, 118.27, 118.02, 117.79, 117.38, 116.81, 115.48 (2C), 111.33, 109.38, 53.22, 51.71, 26.83. ESI-MS: *m/z* 541.2 [M + H]<sup>+</sup>, ESI-HRMS: calcd for C<sub>30</sub>H<sub>25</sub>ClN<sub>4</sub>O<sub>4</sub> [M + H]<sup>+</sup> 541.1637, found 541.1622.

**4.2. Virtual Screening and Hit Identification.** The overall workflow of our docking-based virtual screening is shown in Figure S1 in the Supporting Information. The starting point of our virtual screening was roughly 630,000 small molecules assembled from three commercial compound libraries, including MayBridge, SPECS, and LifeChemicals. Those molecules were first filtered by the following chemical rules: molecular weight <600, hydrogen bond acceptor <10, hydrogen bond donor <5, and CLogP < 6. Then, molecular structures of the qualified molecules were prepared by using the LigPrep module in the Schrödinger software (version 2016), including desalting, protonation assignment, and isomer generation.

All major antiapoptotic BCL-2 family proteins (e.g., BCL-2, MCL-1, and BCL-x<sub>L</sub>) are known to exhibit considerable conformational flexibility around the BH3-domain binding site. In order to tackle this difficulty to improve the chance of discovering small-molecule binders, parallel docking jobs were conducted in our work on multiple structures of MCL-1 and BCL-x<sub>L</sub>. Three representative complex structures for MCL-1 (PDB entries 3WIX, 4HW3, and 4OQ5) and BCL-x<sub>L</sub> (PDB entries 3QKD, 3ZLR, and 4TUH), respectively, were downloaded from the Protein Data Bank (PDB), and they were all processed by using the Protein Preparation Wizard module in the Schrödinger software (Schrödinger Inc., version 2016), including adding hydrogen atoms, setting protonation states, and filling up missing atoms. Molecular docking was executed by using the GOLD software (CCDC, version 2016) because GOLD is considerably more efficient than GLIDE in the Schrödinger software. All small molecules selected at the

previous step were docked into the BH3-domain binding site on the six chosen protein structures, respectively. The binding pocket on MCL-1 or BCL-x<sub>L</sub> was defined as the regions formed by protein atoms within 10 Å from residues T266 or G138, respectively. A genetic algorithm was used for conformational sampling during the docking process, with a sampling efficiency of 30%. For each molecule, a maximum of 10 binding poses were generated. The ChemPLP scoring function was used to select the most promising binding pose as the output.

For each protein structure considered in virtual screening, 40,000 top-ranked molecules were selected and then clustered according to the pairwise similarity among them (computed by using the BIT\_MACCS descriptor). The molecule with the highest ChemPLP score in each cluster was selected as the representative and was added to the candidate list for this particular protein structure. Then, among the intersection of the three obtained candidates list for the given target (MCL-1 or BCL-x<sub>L</sub>), the top-ranked 1000 molecules were subjected to visual inspection. Finally, 349 and 317 molecules were selected as plausible inhibitors for MCL-1 and BCL-x<sub>L</sub>, respectively, by considering their binding mode as well as ligand efficiency (LE = ChemPLP binding score/number of heavy atoms on the given molecule). A detailed list of the finally selected compounds is included as part of the Supporting Information.

Among the finally selected molecules, compound samples of 644 of them were purchased from the TopScience Inc. (Shanghai, China). All obtained compounds were tested in a fluorescence polarization-based binding assay, and the ones with an inhibition ratio >50% at the single dose of 50 μM were further tested in a multidose measurement to derive their inhibition constants (K<sub>i</sub>) on the desired target.

**4.3. Molecular Modeling.** The binding mode of each MCL-1 inhibitor of interest was predicted by molecular docking and then was further refined through MD simulation. To account for the conformational flexibility of MCL-1 in molecular docking, ten representative crystal structures of the human MCL-1 protein were selected from Protein Data Bank (i.e., PDB entries 4OQ6, 4WMU, 4ZBF, SFDO, SFDR, 6QYO, 6U65, 6YBL, 6FS0, and 7NB7). All structures include a small-molecule ligand bound at the BH3-domain-binding pocket, and all of them have an overall resolution better than 2.5 Å. Those ten structures were superimposed by the residues forming the BH3-domain-binding pocket by using the Conformer Cluster module in the Schrödinger software (Figure S3 in the Supporting Information). Each given MCL-1 inhibitor was then docked into the BH3-domain-binding pocket on each of the ten MCL-1 structures by using the GLIDE module in the Schrödinger software at the SP mode (i.e., standard precision), and the binding pose with the best binding score on each MCL-1 structure was recorded for analysis. Then, the most common binding mode observed among all ten MCL-1 structures was selected as the starting point for subsequent MD simulation.

All MD simulations in our work were conducted with the AMBER 18 software. The AmberTools suite was used for preparing input files, where the small-molecule ligand and the protein molecule were assigned appropriate parameters from the GAFF and ff14SB force field, respectively. The complex structure was immersed in a TIP3P water box with a 10 Å boundary at each dimension, and an appropriate number of counterions were added to neutralize the whole system. The whole system was then subjected to a stepwise minimization process to release the internal strain energy. After that, the whole system was heated from 0 to 303 K in 200 ps with a force

constant restraint of 10 kcal/mol Å<sup>2</sup> on all protein atoms. The whole system was further equilibrated for additional 500 ps at the constant temperature of 303 K and the constant pressure of 1 atm. Then, three parallel MD simulations, 1 μs long each, in the NPT ensemble were performed. During this process, the time step was set to 2 fs, and the SHAKE algorithm was used to fix the lengths of all chemical bonds connecting hydrogen atoms. On each finally obtained MD trajectory, a total of 100,000 snapshots were extracted at an interval of 10 ps for analysis. Root-mean-square-deviation (RMSD) values were calculated for the ligand molecule as well as the protein molecule by using the first frame as the reference. Judged by the RMSD values, if any of the three obtained MD trajectories indicated a quasi-stable ligand binding mode, that MD trajectory was subjected to a hierarchical clustering process to identify the largest cluster of complex structure, which was then used to derive the representative binding mode of the given ligand molecule.

#### 4.4. Protein Expression and In Vitro Binding Assay.

The experimental methods adopted for proteins expression and purification were essentially the same as described in our previous work.<sup>44,45</sup> In brief, MCL-1 (residues 152–327), BCL-2 (residues 1–207), and BCL-x<sub>L</sub> (residues 45–233) protein molecules with an 8 × His N-terminal tag were expressed in *E. coli* BL21 (DE3) cells and were induced by 0.4 mM IPTG at 20 °C for 16 h. Then, cells were lysed by low temperature ultrahigh pressure cell disrupter in 25 mM Tris-HCl, pH 8.0 buffer containing 300 mM NaCl, 5 mM βME, 1% (v/v) Triton X-100, 1× protease inhibitor cocktail, and 0.1 mg/mL phenylmethanesulfonyl fluoride (PMSF). The His-TEV-MCL-1, His-TEV-BCL-2, and His-TEV-BCL-x<sub>L</sub> proteins were purified from the soluble fraction using Ni-NTA resin (QIAGEN) at 4 °C. The purified proteins were cleaved by TEV protease (0.5 mg/mL, 4 °C, 15 h) at 4 °C for 16 h. After the removal of His-tags, proteins were further purified through HiLoad Superdex 75 pg column at 4 °C and were confirmed by 10% SDS-PAGE. Finally, the pooled fraction from the purified proteins was concentrated using 10 kDa molecular weight cutoff membrane (Spectrum-Labs).

A fluorescence polarization (FP)-based binding assay successfully applied to our previous work<sup>44,45</sup> was also employed in this work. The sample of a 5-carboxy-fluorescein-labeled 26-residue peptide derived from BID-BH3 (5-FAM-QEDIIR-NIARHLA QVGDSDM-RSIPPG) was purchased from the HD Biosciences Cooperation Company to use as the fluorescein probe in measurement. Each target protein (BCL-2, BCL-x<sub>L</sub>, or MCL-1) was prepared in 180 μL assay buffer (PBS, pH 7.3, 140 mM NaCl, 2.7 mM KCl, 10 mM Na<sub>2</sub>HPO<sub>4</sub>, 1.8 mM KH<sub>2</sub>PO<sub>4</sub>) and was incubated with the compounds under test (1% final DMSO) at 37 °C for 30 min. Then, 20 μL FAM-BID peptide in PBS was added to the protein-compound mixture solution and incubated at 37 °C for 20 min. Final concentrations of BCL-2, BCL-x<sub>L</sub>, and MCL-1 were 445, 205, and 145 nM, respectively. Final concentration of the BID-BH3 peptide was 10 nM. At last, the solutions were transferred into 384-well, black, flat-bottom plates (from Corning Inc.) with 60 μL per well and three wells per sample. Polarization values in millipolarization units (mP) were measured at an excitation wavelength at 485 nm and an emission wavelength at 535 nm with a TECAN Spark multimode microplate reader (TECAN Group Ltd.). For each measurement, a positive control containing the target protein (BCL-2, BCL-x<sub>L</sub>, or MCL-1) and the BID-BH3 peptide dissolved in 1% (v/v) [D<sub>6</sub>]DMSO and a negative control

containing only the BID-BH3 peptide dissolved in 1% (v/v) [D<sub>6</sub>]DMSO were included on each plate.

Each compound was tested against all three target proteins (BCL-2, BCL-x<sub>L</sub>, and MCL-1) at seven doses, i.e., 1 nM, 10 nM, 100 nM, 1 μM, 10 μM, 50 μM and 100 μM. At each concentration, the average value of three parallel measurements was used to perform a nonlinear fitting to obtain the dose-dependent binding curve by using the GraphPad Prism software. Concentration of the given compound when 50% of the bound peptide was displaced (IC<sub>50</sub>) was derived from this binding curve. The competitive inhibition constant (K<sub>i</sub>) of each tested compound was then calculated with the equation developed by Wang and co-workers<sup>47</sup> assuming that a binary complex with the target protein was formed. In our binding assay, ABT-199 was employed as a reference compound (K<sub>i</sub> < 1 nM for BCL-2 and K<sub>i</sub> < 1 nM for BCL-x<sub>L</sub>, but no obvious binding to MCL-1 by our measurement) and A1210477 was employed as another (K<sub>i</sub> < 10 nM for MCL-1 but no obvious binding to BCL-2 and BCL-x<sub>L</sub> by our measurement).

**4.5. <sup>1</sup>H–<sup>15</sup>N-Heteronuclear Single-Quantum Coherence Spectroscopy.** The human MCL-1 protein (172–327aa) was used in this experiment. The pET28a-His-hMCL-1 vector was expressed in the *E. coli* BL21 (DE3) cells. Cells were grown at 37 °C in the M9 medium containing <sup>15</sup>N-ammonium chloride and Kana. Protein expression was induced by addition of 0.4 mM IPTG at 37 °C for 4 h. Cells were lysed in 25 mM Tris (hydroxymethyl) aminomethane (Tris)-HCl buffer at pH 7.0 containing 100 mM NaCl and 0.1 mg/mL PMSF. <sup>15</sup>N-labeled His-hMCL-1 protein was purified from the soluble fraction by using the Ni-NTA resin (QIAGEN), and further purified through a HiLoad Superdex 75 pg column. <sup>1</sup>H–<sup>15</sup>N HSQC NMR spectra were recorded on an Agilent 800 MHz NMR spectrometer at 25 °C. The <sup>15</sup>N-labeled His-hMCL-1 protein was dissolved in 20 mM sodium phosphate buffer at pH 6.8, with 1 mM DTT, 2% DMSO-*d*<sub>6</sub>, and 10% D<sub>2</sub>O. HSQC NMR spectra of the protein in its free form were recorded first. Then, the tested compound dissolved in DMSO-*d*<sub>6</sub> was added into the above solution, which was incubated at 4 °C for 1 h and then centrifuged. The final concentration of the protein was 0.15 mM. After that, HSQC NMR spectra of the protein-compound complex were recorded. The NMR spectra were processed and analyzed by using the Sparky software. The HSQC spectrum of hMCL-1 in its free form can be obtained from the Biological Magnetic Resonance Data Bank (<http://www.bmrb.wisc.edu/>, access number 19654), which was used as the reference for assigning residue chemical shifts.

**4.6. Cytotoxicity Evaluation.** The cytotoxicity activities of all tested compounds were measured in a CCK-8 (Cell Counting Kit-8) colorimetric assay. The CCK-8 kit was purchased from TargetMol (catalog #C0005, TargetMol, China). Cell lines employed in this assay included H929, RS4;11, HL-60, MV-4–11, HeLa, and HEK293T, which were all originally obtained from the American Type Culture Collection (ATCC, Manassas, VA). Cells were cultured in Dulbecco's Modified Eagle's Medium (HEK293T), RPMI 1640 Medium (H929, RS4;11, HeLa, and HL-60), or Iscove's Modified Dulbecco's Medium (MV-4–11) with 10% heat inactivated fetal bovine serum (FBS) and supplemented with 1% penicillin-streptomycin (P/S), and were grown at 37 °C in a humidified atmosphere with 5% CO<sub>2</sub>. After that, cells were seeded in a 96-well plate at an appropriate density (i.e., 8000 for H929, 16,000 for RS4;11, 8000 for HeLa, 16,000 for HL-60, 8000 for MV-4–11, and 10,000 for HEK293T) at 100 μL per



well to maintain cells in the exponential phase of growth. Then, cells were incubated in a CO<sub>2</sub> incubator for 48 h at 37 °C with the tested compound at a series of doses. Here, the dose profiles were set differently on different cell lines in order to obtain optimal outcomes, i.e., 2.5, 5, 10, 20, and 40 μM in the cases of HL-60, HeLa, RS4;11, and HEK293T; 0.907, 1.633, 2.940, 5.292, 9.526, 17.147, 30.864, 55.556, and 100 μM in the case of MV-4–11; and 1.25, 2.5, 5, 10, 20, 40, and 80 μM in the case of H929. Note that each given compound of each dose was prepared in triplicate wells. After incubation, the CCK-8 solution of 10 μL was added to each well, and the 96-well plate was incubated at 37 °C in the CO<sub>2</sub> incubator for another 2 h.

The absorbance values (OD) at 450 and 650 nm (as the reference) were recorded with a TECAN Spark multimode microplate reader (TECAN Group Ltd.). The absorbance values detected at the same wavelength for the wells containing only the medium and the wells containing the medium plus the cells were defined as the blank and the control, respectively. Inhibition of cell viability by the compound under test was calculated with the following equation:

$$\text{cell viability inhibition (\%)} \\ = \left[ 1 - \frac{(\text{OD (compound)} - \text{OD (blank)})}{(\text{OD (control)} - \text{OD (blank)})} \right] \times 100\%$$

Concentration at 50% inhibition (IC<sub>50</sub>) of each tested compound was derived by a nonlinear fitting of the average inhibition rates measured at different doses by using the Graphpad Prism software.

**4.7. Kinetics Study in Cells.** MV-4–11 cells were seeded in 6-well cell culture plates at  $1.2 \times 10^6$  cells per well (2 mL), which were then treated with the given compound at a total concentration of 40 μM (5% final DMSO). At predetermined time points (0, 1, 2, 3, 5, 7, and 8 h), one well of cells was collected and centrifuged immediately at 200G and 4 °C for 5 min. The supernatants were analyzed by LC-MS/MS (model 4000 Q-TRAP from AB SciEX, USA) to determine the extracellular partition of the given compound. The cells were lysed in the RIPA lysis buffer (50 mM Tris, pH 7.4, 150 mM NaCl, 1% Triton X-100, 0.1% SDS, 1% sodium deoxycholate (catalog #P0013B, Beyotime, China) for 30 min. Then, the lysate samples were centrifuged at 12,000 rpm for 20 min to collect the supernatants for LC-MS/MS analysis to determine the intracellular partition of the given compound.

**4.8. Flow Cytometry.** MV-4–11 cells were incubated with A1210477 (catalog #114401, TargetMol, China) of 1 and 5 μM, AZD5991 (catalog #BCP23513, Biochempartner, China) of 1 and 5 μM, and GQN-B37-Me of 1, 5, 10, 20, 30, and 40 μM in a six-well cell culture plate for 24 h. Each sample was collected, centrifuged and washed twice with PBS, and dispersed in 100 μL 1Annexin V binding buffer. Then, each sample was stained with 5 μL Annexin V-FITC and 5 μL propidium iodide staining solution (catalog #556547, BDPharmingen, USA), respectively, in dark at the room temperature for 15 min. All samples were analyzed using a Beckman flow cytometer (CytoFlex S, Beckman, USA).

**4.9. Western Blot.** H929 cells were treated with AZD5991 of 0.5 μM (catalog #BCP23513, Biochempartner, China) and GQN-B37-Me of 5, 10, 20, and 40 μM for 24 h, and then were lysed in an ice-cold RIPA lysis buffer (catalog #P0013B, Beyotime, China). Lysate samples were centrifuged at 12,000 rpm for 20 min at 4 °C to collect the supernatants. Protein

concentration was assessed using the BCA protein assay kit (catalog #EB15DA0007, Sangon Biotech, China). Each sample was heated at 100 °C for 8 min and run on 12.5% SDS polyacrylamide gels using a Bio-Rad Mini-PROTEANTetra electrophoresis apparatus. Then, the protein was transferred onto polyvinylidene difluoride (PVDF) membranes (Millipore, USA) using a Bio-Rad Trans-BlotTurbo electrotransfer apparatus. Blots on PVDF membranes were blocked for 1 h at room temperature with 5% nonfat milk in Tris-buffered saline with 0.1% Tween-20 (TBST). Blots were incubated with PARP (catalog #9532, Cell Signaling Technology, USA), caspase-3 (catalog #9662, Cell Signaling Technology, USA), and GAPDH (catalog #2118, Cell Signaling Technology, USA) antibodies in TBST with 5% nonfat milk at a 1:1000 dilution at 4 °C overnight. Blots were washed with TBST three times and then were incubated at a 1:4000 dilution of HRP-conjugated goat antimouse or goat antirabbit IgG secondary antibody (catalog #7074 and #7076, Cell Signaling Technology, USA) for 2 h at room temperature. After that, blots were washed with TBST three times again and were detected using enhanced chemiluminescence (ECL) reagents.

**4.10. Coimmunoprecipitation.** H929 cells were seeded in a six-well cell culture plate at a suitable density, which were then incubated with A1210477 of 2 μM (catalog #114401, TargetMol, China), AZD5991 of 0.5 μM (catalog #BCP23513, Biochempartner, China), and GQN-B37-Me of 10, 20, or 40 μM at 37 °C for 10 h. After that, cells were harvested and lysed in the IP buffer (20 mM Tris, pH 7.5, 150 mM NaCl, 1% Triton X-100) (catalog #P0013, Beyotime, China) supplemented with 1% PMSF at 4 °C for 30 min. After centrifugation at 12,000 rpm and 4 °C for 15 min, supernatants were collected and normalized to the protein contents using the BCA protein Assay kit (catalog #EB15DA0007, Sangon Biotech, China). An volume of 10 μL of the MCL-1 antibody (catalog #sc-12756, Santa Cruz Biotechnology, USA) was added to an input volume of 100 μL supernatants. The mixture was incubated at 4 °C overnight on a tube rotator. Then, the precleared 30 μL of Protein A/G Magnetic Beads (catalog #SB-PR001-M, ShareBio, China) was added and incubated at 4 °C for 2 h with constant rotation. The beads were centrifuged and washed with the IP buffer three times for the following Western blot analysis using the MCL-1 antibody (catalog #sc-12756, Santa Cruz Biotechnology, USA), the BIM antibody (catalog #2933, Cell Signaling Technology, USA), and GAPDH (catalog #2118, Cell Signaling Technology, USA).

**4.11. In Vivo Antitumor Study.** All animal experimental procedures were approved by the Institutional Animal Care and Use Committee of SMOC (IACUC no. 2019–0011, Shanghai Model Organisms Center). Healthy female M-NSG mice of 4–5 weeks old were purchased from the Shanghai Model Organisms Center (Shanghai, China). Tumor implantation were conducted when mice were 6 weeks old. Five  $\times 10^6$  MV-4–11 cells were injected subcutaneously in the right flank of the mice. GQN-B37-Me and AZD5991 were formulated in 10% solutol and saline solution (0.9% NaCl). Tumor growth was monitored, while tumor volume and body weight were measured twice weekly using an electronic caliper. The tumor volume was calculated as  $(\text{length} \times \text{width}^2)/2$ . When the mean tumor size reached approximately 250 mm<sup>3</sup>, mice were randomized into five groups and intraperitoneally treated with vehicle, AZD5991 (10 mg/kg), or GQN-B37-Me (12.5 or 50 mg/kg) every 2 days for 20 days. Tumor volumes and weights of the mice were measured every 2 days. During this process, the mice were given

free access to diet and water. Tumor growth inhibition (TGI) in percentage was calculated as

$$\text{TGI}(\%) = \left[ 1 - \frac{(\text{mean volume (treated day } x) - \text{mean volume (treated day 0)})}{(\text{mean volume (vehicle day } x) - \text{mean volume (vehicle day 0)})} \right] \times 100\%$$

After 20 days, mice were executed, and their main organs and tumors were taken out for cryo-sectioning. Toxicity, antiproliferation, and apoptosis evaluation were detected using the HE (catalog #BA4025, BASO, China),  $K_i$ -67 (catalog #ab15580, ABcam, UAS), and cleaved-PARP (catalog #ab32064, ABcam, USA) antibodies.

**4.12. Stability in GSH.** To a 20 mL sample bottle dried with argon gas, 10 mL DMSO was added together with 10  $\mu$ L of a concentrated storage of 10 mM GQN-B37-Me, 52  $\mu$ L DIPEA, and 1 mL PBS buffer solution. A total amount of 15.4 mg GSH was added to the above solution and stirred at the room temperature. At predetermined time points (i.e., 5, 30, 60, 90, and 120 min), 20  $\mu$ L sample solution was taken out and then analyzed by HPLC, where the methanol percentage was increased from 5 to 95% over 16 min.

**4.13. Stability in Liver Microsomes.** The sample of human liver microsome was purchased from CORNING, USA (catalog #452161), which was a mixture of five major P450s (i.e., CYP1A2, 2C9, 2C19, 2D6, and 3A4). Monkey, dog, and rat pooled liver microsomes were also purchased from CORNING, USA (catalog #452413, #452601, and #452501). GQN-B37-Me was dissolved in DMSO at 2 mM, and 5  $\mu$ L of this solution was added to the 15  $\mu$ L of the PBS buffer. 0.75  $\mu$ L of the above diluted 0.5 mM solution was preincubated with 9.38  $\mu$ L liver microsomes (0.2 mg/mL) in 239.88  $\mu$ L PBS at the room temperature for 5 min. Then, 15  $\mu$ L of the NADPH solution (3 mM) was added to initiate the reaction. After incubation at 37 °C for certain time (0, 5, 10, 20, 30, and 60 min), 90  $\mu$ L of cold acetonitrile was added to quench and precipitate the P450 proteins. Finally, samples were centrifuged at 10,000 rpm for 10 min, and the supernatants were analyzed by LC-MS/MS.

## ■ ASSOCIATED CONTENT

### SI Supporting Information

The Supporting Information is available free of charge at <https://pubs.acs.org/doi/10.1021/acsomega.4c02021>.

Part 1: workflow of the virtual screening conducted in our work; Part 2: prediction of ligand binding mode through molecular modeling; Part 3: flow cytometric analysis of GQN-B37-Me; Part 4: evaluation of in vitro stability of GQN-B37-Me; Part 5: HPLC traces for all new compounds described in this study (PDF)

Molecular formula strings and other basic information of all candidate compounds selected in virtual screening (CSV); molecular formula strings of all newly synthesized compounds reported in this study (CSV); the predicted binding modes of LC126 and GQN-B37-E as shown in Figure 3b (PDB); and statement on the ethnicity of all animal experiments performed in this work (ZIP)

## ■ AUTHOR INFORMATION

### Corresponding Authors

**Yong Chu** – Department of Medicinal Chemistry, School of Pharmacy, Fudan University, Shanghai 201203, People's Republic of China; Email: [cy110@fudan.edu.cn](mailto:cy110@fudan.edu.cn)

**Hong Liu** – State Key Laboratory of Drug Research, Shanghai Institute of Materia Medica, Chinese Academy of Sciences, Shanghai 201203, China; [orcid.org/0000-0003-3685-6268](https://orcid.org/0000-0003-3685-6268); Email: [hliu@simmm.ac.cn](mailto:hliu@simmm.ac.cn)

**Renxiao Wang** – Department of Medicinal Chemistry, School of Pharmacy, Fudan University, Shanghai 201203, People's Republic of China; [orcid.org/0000-0003-0485-0259](https://orcid.org/0000-0003-0485-0259); Email: [wangrx@fudan.edu.cn](mailto:wangrx@fudan.edu.cn)

### Authors

**Qineng Gong** – Department of Medicinal Chemistry, School of Pharmacy, Fudan University, Shanghai 201203, People's Republic of China

**Chunpu Li** – State Key Laboratory of Drug Research, Shanghai Institute of Materia Medica, Chinese Academy of Sciences, Shanghai 201203, China; [orcid.org/0000-0002-3000-0728](https://orcid.org/0000-0002-3000-0728)

**Haojie Wang** – Department of Medicinal Chemistry, School of Pharmacy, Fudan University, Shanghai 201203, People's Republic of China

**Jinrui Cao** – Department of Medicinal Chemistry, School of Pharmacy, Fudan University, Shanghai 201203, People's Republic of China

**Zuo Li** – Department of Medicinal Chemistry, School of Pharmacy, Fudan University, Shanghai 201203, People's Republic of China

**Mi Zhou** – Department of Medicinal Chemistry, School of Pharmacy, Fudan University, Shanghai 201203, People's Republic of China

**Yan Li** – Department of Medicinal Chemistry, School of Pharmacy, Fudan University, Shanghai 201203, People's Republic of China; [orcid.org/0000-0002-8259-2470](https://orcid.org/0000-0002-8259-2470)

Complete contact information is available at:

<https://pubs.acs.org/doi/10.1021/acsomega.4c02021>

### Author Contributions

<sup>§</sup>Q.G., C.L., and H.W. had equal contributions to this work.

### Notes

The authors declare no competing financial interest.

## ■ ACKNOWLEDGMENTS

This study was financially supported by the National Natural Science Foundation of China (Grant No. 81725022) and Science and Technology Commission of Shanghai Municipality (Grant No. 20S11900500).

## ■ REFERENCES

- (1) Aguirre-Ghiso, J. A. Models, mechanisms and clinical evidence for cancer dormancy. *Nat. Rev. Cancer* **2007**, *7*, 834–846.
- (2) Hanahan, D.; Weinberg, R. A. Hallmarks of cancer: the next generation. *Cell* **2011**, *144*, 646–674.
- (3) Hanahan, D. Hallmarks of cancer: new dimensions. *Cancer Discovery* **2022**, *12*, 31–46.
- (4) Kerr, J. F. R.; Wyllie, A. H.; Currie, A. R. Apoptosis: a basic biological phenomenon with wide-ranging implications in tissue kinetics. *Br. J. Cancer* **1972**, *26*, 239–257.
- (5) Jin, Z.; El-Deiry, W. S. Overview of cell death signaling pathways. *Cancer Biol. Ther.* **2005**, *4*, 139–163.

- (6) Danial, N. N.; Korsmeyer, S. J. Cell death: critical control points. *Cell* **2004**, *116*, 205–219.
- (7) Ashkenazi, A.; Dixit, V. M. Death receptors: signaling and modulation. *Science* **1998**, *281*, 1305–1308.
- (8) Czabotar, P. E.; Lessene, G.; Strasser, A.; Adams, J. M. Control of apoptosis by the BCL-2 protein family: implications for physiology and therapy. *Nat. Rev. Mol. Cell Biol.* **2014**, *15*, 49–63.
- (9) Sarosiek, K. A.; Chi, X.; Bachman, J. A.; Sims, J. J.; Montero, J.; Patel, L.; Flanagan, A.; Andrews, D. W.; Sorger, P.; Letai, A. BID preferentially activates BAK while BIM preferentially activates BAX, affecting chemotherapy response. *Mol. Cell* **2013**, *51*, 751–765.
- (10) Luo, X.; Budihardjo, I.; Zou, H.; Slaughter, C.; Wang, X. Bid, a Bcl-2 interacting protein, mediates cytochrome c release from mitochondria in response to activation of cell surface death receptors. *Cell* **1998**, *94*, 481–490.
- (11) Youle, R. J.; Strasser, A. The BCL-2 protein family: opposing activities that mediate cell death. *Nat. Rev. Mol. Cell Biol.* **2008**, *9*, 47–59.
- (12) Singh, R.; Letai, A.; Sarosiek, K. Regulation of apoptosis in health and disease: the balancing act of BCL-2 family proteins. *Nat. Rev. Mol. Cell Biol.* **2019**, *20*, 175–193.
- (13) Adams, J. M.; Cory, S. The Bcl-2 apoptotic switch in cancer development and therapy. *Oncogene* **2007**, *26*, 1324–1337.
- (14) Diepstraten, S. T.; Anderson, M. A.; Czabotar, P. E.; Lessene, G.; Strasser, A.; Kelly, G. L. The manipulation of apoptosis for cancer therapy using BH3-mimetic drugs. *Nat. Rev. Cancer* **2022**, *22*, 45–64.
- (15) Oltersdorf, T.; Elmore, S. W.; Shoemaker, A. R.; Armstrong, R. C.; Augeri, D. J.; Belli, B. A.; Bruncko, M.; Deckwerth, T. L.; Dinges, J.; Hajduk, P. J.; Joseph, M. K.; Kitada, S.; Korsmeyer, S. J.; Kunzer, A. R.; Letai, A.; Li, C.; Mitten, M. J.; Nettlesheim, D. G.; Ng, S.; Nimmer, P. M.; O'Connor, J. M.; Oleksijew, A.; Petros, A. M.; Reed, J. C.; Shen, W.; Tahir, S. K.; Thompson, C. B.; Tomaselli, K. J.; Wang, B.; Wendt, M. D.; Zhang, H.; Fesik, S. W.; Rosenberg, S. H. An inhibitor of Bcl-2 family proteins induces regression of solid tumours. *Nature* **2005**, *435*, 677–681.
- (16) Tse, C.; Shoemaker, A. R.; Adickes, J.; Anderson, M. G.; Chen, J.; Jin, S.; Johnson, E. F.; Marsh, K. C.; Mitten, M. J.; Nimmer, P.; Roberts, L.; Tahir, S. K.; Xiao, Y.; Yang, X.; Zhang, H.; Fesik, S.; Rosenberg, S. H.; Elmore, S. W. ABT-263: a potent and orally bioavailable Bcl-2 family inhibitor. *Cancer Res.* **2008**, *68*, 3421–3428.
- (17) Souers, A. J.; Levenson, J. D.; Boghaert, E. R.; Ackler, S. L.; Catron, N. D.; Chen, J.; Dayton, B. D.; Ding, H.; Enschede, S. H.; Fairbrother, W. J.; Huang, D. C.; Hymowitz, S. G.; Jin, S.; Khaw, S. L.; Kovar, P. J.; Lam, L. T.; Lee, J.; Maecker, H. L.; Marsh, K. C.; Mason, K. D.; Mitten, M. J.; Nimmer, P. M.; Oleksijew, A.; Park, C. H.; Park, C. M.; Phillips, D. C.; Roberts, A. W.; Sampath, D.; Seymour, J. F.; Smith, M. L.; Sullivan, G. M.; Tahir, S. K.; Tse, C.; Wendt, M. D.; Xiao, Y.; Xue, J. C.; Zhang, H.; Humerickhouse, R. A.; Rosenberg, S. H.; Elmore, S. W. ABT-199, a potent and selective BCL-2 inhibitor, achieves antitumor activity while sparing platelets. *Nat. Med.* **2013**, *19*, 202–208.
- (18) Juin, P.; Geneste, O.; Gautier, F.; Depil, S.; Camponne, M. Decoding and unlocking the BCL-2 dependency of cancer cells. *Nat. Rev. Cancer* **2013**, *13*, 455–465.
- (19) Andersen, M. H.; Becker, J. C.; Thor Straten, P. The antiapoptotic member of the Bcl-2 family Mcl-1 is a CTL target in cancer patients. *Leukemia* **2005**, *19*, 484–485.
- (20) Yecies, D.; Carlson, N. E.; Deng, J.; Letai, A. Acquired resistance to ABT-737 in lymphoma cells that up-regulate MCL-1 and BFL-1. *Blood* **2010**, *115*, 3304–3313.
- (21) Song, L.; Coppola, D.; Livingston, S.; Cress, D.; Haura, E. B. Mcl-1 regulates survival and sensitivity to diverse apoptotic stimuli in human non-small cell lung cancer cells. *Cancer Biol. Ther.* **2005**, *4*, 267–276.
- (22) Ding, Q.; He, X.; Xia, W.; Hsu, J. M.; Chen, C. T.; Li, L. Y.; Lee, D. F.; Yang, J. Y.; Xie, X.; Liu, J. C.; Hung, M. C. Myeloid cell leukemia-1 inversely correlates with glycogen synthase kinase-3 $\beta$  activity and associates with poor prognosis in human breast cancer. *Cancer Res.* **2007**, *67*, 4564–4571.
- (23) Touzeau, C.; Dousset, C.; Le Gouill, S.; Sampath, D.; Levenson, J. D.; Souers, A. J.; Maiga, S.; Bene, M. C.; Moreau, P.; Pellat-Deceunynck, C.; Amiot, M. The Bcl-2 specific BH3 mimetic ABT-199: a promising targeted therapy for t(11;14) multiple myeloma. *Leukemia* **2014**, *28*, 210–212.
- (24) Tong, J.; Wang, P.; Tan, S.; Chen, D.; Nikolovska-Coleska, Z.; Zou, F.; Yu, J.; Zhang, L. Mcl-1 degradation is required for targeted therapeutics to eradicate colon cancer cells. *Cancer Res.* **2017**, *77*, 2512–2521.
- (25) Qin, J. Z.; Xin, H.; Sitailo, L. A.; Denning, M. F.; Nickoloff, B. J. Enhanced killing of melanoma cells by simultaneously targeting Mcl-1 and NOXA. *Cancer Res.* **2006**, *66*, 9636–9645.
- (26) Akgul, C. Mcl-1 is a potential therapeutic target in multiple types of cancer. *Cell. Mol. Life Sci.* **2009**, *66*, 1326–1336.
- (27) Wertz, I. E.; Kusam, S.; Lam, C.; Okamoto, T.; Sandoval, W.; Anderson, D. J.; Helgason, E.; Ernst, J. A.; Eby, M.; Liu, J.; Belmont, L. D.; Kaminker, J. S.; O'Rourke, K. M.; Pujara, K.; Kohli, P. B.; Johnson, A. R.; Chiu, M. L.; Lill, J. R.; Jackson, P. K.; Fairbrother, W. J.; Seshagiri, S.; Ludlam, M. J.; Leong, K. G.; Dueber, E. C.; Maecker, H.; Huang, D. C.; Dixit, V. M. Sensitivity to antitubulin chemotherapeutics is regulated by MCL1 and FBW7. *Nature* **2011**, *471*, 110–114.
- (28) Wei, S. H.; Dong, K.; Lin, F.; Wang, X.; Li, B.; Shen, J. J.; Zhang, Q.; Wang, R.; Zhang, H. Z. Inducing apoptosis and enhancing chemosensitivity to gemcitabine via RNA interference targeting Mcl-1 gene in pancreatic carcinoma cell. *Cancer Chemother Pharmacol* **2008**, *62*, 1055–1064.
- (29) Denis, C.; Santos, J. S. O.; Bureau, R.; Voisin-Chiret, A. S. Hot-spots of mcl-1 protein. *J. Med. Chem.* **2020**, *63*, 928–943.
- (30) Day, C. L.; Chen, L.; Richardson, S. J.; Harrison, P. J.; Huang, D. C.; Hinds, M. G. Solution structure of proapoptotic Mcl-1 and characterization of its binding by proapoptotic BH3-only ligands. *J. Biol. Chem.* **2005**, *280*, 4738–4744.
- (31) Yang, T.; Kozopas, K. M.; Craig, R. W. The intracellular distribution and pattern of expression of mcl-1 overlap with, but are not identical to, those of bcl-2. *J. Cell Biol.* **1995**, *128*, 1173–1184.
- (32) Negi, A.; Murphy, P. V. Development of Mcl-1 inhibitors for cancer therapy. *Eur. J. Med. Chem.* **2021**, *210*, No. 113038.
- (33) Zhu, P.-J.; Yu, Z.-Z.; You, Q.-D.; Jiang, Z.-Y. Myeloid cell leukemia-1 inhibitors: a growing arsenal for cancer therapy. *Drug Discovery Today* **2020**, *25* (10), 1873–1882.
- (34) Bruncko, M.; Wang, L.; Sheppard, G. S.; Phillips, D. C.; Tahir, S. K.; Xue, J.; Erickson, S.; Fidanze, S.; Fry, E.; Hasvold, L.; Jenkins, G. J.; Jin, S.; Judge, R. A.; Kovar, P. J.; Madar, D.; Nimmer, P.; Park, C.; Petros, A. M.; Rosenberg, S. H.; Smith, M. L.; Song, X.; Sun, C.; Tao, Z. F.; Wang, X.; Xiao, Y.; Zhang, H.; Tse, C.; Levenson, J. D.; Elmore, S. W.; Souers, A. J. Structure-guided design of a series of MCL-1 inhibitors with high affinity and selectivity. *J. Med. Chem.* **2015**, *58*, 2180–2194.
- (35) Lee, T.; Christov, P. P.; Shaw, S.; Tarr, J. C.; Zhao, B.; Veerasamy, N.; Jeon, K. O.; Mills, J. J.; Bian, Z.; Sensintaffar, J. L.; Arnold, A. L.; Fogarty, S. A.; Perry, E.; Ramsey, H. E.; Cook, R. S.; Hollingshead, M.; Millin, D. M.; Lee, K. M.; Koss, B.; Budhraj, A.; Opferman, J. T.; Kim, K.; Arteaga, C. L.; Moore, W. J.; Olejniczak, E. T.; Savona, M. R.; Fesik, S. W. Discovery of potent myeloid cell leukemia-1 (mcl-1) inhibitors that demonstrate in vivo activity in mouse xenograft models of human cancer. *J. Med. Chem.* **2019**, *62*, 3971–3988.
- (36) Zhu, P.-J.; Yu, Z.-Z.; Lv, Y.-F.; Zhao, J.-L.; Tong, Y.-Y.; You, Q.-D.; Jiang, Z.-Y. Discovery of 3,5-Dimethyl-4-Sulfonyl-1H-Pyrrole-Based Myeloid Cell Leukemia 1 Inhibitors with High Affinity, Selectivity, and Oral Bioavailability. *J. Med. Chem.* **2021**, *64* (15), 11330–11353.
- (37) Lu, X.; Liu, Y.-C.; Orvig, C.; Liang, H.; Chen, Z.-F. Discovery of a Copper-Based Mcl-1 Inhibitor as an Effective Antitumor Agent. *J. Med. Chem.* **2020**, *63* (17), 9154–9167.
- (38) Lu, X.; Wu, M.-F.; Wu, J.-L.; Zhang, H.-Q.; Liang, H.; Chen, Z.-F. Platinum-Based Mcl-1 Inhibitor Targeting Mitochondria Achieves Enhanced Antitumor Activity as a Single Agent or in Combination with ABT-199. *J. Med. Chem.* **2023**, *66* (13), 8705–8716.
- (39) Romanov-Michailidis, F.; Hsiao, C.-C.; Uner, L. M.; Jerhaoui, S.; Surkyn, M.; Miller, B.; Vos, A.; Dominguez Blanco, M.; Bueters, R.; Vinken, P.; Bekkers, M.; Walker, D.; Pietrak, B.; Eyckmans, W.; Dores-Sousa, J. L.; Joo Koo, S.; Lento, W.; Bauser, M.; Philippar, U.;

Rombouts, F. J. R. Discovery of an Oral, Beyond-Rule-of-Five Mcl-1 Protein–Protein Interaction Modulator with the Potential of Treating Hematological Malignancies. *J. Med. Chem.* **2023**, *66* (9), 6122–6148.

(40) Caenepeel, S.; Brown, S. P.; Belmontes, B.; Moody, G.; Keegan, K. S.; Chui, D.; Whittington, D. A.; Huang, X.; Poppe, L.; Cheng, A. C.; Cardozo, M.; Houze, J.; Li, Y.; Lucas, B.; Paras, N. A.; Wang, X.; Taygerly, J. P.; Vimolratana, M.; Zancanella, M.; Zhu, L.; Cajulis, E.; Osgood, T.; Sun, J.; Damon, L.; Egan, R. K.; Greninger, P.; McClanaghan, J. D.; Gong, J.; Moujalled, D.; Pomilio, G.; Beltran, P.; Benes, C. H.; Roberts, A. W.; Huang, D. C.; Wei, A.; Canon, J.; Coxon, A.; Hughes, P. E. Amg 176, a selective mcl1 inhibitor, is effective in hematologic cancer models alone and in combination with established therapies. *Cancer Discovery* **2018**, *8*, 1582–1597.

(41) Caenepeel, S.; Karen, R.; Belmontes, B.; Verlinsky, A.; Tan, H.; Yang, Y.; Chen, X.; Li, K.; Allen, J.; Wahlstrom, J.; Canon, J.; Coxon, A.; Hughes, P. Abstract 6218: Discovery and preclinical evaluation of AMG 397, a potent, selective and orally bioavailable MCL1 inhibitor. *Cancer Res.* **2020**, *80* (16 Supplement), 6218.

(42) Tron, A. E.; Belmonte, M. A.; Adam, A.; Aquila, B. M.; Boise, L. H.; Chiarparin, E.; Cidado, J.; Embrey, K. J.; Gangl, E.; Gibbons, F. D.; Gregory, G. P.; Hargreaves, D.; Hendricks, J. A.; Johannes, J. W.; Johnstone, R. W.; Kazmirski, S. L.; Kettle, J. G.; Lamb, M. L.; Matulis, S. M.; Nooka, A. K.; Packer, M. J.; Peng, B.; Rawlins, P. B.; Robbins, D. W.; Schuller, A. G.; Su, N.; Yang, W.; Ye, Q.; Zheng, X.; Secrist, J. P.; Clark, E. A.; Wilson, D. M.; Fawell, S. E.; Hird, A. W. Discovery of Mcl-1-specific inhibitor AZD5991 and preclinical activity in multiple myeloma and acute myeloid leukemia. *Nat. Commun.* **2018**, *9*, 5341.

(43) Szlavik, Z.; Csekei, M.; Paczal, A.; Szabo, Z. B.; Sipos, S.; Radics, G.; Proszenyak, A.; Balint, B.; Murray, J.; Davidson, J.; Chen, I.; Dokurno, P.; Surgenor, A. E.; Daniels, Z. M.; Hubbard, R. E.; Le Toumelin-Braizat, G.; Claperon, A.; Lysiak-Auvity, G.; Girard, A. M.; Bruno, A.; Chanrion, M.; Colland, F.; Maragno, A. L.; Demarles, D.; Geneste, O.; Kotschy, A. Discovery of S64315, a Potent and Selective Mcl-1 Inhibitor. *J. Med. Chem.* **2020**, *63*, 13762–13795.

(44) Yang, C.; Chen, S.; Zhou, M.; Li, Y.; Li, Y.; Zhang, Z.; Liu, Z.; Ba, Q.; Li, J.; Wang, H.; Yan, X.; Ma, D.; Wang, R. Development of 3-phenyl-N-(2-(3-phenylureido)ethyl)-thiophene-2-sulfonamide compounds as inhibitors of antiapoptotic Bcl-2 family proteins. *ChemMedChem.* **2014**, *9*, 1436–1452.

(45) Li, Y.; Fan, W.; Gong, Q.; Tian, J.; Zhou, M.; Li, Q.; Uwituze, L. B.; Zhang, Z.; Hong, R.; Wang, R. Structure-based optimization of 3-phenyl-n-(2-(3-phenylureido)ethyl) thiophene-2-sulfonamide derivatives as selective mcl-1 inhibitors. *J. Med. Chem.* **2021**, *64*, 10260–10285.

(46) Baell, J. B.; Holloway, G. A. New substructure filters for removal of pan assay interference compounds (PAINS) from screening libraries and for their exclusion in bioassays. *J. Med. Chem.* **2010**, *53*, 2719–2740.

(47) Nikolovska-Coleska, Z.; Wang, R.; Fang, X.; Pan, H.; Tomita, Y.; Li, P.; Roller, P. P.; Krajewski, K.; Saito, N. G.; Stuckey, J. A.; Wang, S. Development and optimization of a binding assay for the XIAP BIR3 domain using fluorescence polarization. *Anal. Biochem.* **2004**, *332*, 261–273.